MECHANISM OF OXYGEN ABSORPTION BY ZIRCONIUM(Dissertation_全文)

AUTHOR(S):

Yamamoto, Masahiro

MECHANISM OF OXYGEN ABSORPTION BY ZIRCONIUM

1990

Masahiro Yamamoto

MECHANISM OF OXYGEN ABSORPTION BY ZIRCONIUM

1990

Masahiro Yamamoto

Contents

Introduction

Background of This Work

Oxidation of transition metals has been a practical problem of corrosion of structural materials, because the transition metals have a high affinity for oxygen and the transition metal oxides are easily formed at their surfaces. The oxide films formed, on the other hand, have useful properties and they are used, for example, as a protective oxide film under corrosive conditions and a thin oxide film insulator in electronic devices. Thereby, the metal oxidation has been studied from a point of view of chemical kinetics of corrosion, and recently the microscopic oxidation mechanism of the surface of transition metals has been studied by using modern techniques of surface science.

The mechanism of initial oxidation of zirconium is investigated in the present study. The zirconium-oxygen system has the following characteristics.

1) Metallic zirconium has a high affinity for oxygen.[1] As shown in Fig. I-1, the heat of oxide formation is the second greatest in the 4d transition metals. The heat of formation of zirconium oxide per oxygen atom is almost two times greater than that of water per oxygen atom. Zirconium has a high affinity also for some other light elements such as hydrogen, carbon and nitrogen. Then zirconium is used as a getter material in a vacuum system. The high affinity, on the other hand, makes it difficult to prepare a clean surface of zirconium.

2) No lower oxides have been generally recognized in the zirconium-

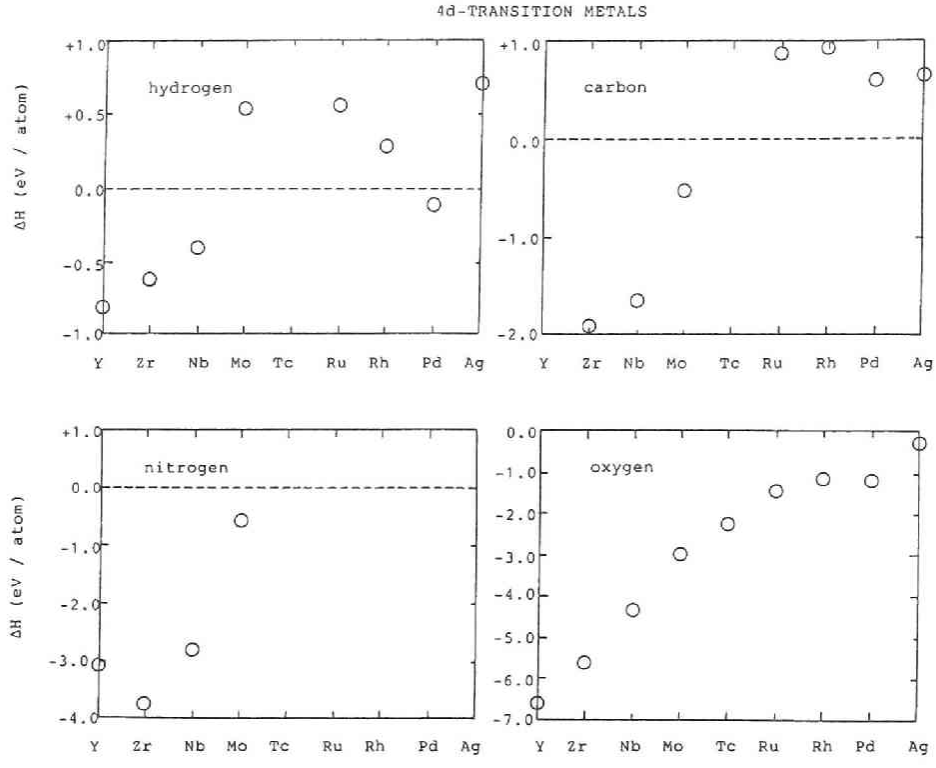

Fig. I-1. Heat of hydrogen absorption by 4d-transition metals and heat of formation of carbide, nitride and oxide of 4d-transition metal elements.

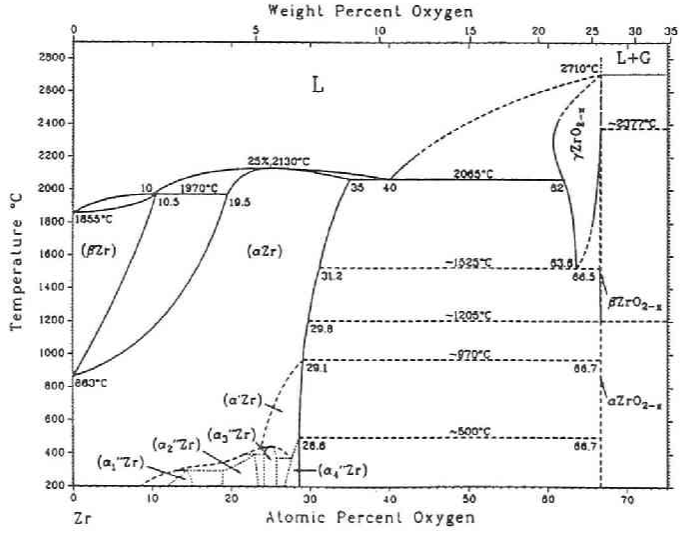

Fig. I-2. Assessed zirconium-oxygen phase diagram.[2]
——— :evaluated - - - - - :probable ····· :uncertain

oxygen system.[1-2] (*cf.* the titanium-oxygen system) Fig. I-2 shows the phase diagram of the zirconium-oxygen system.[2] A large amount of oxygen is soluble in α-zirconium, *e.g.* 28.6 atomic percent at 773 K. There is a coexisting phase of the α-zirconium with maximum oxygen concentration of 28.6 atomic percent and of the nonstoichiometric oxide ZrO_{2-x}. The simplicity of the phase diagram, *i.e.* there are no lower oxides, makes it easy to clarify experimentally the oxidation states of zirconium and to construct a model of oxygen absorption. There are three oxide phases: monoclinic phase at low temperatures, tetragonal phase at intermediate temperatures and cubic phase at high temperatures. Since the phase transition from the monoclinic to the tetragonal structure causes a large volume change, the zirconium oxide partially stabilized by the oxides such as Y_2O_3, CaO and MgO is used in practice.[3] In pure metallic zirconium structural phase transition from the h.c.p. α-phase to the b.c.c. β-phase occurs at 1136 K. In the present study oxidation of zirconium at temperatures below 1136 K is investigated.

3) Zirconium is the sixth greatest in abundance in transition metal elements in the earth's crust.

4) Zirconium and its alloys have considerable technological importance. Zirconium is used as a nuclear material because it has a small cross section of absorption for thermal neutrons. In addition, as already mentioned above, zirconium is used as a getter material and its oxide is widely used as a ceramic material (*e.g.* refractories and oxygen sensors).

It may be expected from the characteristics of the zirconium-oxygen system mentioned above that the study on the initial oxidation of

zirconium gives a basic understanding of the initial oxidation of transition metal.

Survey of Studies on Metal Oxidation

It is well known that the oxidation of transition metal goes through the three processes: dissociative adsorption of oxygen molecule, nucleation of oxide at the surface and growth of oxide film. A schematic diagram of the three processes are shown in Fig. I-3. It has been a main object of the study on metal oxidation to obtain a knowledge of the rate of oxide growth, because the oxide is formed at the very early stage of oxidation at an atmospheric pressure and high temperatures.

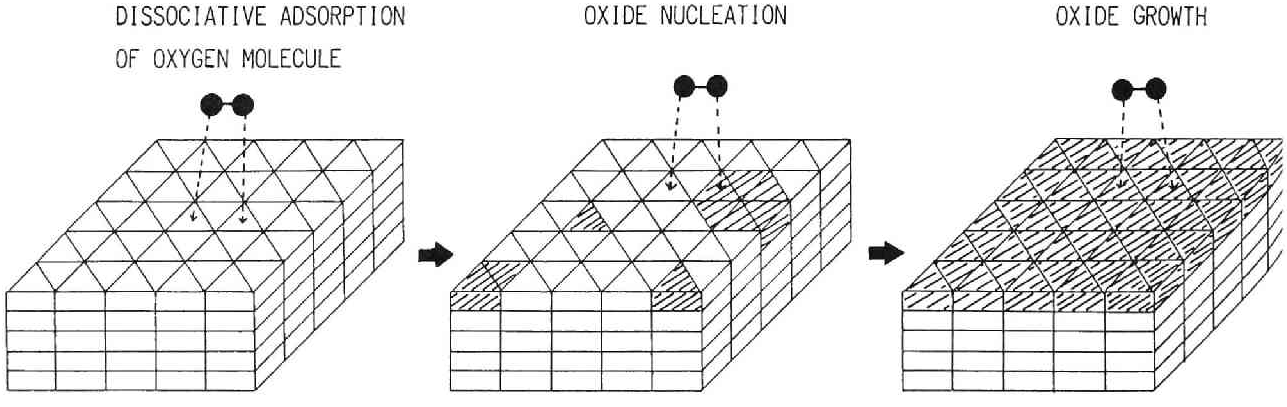

Fig. I-3. Schematic diagram of the three processes of metal oxidation

The kinetics of oxide growth has been discussed by using the Wagner theory for thick films and the Cabrera-Mott theory for thin

films.[4-7]

1) The Wagner theory for thick films[4-6]

Parabolic law (*i.e.* $L^2 \propto t$;L is thickness of the oxide film.) of the rate of growth of the oxide film thicker than 1 μm has been explained by this theory. Diffusion of ion species which pass through the oxide is a rate-limiting process. No net current throughout the film is assumed, *i.e.* ion current is compensated by electron current. Based on an approximation of local equilibrium in the film the parabolic rate constant are given using phenomenological kinetic parameters. The theory has been improved by including the effects of point defects in the oxide. However, it is difficult to apply the theory to the measured results, because some kinetic parameters cannot be unambiguously determined experimentally.

2) The Cabrera-Mott theory for thin films[4-5,7]

In this theory electrons are assumed to traverse the oxide film either by thermionic emission or by tunnelling from the metal to the oxygen adatoms at the surface. Strong uniform field between the oxygen ion at the surface and the oxide/metal interface is created. This strong uniform field in the oxide film is the driving force to transfer the oxygen ion. The field becomes weaker as the film becomes thicker, and the growth rate is reduced. There are several related theories and a corresponding number of growth laws, *e.g.* inverse logarithmic, logarithmic, cubic and parabolic law. However, it seems that there is no consensus on what theories or assumptions are reasonable to explain the growth of the thin films.[5]

The adsorption and nucleation processes had not been discussed until quite recently. The modern techniques of surface science have been used to

investigate the processes of the initial oxidation of the metal surface. However, almost all the studies have been concerned with the metal oxidation at room temperature. Dynamic properties of oxidation at high temperatures have not been investigated in detail.

Survey of Studies on Oxidation of Zirconium

A number of studies on oxidation of zirconium have been reported in the 1960s. These studies have been concerned with the rate of oxygen absorption by the oxide-covered zirconium. A review on these studies in the 1960s was given by Rosa.[8] He has concluded the following: (i)The rate of oxygen absorption by the oxide-covered zirconium can be best expressed by the parabolic law. (ii)This fact suggests that the rate of oxygen absorption is limited by the oxygen diffusion into the bulk with a moving boundary of oxide/metal interface. (iii)Little is known about the initial oxidation of zirconium. These studies on the oxidation of zirconium, however, yielded inconsistent results from different investigators because of insufficient preparation of specimen surfaces. The specimen surface had been prepared under low vacuum conditions in these studies, therefore the surface of zirconium was possibly contaminated with oxygen, carbon, hydrocarbon, water, *etc.*

In the 1970s a few investigators have reported the oxidation of zirconium the surface of which is cleaned by annealing under high vacuum conditions.[9-10] A linear rate of oxygen absorption has been observed before a parabolic rate has been observed. It has been suggested that the linear rate is limited by the adsorption of oxygen molecules. However, the

rate of oxygen absorption has not been discussed in detail in these studies, because the oxidation state of the surface in these measurements have not been determined by surface spectroscopic measurements.

In the 1980s surface oxidation of zirconium at room temperature has been investigated by using surface spectroscopies such as AES(Auger electron spectroscopy),[11-13] XPS(X-ray photoelectron spectroscopy),[14] LEED(low energy electron diffraction),[15-16] UPS(ultraviolet photoelectron spectroscopy),[17] EELS(electron energy loss spectroscopy),[18-19] SES(secondary electron emission spectroscopy)[20-21] and $\Delta\phi$ (change of work function).[22] Changes in the structure of surface, the electronic structure and the oxygen concentration by oxidation of zirconium at room temperature have been studied in detail. However, the knowledge of the dynamic properties of the oxidation of zirconium at high temperatures has not been given in these studies.

Outline of This Work

The present thesis deals with the study on the mechanism of initial oxidation of zirconium at high temperatures and at low oxygen pressures. Dynamic properties of the oxidation of zirconium become important at high temperatures and at low oxygen pressures, because the dynamic competition between the adsorption of oxygen at the surface and the diffusion of oxygen into the bulk should be considered. The rate of oxygen absorption by metallic zirconium with a clean surface and the characterization of the oxidation state of the surface are discussed in detail in this study.

In Chapter 1, pressure dependence of the rate of oxygen absorption by zirconium at 1073 K is discussed. The rate of oxygen absorption, the

electric resistivity and the effective emissivity have been measured. The condition under which the oxide is formed at the surface due to the increase in the adsorption rate with increasing oxygen pressure is determined. A model of oxygen absorption which is based on the oxygen diffusion process is constructed and the experimental results are explained using this model.

In Chapter 2, kinetics of oxygen absorption by α-zirconium is discussed. The temperature dependence of the rate of oxygen absorption at high temperatures of 973 - 1098 K and at low oxygen pressures of 6.7×10^{-5} - 1.3×10^{-4} Pa has been measured. The absorption rate is found to be almost linear, and the surface of zirconium is confirmed to remain in α-zirconium by using the secondary ion mass spectroscopy. The absorption rate is explained by using a model in which the absorption process comprises three successive steps: dissociative adsorption of oxygen molecules on the zirconium surface, transfer of adatoms at the surface site to the outermost bulk sites and diffusion of oxygen atoms into the bulk. The absorption rate is found to be limited by the adsorption under the conditions studied. Some kinetic parameters such as the activation energy for the adsorption, the interaction energy between adatoms and the energy difference between the adsorption site and the bulk site have been evaluated.

In Chapter 3, secondary ion mass spectroscopy (SIMS) has been used to investigate the change in the chemical composition of the zirconium surface by oxidation at high temperatures of 773 - 1073 K and at low pressures of 6.7×10^{-5} - 1.3×10^{-3} Pa. The chemical composition is characterized by the increase in the yields of the secondary ions of Zr^+, ZrO^+ and ZrO_2^+. The yield of the Zr^+ ion emission from the oxide surface

is found to be increased by *ca.* 300 times. The physical origin of the increase is discussed by using a resonance tunnelling theory for ion emission.

In Chapter 4, an anomaly in the rate of oxygen absorption by zirconium, *i.e.* the rate anomalously increased at the nucleation stage of oxidation, is discussed. The rate of oxygen absorption at the nucleation stage is numerically evaluated by using a model in which the nucleation and growth of the oxide at the surface is simulated by the so-called autocatalytic reaction.

In Chapter 5, changes in the work function of zirconium by oxidation at high temperatures is investigated and the oxidation states at the surface is discussed. The decrease in the work function at the initial stage of oxidation, which corresponds to the stage of dissociative adsorption, suggests that oxygen adatoms are adsorbed at subsurface sites. The potential for oxygen adsorption is calculated by using an effective medium theory and the physical origin of decrease is discussed. The increase in the work function are explained by the change in electronic structure as a result of the oxide formation at the surface.

In Chapter 6, changes in the electronic structure of zirconium by oxidation at room temperature and high temperatures is investigated by the use of Auger electron spectroscopy(AES), electron energy loss spectroscopy (EELS) and secondary electron emission spectroscopy(SES). The oxygen concentration at the surface and the thickness of the oxide film are estimated by using the results of Auger electron spectroscopy.

In the final chapter the results described in Chapters 1-6 are summarized.

References for Introduction

1. E. Fromm and E. Gebhardt, in *Gase und Kohlenstoff in Metallen*, (Springer, Berlin, 1976), pp. 397-440.
2. J. P. Abriata, J. Garces and R. Versaci, *Bull. Alloy Phase Diagrams*, 1986, 7, 116.
3. *Science and Technology of Zirconia, Advances in Ceramics Vol. 3*, ed. A. H. Heuer and L. W. Hobbs (The American Ceramic Society, Columbus, 1981).
4. A. T. Fromhold, Jr., in *Theory of Metal Oxidation, Vol. I*, (North-Holland, Amsterdam, 1976).
   A. T. Fromhold, Jr., in *Theory of Metal Oxidation, Vol. II*, (North-Holland, Amsterdam, 1980).
5. A. Atkinson, *Review Mod. Phys.*, 1985, 57, 437.
6. C. Wagner, *Z. Phys. Chem.*, 1933, B21, 25.
7. N. Cabrera and N. F. Mott, *Rep. Prog. Phys.*, 1949, 12, 163.
8. C. J. Rosa. *J. Less-Common Metals*, 1968, 16, 173, and references are therein.
9. M. Dechamps and P. Lehr, *C. R. Acad. Sci.*, 1970, C270, 169.
10. M. Nagasaka, E. Ueda and T. Yamashina, *Vacuum*, 1973, 23, 51.
11. J. S. Foord, P. J. Goddard and R. M. Lambert, *Surf. Sci.*, 1980, 94, 339.
12. P. Sen, D. D. Sarma, R. C. Budhani, K. L. Chopra and C. N. R. Rao, *J. Phys. F*, 1984, 14, 565.
13. J. M. Sanz, C. Palacio, Y. Casas and J. M. Martinez-Duart, *Surf. Interface Anal.*, 1987, 10 ,177.
14. C. Moranz, J. M. Sanz, L. Galán, L. Soriano and F. Rueda,

Surf. Sci. 1989, 218, 331.

15. K. C. Hui, R. H. Milne, K. A. R. Mitchell, W. T. Moore and M. Y. Zhou, *Solid State Commun.*, 1985, 56, 83.
16. P. C. Wang, K. C. Hui, B. K. Zhong and K. A. R. Mitchell, *Solid State Commun.*, 1987, 62, 293.
17. R. L. Tapping, *J. Nucl. Mater.*, 1982, 107, 151.
18. K.-O. Axelsson, K. -E. Keck and B. Kasemo, *Surf. Sci.*, 1985, 164, 109.
19. G. R. Corallo, D. A. Asbury, R. E. Gilbert and G. B. Hoflund, *Phys. Rev. B*, 1987, 35, 9451.
20. C. Palacio, J. M. Sanz and J. M. Martinez-Duart, *Surf. Sci.*, 1987, 191, 385.
21. P. Aebi, M. Erbudak, A. Leonardi and F. Vanini, *J. Electron. Spectrosc. Relat. Phenom.*, 1987, 42, 351.
22. K. Giffiths, *J. Vac. Sci. Technol. A*, 1988, 6, 210.

Chapter 1

Pressure Dependence of the Rate of Oxygen Absorption by Zirconium*

Introduction

Zirconium has an extremely large chemical affinity for oxygen. The surface of metallic zirconium is unavoidably contaminated by oxygen, even at room temperature, once it has been in contact with the air. At elevated temperatures the contamination is serious even under a considerably high vacuum. A UHV apparatus is necessary for the careful treatment of metallic zirconium.

UHV apparatus has not been used in most studies on the oxidation mechanism of zirconium. The absorption of oxygen has been investigated under near-normal atmospheric pressures of oxygen.[1-4] As a consequence of the prompt formation of an oxide film over the specimen surface, the observed rate of oxygen absorption is determined by diffusion of oxygen through the oxide phase layer. However, no reliable data have been obtained in the experiments because the scab-like oxide scale is always produced under the conditions of such higher pressures.

It is impossible to obtain explicit information concerning oxygen attack on the metal phase once the surface has been covered by

---

* published in *J. Chem. Soc., Faraday Trans. 1*, 1988, 84, 4235.

the oxide layer. It is expected that the formation of the oxide phase at the surface is inhibited by lowering the oxygen pressure. Some experiments have been carried out without paying special attention to cleaning the surface of the specimen in the pressure range 10^{-1} - 10^{-4} Pa. An effective analysis has been confined to the diffusion of oxygen through the surface oxide layer.[5-7] The absorption of oxygen in the absence of the oxide phase on the metal surface has not been realized even at very low pressures. A non-trivial amount of oxygen must have remained on the surface as a result of the deficient decontamination treatment.

The purpose of the present work is to investigate the pressure dependence of oxygen absorption by metallic zirconium with a clean surface under constant pressures of 10^{-1} - 10^{-5} Pa at 1073K.

Experimental

Apparatus

The apparatus was constructed on the basis of a UHV system ensuring evacuation to 10^{-8} Pa by the use of a turbomolecular pump(0.11 m^3s^{-1}) and a titanium-getter pump. The arrangement of the apparatus is shown in Fig. 1-1.

The specimen chamber was of a cylindrical form 0.20 m in diameter and 0.12 m in length. This dimension was sufficient to prevent the occurrence of significant pressure gradient for any rapid introduction of oxygen gas into the specimen chamber. In the blank test it was confirmed that once the vacuum system had been baked-out at *ca.* 550 K over 10 h,

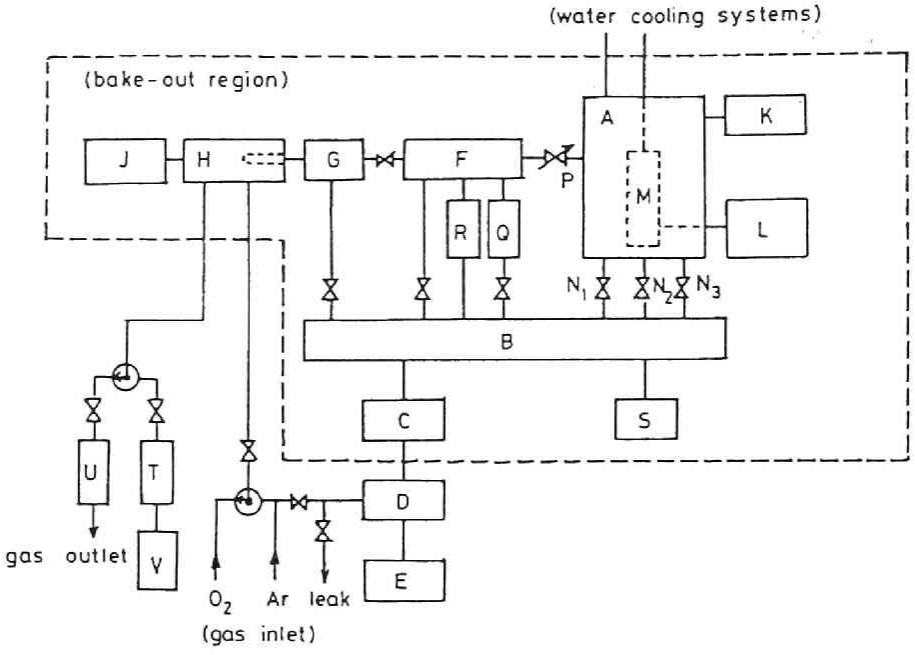

Fig. 1-1 Arrangement of the apparatus employed. A, Specimen chamber; B, vacuum chamber; C, Ti-sorption pump; D, turbomolecular pump; E, rotary pump; F, main storage tank for purified oxygen gas; G, auxiliary storage tank for purified oxygen gas; H, oxygen gas purifier; J, electric power system and control system; K, two pressure gauges (for UHV. and HV); L, electric power system and control; M, specimen holder; N_1, main valve (VAT); N_2, valve (Nupro); N_3, variable leak valve; P, automatic pressure control valve; Q, pressure gauge; R, diaphragm gauge (Baratron); S, pressure gauge (for UHV); T, trap; U, flowmeter; V, rotary pump.

the pressure in the specimen chamber did not exceed a value of 6.5×10^{-7} Pa in the situation where all valves were closed for 40 h. The pressure of oxygen in the specimen chamber was measured using a Schultz-Phelps gauge for pressures $> 10^{-2}$ Pa, and a Bayard-Alpert gauge for pressures $< 10^{-2}$ Pa.

The oxygen gas was purified by allowing it to penetrate the wall of a silver tube heated to 850K. The mass-spectroscopic analysis of the purified oxygen gas gave peak heights of 1.5×10^{-4} for H, 1.0×10^{-4} for H_2 and 6.6×10^{-3} for CO_2 relative to the peak height for O_2. The purified oxygen gas was stored in the main and auxiliary

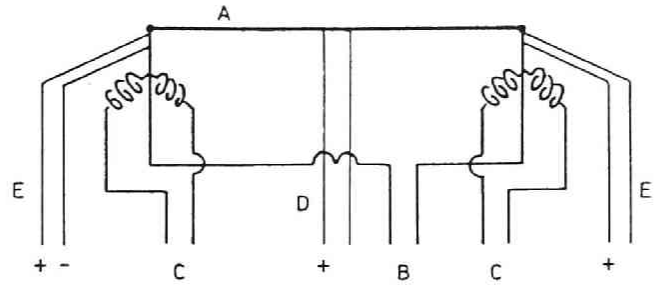

Fig. 1-2 Arrangement of the specimen. A, Zirconium specimen (0.25 mm in diameter, 60 mm in length); B, Pt wires (0.30 mm in diameter) for the circuit; C, supplementary heaters (Pt 0.30 mm in diameter); D, thermocouple (Pt–PtRh13% 0.025 mm in diameter); E, thermocouples (Pt–PtRh13% 0.030 mm in diameter).

storage tanks, each of whose volumes was known exactly: 52.0 cm^3 for the storage tank and 48.8 cm^3 for the auxiliary storage tank.

The circuits for heating the specimen and the arrangement of the supplementary heating system and thermocouples are shown in Fig. 1-2. The specimen of metallic zirconium wire of 0.25 mm diameter and 60 mm length was connected with platinum wires 0.30mm in diameter by welding at both ends, and was heated by passing an electric current of 60Hz through the circuit. The unavoidable temperature drop which occurred near each end of the specimen was compensated by supplying heat from a supplementary platinum heater, through which a d.c. current controlled automatically was passed. A Pt-PtRh13% thermocouple 0.025mm in diameter was welded to the specimen at the centre, and the temperature of the specimen was monitored with the aid of this thermocouple. The two other thermocouples, each of diameter 0.030mm, were welded to the specimen at both ends. Uniformity in temperature over the specimen was maintained with these three thermocouples.

The constancy and uniformity of temperature of the specimen were satisfactorily maintained by controlling strictly the electric power supply with the help of automatic thermoregulators connected to

the thermocouples. On heating the specimen, the electric resistance, power and other necessary quantities were determined from the experimental data with the help of an on-line computer. The data obtained were recorded continuously. The disturbance caused by the reaction heat produced was considered negligible because the reaction took place under a low oxygen pressure in every case. The electric power required to keep the temperature constant was equal to the rate of the energy lost by the thermal radiation from the whole surface, on the assumption that the energy lost by other means, *e.g.* thermal conductance, *etc.* was negligible in comparison with the thermal radiation energy. The change in the electric power was equivalent to the change in the effective emissivity of the specimen. The electric power supplied was determined from the data for the current and the corresponding resistivity.

Specimen

Metallic zirconium of MARZ-grade (99.99 % Zr) guaranteed by MRC (Materials Research Corporation) was used. A wire 0.25 mm in diameter and 10 cm in length was mechanically polished, and was degreased in acetone by ultrasonic treatment. Both the ends of the wire were cut off to give a specimen of length 6.0 cm. According to the list of impurities indicated by MRC the content of oxygen in zirconium is *ca.* 11 ppm, which is the maximum impurity listed. In reality, much more oxygen was probably introduced into our specimen, because the equilibrium pressure of zirconium oxide with oxygen is 10^{-174} Pa at 300 K. It is impossible to remove oxygen from the specimen merely by means of evacuation once oxygen has been absorbed by zirconium.

The equilibrium pressure is 10^{-42} Pa, even at 1000 K. Such a low pressure cannot be attained by the use of a vacuum pump at present.

Preparation of a Clean Surface

When the purity of the metallic zirconium used is very high, the oxygen contamination may be regarded as being confined within a small region near the surface of the specimen, because the diffusion rate of oxygen is trivial at room temperature. This means that the average concentration of oxygen over the whole specimen is still very small. In such a situation it is expected that a clean surface can be prepared by annealing the specimen under UHV at a high temperature.[8] When the temperature is elevated, the diffusion constant increases by an inverse factor of the exponential function of inverse temperature. Thus the flux of oxygen into the bulk will increase rapidly with increasing temperature. The surface concentration of oxygen will diminish when the flux from the gas phase onto the surface is restricted within a very small magnitude by keeping the pressure low. The diffusion will cease when the concentration gradient vanishes, and then a clean surface will have to be prepared.

After the specimen was placed in the specimen chamber, the vacuum system was baked-out at 523 K for 10 h. The specimen was then annealed under 10^{-8} Pa for 24 h at 1100 K. In the annealing treatment the effective emissivity, which is a measure of the degree of surface coverage by oxygen, decreased with time to a constant final value, regarded as the establishment of surface decontamination. From Auger electron spectroscopy it was confirmed that the surface impurities had

been almost fully removed by this treatment.[8]

Operation

After surface decontamination, the specimen was rapidly cooled by switching off the electric current, and purified oxygen gas was introduced into the storage tanks. The pressure in the tank was measured with a diaphragm gauge and with a pressure gauge capable of measuring pressures of 10^{-1} - 10^{2} Pa and 10^{1} - 10^{4} Pa, respectively.

The main valve was closed during each oxygen absorption reaction. A small amount of the oxygen in the specimen chamber was leaked at a constant rate through the leak valves, and a balancing amount of oxygen was introduced into the specimen chamber to hold the pressure constant. Thus a steady state was attained with respect to oxygen, even after the specimen started to absorb oxygen. The accumulation of impurities, such as H_2, CO, CO_2 *etc.*, which would steadily emerge from the wall of the specimen chamber during the experiment, was avoided by this procedure. The amount of oxygen introduced into the chamber was calculated from the decrease in oxygen pressure in the storage tank. The flow rate of the outlet oxygen gas was regulated so as to be held at *ca.* one tenth of the rate of absorption of oxygen to be lost.

After the preliminary test, the inlet valve was closed and the main valve was opened. The specimen chamber was evacuated to *ca.* 10^{-8} Pa. The specimen was heated at a given temperature by an electric current. Measurements were started at the same time as the oxygen gas was introduced into the chamber to establish the conditions

of fixed pressure.

Results

The amount of oxygen absorbed by the specimen, its electric resistivity and the effective emissivity of its surface were measured as functions of time under constant pressures of oxygen of 1.33×10^{-1}, 1.46×10^{-2}, 1.46×10^{-3}, 1.46×10^{-4} and 1.46×10^{-5} Pa. The experimental results are shown in Fig. 1-3 and Fig. 1-4. Table 1-1 gives the results of an X-ray diffraction analysis of the products of oxygen absorption.

The apparent surface area of the specimen was calculated from the values of its length and weight. The area did not remain unchanged during the experiment, which was accompanied by thermal expansion, the incorporation of oxygen to form α-zirconium and the formation of the oxide phase. According to calculations, the change amounts to $<$ 5.0%, which is less than the uncertainty inherent in the volumetric measurement method used in this investigation.[9]

Under the condition of 1.33×10^{-1} Pa, the amount of oxygen absorbed by zirconium was nearly proportional to the square root of time. This suggests that the rate of the absorption of oxygen by zirconium is determined by diffusion of oxygen through the surface oxide layer, whose thickness increases with the progress of the reaction. A slight deviation from the linear relation is obtained in the initial period of 0 - 600 s (termed the first stage) and may be attributed to a surface process, as confirmed by the trend in the corresponding effective emissivity.

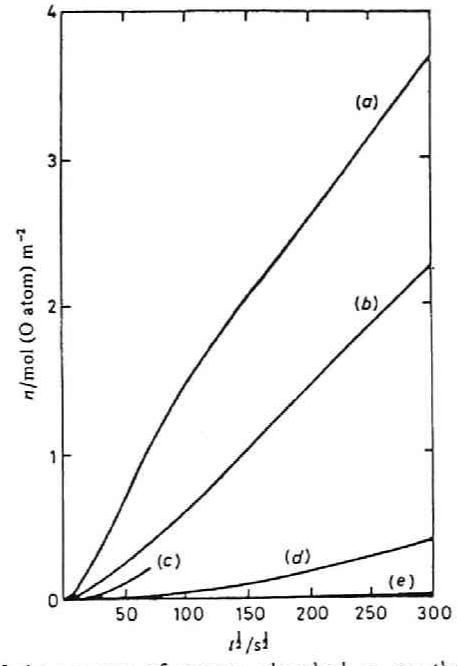

Fig. 1-3 Dependence of the amount of oxygen absorbed, n, on the square root of time, t, under constant pressures of oxygen at 1073 K. (a) 1.33×10^{-1}, (*b*) 1.46×10^{-2}, (*c*) 1.46×10^{-3}, (*d*) 1.46×10^{-4} and (*e*) 1.46×10^{-5} Pa.

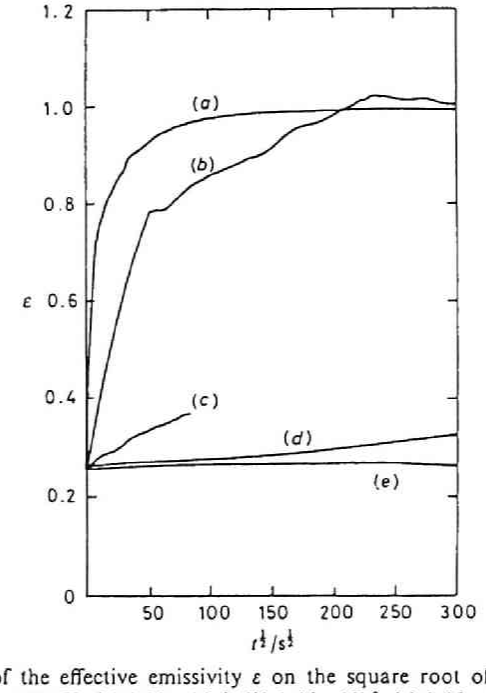

Fig. 1-4 Dependence of the effective emissivity ε on the square root of time t under constant pressures of oxygen at 1073 K. (*a*) 1.33×10^{-1}, (*b*) 1.46×10^{-2}, (*c*) 1.46×10^{-3}, (*d*) 1.46×10^{-4} and (*e*) 1.46×10^{-5} Pa.

Table 1-1 X-Ray diffraction analysis of the specimen following oxygen absorption at 1073 K

oxygen gas		composition	
pressure /Pa	time/h	surface[a]	powdered bulk specimen
1.33×10^{-1}	27	ZrO_2	$ZrO_2 + \alpha$-Zr
1.46×10^{-2}	44	ZrO_2	$ZrO_2 + \alpha$-Zr
1.46×10^{-3}	24	ZrO_2	$ZrO_2 + \alpha$-Zr
1.46×10^{-4}	24	α-Zr	α-Zr
1.46×10^{-5}	24	α-Zr	α-Zr

[a] The data may be regarded as the contribution from within *ca.* 1.7×10^{-5} m of the surface, according to our crude estimation.

The effective emissivity under these conditions rises rapidly immediately the oxygen absorption starts. The gradient of the curve becomes smaller with time, and almost vanishes within *ca.* 6.0×10^3 s. The large initial gradient suggests the rapid formation of the oxide film over the surface. However, the film would still be thin at the end of the first stage, and would be stabilized by the successive supply of oxygen over a period of 50 - 4000 s in which the effective emissivity changes greatly in gradient (the second stage). In the third stage, represented by the period > 4000 s, the effective emissivity increases gradually. Such a change would be associated with an increase in the thickness of the oxide layer through which the diffusion of oxygen takes place.

The surface of a specimen which has undergone this treatment is covered completely with a dark layer which sticks firmly to the metallic zirconium substrate. No pattern other than that of zirconium oxide was given in the X-ray diffraction spectrum for the surface. However, metallic zirconium and zirconium dioxide was shown in the X-ray diffraction pattern for the whole specimen ground into a powder, as

shown in Table 1-1. The lattice spacing of metallic zirconium observed was greater than the normal lattice spacing of α-zirconium. This suggests the formation of a solid solution of oxygen in zirconium.

At 1.46×10^{-2} Pa the amount of the oxygen absorbed also showed a nearly linear relationship to the square root of time, except in an initial period of *ca.* 6.0×10^{3} s. The gradient of the effective emissivity curve in the initial period was considerably smaller than that in the corresponding stage for the higher pressure. A decrease in the oxygen pressure led to a marked delay in the formation of the oxide film. The effective emissivity exhibited a slow fluctuation in the second stage, unlike the higher pressure case. Such a tendency may be regarded as evidence of inhomogeneous growth of the oxide phase at the surface. The results of an X-ray analysis of the surface product and of the whole product are almost the same as the respective results obtained in the higher pressure case.

At 1.46×10^{-3} Pa the relationship between the amount of oxygen absorbed and the square root of time deviates from linearity relation (see Fig. 1-5). It became difficult to hold the temperature uniform over the entire surface as oxygen absorption increased and the experiment was interrupted in a short time. Such a situation may be attributed to the increasing inhomogeneity of the surface as a result of the localized formation of the oxide phase on the metallic phase, as supported by the trend in the corresponding effective emissivity curve. The effective emissivity is nearly proportional to the square root of time. The sticking probability of oxygen was taken as *ca.* 0.35 on the basis of the experimental curve. The result of the X-ray analysis of a specimen exposed to a long period of oxidation

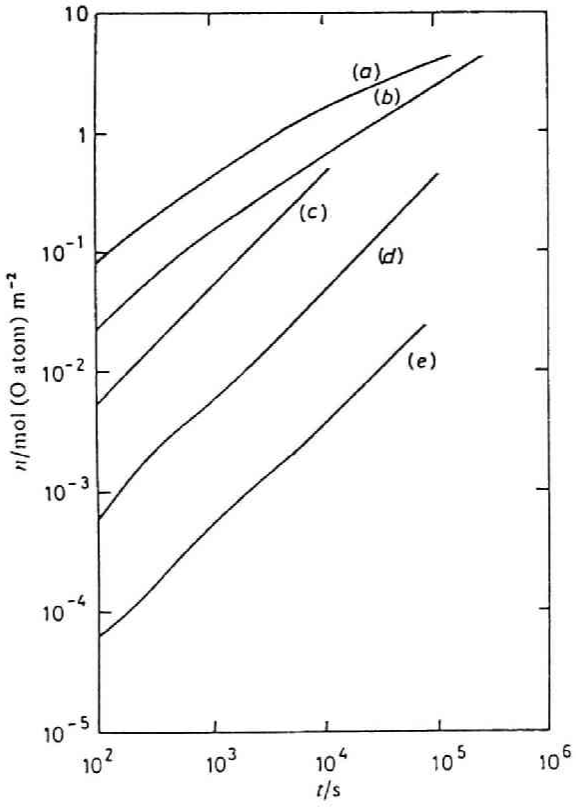

Fig. 1-5 Relationship between the amount of oxygen, n, and time, t, at 1073 K. The data were replotted from the diagram of Fig. 1-1. (*a*) 1.33×10^{-1}, (*b*) 1.46×10^{-2}, (*c*) 1.46×10^{-4}, (*d*) 1.46×10^{-4} and (*e*) 1.46×10^{-5} Pa.

was identical to the results obtained for higher pressures.

At 1.46×10^{-4} Pa the rate of oxygen absorption remained almost unchanged from the start to the end of the run, *i.e.* a linear relation was valid between the amount absorbed by the specimen and time, as shown in Fig. 1-5. The sticking probability was obtained as 0.35 from the experimental curve. The gradient of the effective emissivity curve was *ca.* one twentieth of that at each corresponding stage for 1.46×10^{-3} Pa. No pattern other than that of α-zirconium was found in the X-ray diffraction analysis for the specimens prepared as mentioned previously. There was

also no evidence for the conversion of metallic zirconium into the oxide. However, X-ray diffraction analysis showed that the phase of metallic zirconium remaining at the surface would be in the state of a solid solution of oxygen. The intensity of the (101) diffraction line was less than that of (200), in contrast to the normal case of metallic zirconium.

At 1.46×10^{-5} Pa the total absorption of oxygen was very slight even after a very long time. The amount absorbed is in proportion to time throughout the progress of the reaction, like the case at 1.46×10^{-4} Pa, as shown in Fig. 1-5. The sticking probability was 0.30: the decrease in sticking probability was caused by the increasing relative contribution of the impurities. As mentioned, a satisfactorily clean surface has been prepared in this experiment. Nevertheless, it is impossible to avoid the slight impurities which will emerge from the chamber wall under very low pressures. No oxide pattern was found in the X-ray diffraction analysis of the surface material and for the whole specimen after the run. The changes in electric resistivity and in effective emissivity were both very slight. In each case there was no evidence for the conversion of metallic zirconium into the oxide.

Discussion

In the case of no formation of the oxide phase, as realized under the condition of oxygen pressures $< 10^{-3}$ Pa, the surface reaction process, which determines the boundary condition of the diffusion in the bulk, may be represented by

$$\tfrac{1}{2}O_2(\text{gas}) \underset{r}{\rightarrow} O(\text{ads}) \rightleftarrows O(\text{in Zr}) \tag{1-1}$$

with

$$v = k_1 p \tag{1-2}$$

because the amount of oxygen absorbed by zirconium is in proportion to the oxygen pressure. Here p is the pressure of oxygen gas, v is the rate of oxygen adsorption and k_1 is the rate constant. Even under oxygen pressures $\geq 10^{-2}$ Pa the formation of the oxide film at the specimen surface was not complete in the initial period. For this initial period under 10^{-2} and 10^{-1} Pa the experimental results suggested

$$\tfrac{1}{2}O_2(\text{gas}) \rightleftharpoons O(\text{ads}) \underset{v}{\rightarrow} O(\text{in Zr}) \tag{1-3}$$

with

$$\left.\begin{aligned} [O(\text{ads})] &= k_2 p^{\frac{1}{2}} \\ v &= k_3[O(\text{ads})] = k_2 k_3 p^{\frac{1}{2}} \end{aligned}\right\} \tag{1-4}$$

where the k are the rate constants. Here the mechanism has been considered in the situation of no oxide formation.

Once the surface film of the oxide phase has been completed, the surface process must be written as

$$\tfrac{1}{2}O_2(\text{gas}) \rightleftharpoons O(\text{ads})(\text{on oxide}) \underset{v_{ox}}{\rightarrow} O\text{—}Zr(\text{in oxide}). \tag{1-5}$$

We have the relations

$$\left.\begin{aligned}[\mathrm{O(ads)}] &= k_4 p^{\frac{1}{2}} \\ v_{ox} &= k_5[\mathrm{O}](c_e - c_s) = k_4 k_5 p^{\frac{1}{2}}(c_e - c_s)\end{aligned}\right\} \tag{1-6}$$

where c_e denotes the upper limit of concentration of empty sites accessible for occupation by oxygen at the surface, and c_s is the oxygen concentration at the surface. Throughout the present paper the concentration is given by the O/Zr in atomic ratio.

For the diffusion of oxygen into the solid, the boundary-value problem should distinguish between the case where no oxide phase is formed at the surface [Fig. 1-6(b)] and the case where the growing oxide layer whose thickness is $x(t)$ is formed on the surface [Fig. 1-6(a)]. In the former case we have the differential equation

$$\frac{\partial c}{\partial t} = \frac{1}{r}\frac{\partial}{\partial r}\left(rD\frac{\partial c}{\partial r}\right) \tag{1-7}$$

specified by the boundary conditions

$$\left(\frac{\partial c}{\partial r}\right)_{r=0} = 0; \quad D\left(\frac{\partial c}{\partial r}\right)_{r=a} = v \tag{1-8}$$

and by the initial condition

$$c = 0 \quad \text{for} \quad t = 0 \tag{1-9}$$

where D is the diffusion constant of oxygen thought α-zirconium, and a is the radius of the cylindrical specimen. For our numerical computation we use $D = 2.79 \times 10^{-14}\ \mathrm{m^2 s^{-1}}$ recommended in ref.[1] and [10]. In the latter case we construct the differential equations

$$\frac{\partial c}{\partial t} = \frac{1}{r}\frac{\partial}{\partial r}\left(rD\frac{\partial c}{\partial r}\right) \quad \text{for} \quad r = [0, x(t)] \tag{1-10}$$

$$\frac{\partial c}{\partial t} = \frac{1}{r}\frac{\partial}{\partial r}\left(rD_{ox}\frac{\partial c}{\partial r}\right) \quad \text{for} \quad r = [x(t), a] \tag{1-11}$$

specified by the boundary conditions

$$\left.\begin{aligned} \left(\frac{\partial c}{\partial r}\right)_{r=0} = 0; \quad D_{ox}\left(\frac{\partial c}{\partial r}\right)_{r=a} = v \\ \frac{\partial x}{\partial t} = \frac{1}{c_o - c_m}\left[D\left(\frac{\partial c}{\partial r}\right)_{r=x-0} - D_{ox}\left(\frac{\partial c}{\partial r}\right)_{r=x+0}\right] \end{aligned}\right\} \tag{1-12}$$

and by the initial condition

$$c = 0 \quad \text{for} \quad t = 0 \tag{1-13}$$

where D_{ox} is the diffusion constant of oxygen through the

zirconium oxide phase. A value of $D_{ox} = 1.55 \times 10^{-13}$ $m^2 s^{-1}$ has been recommended.[1] c_m and c_o represent the oxygen concentration in a solid solution of oxygen in α-zirconium in the state of the maximum solubility and the minimum concentration of oxygen in zirconium oxide phase, respectively. These concentrations can be estimated from the phase diagram of the oxygen-zirconium system.[1,11-14] We obtained $c_m = 0.41$ and $c_o = 1.95$. The regions of $[0, x(t)]$ and $[x(t), a]$ represent the phase of the solid solution of oxygen in zirconium and the oxide phase, respectively, as shown in Fig. 1-6(a).

By means of the finite difference method we numerically solved the boundary value problems specified above, and compare the results of the numerical calculation with the corresponding experimental results in Fig. 1-7. We obtained good agreement in each case, except for slight deviations occurring for the formation of the oxide layer.

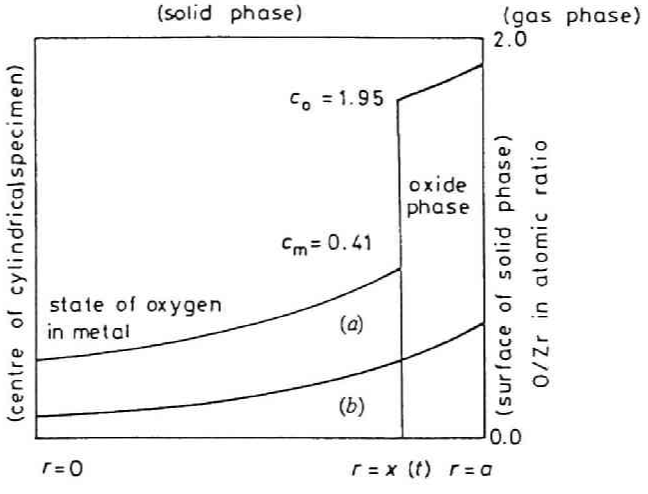

Fig. 1-6 Profile of the concentration distribution in the solid phase in the presence (*a*) and absence (*b*) of the oxide layer.

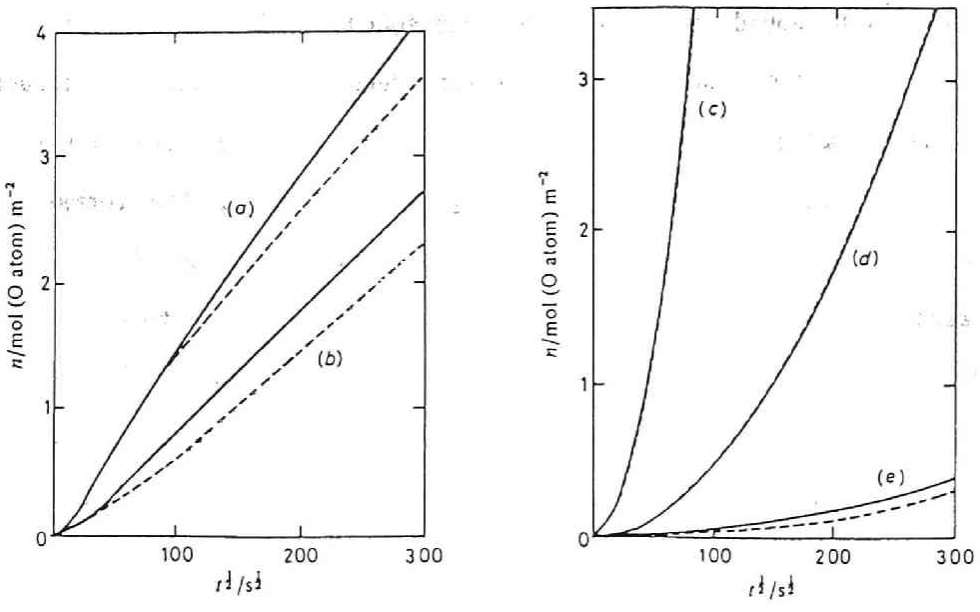

Fig. 1–7 Comparison of calculated (—) and experimental (---) results for the relationship between the amount of oxygen absorbed, n, and the square root of time, t. (*a*) 1.33×10^{-1}, (*b*) 1.46×10^{-2}, (*c*) 1.46×10^{-3}, (*d*) 1.46×10^{-4} and (*e*) 1.46×10^{-5} Pa.

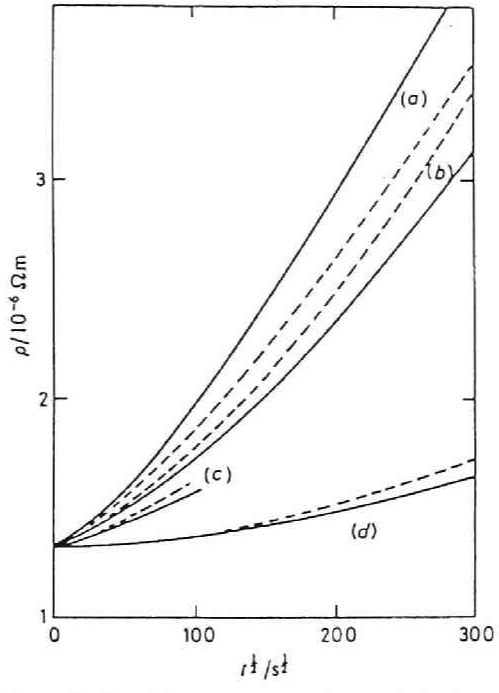

Fig. 1–8 Comparison of the calculated (—) and experimental (---) results for the relationship between the electric resistivity, ρ, and the square root of time, t. (*a*) 1.33×10^{-1}, (*b*) 1.46×10^{-2}, (*c*) 1.46×10^{-4} and (*d*) 1.46×10^{-5} Pa.

The deviation would be a natural consequence of the simplifications employed in the calculation: temperature, composition, structure *etc.* have always been assumed to be homogeneous over the surface even in the (probably) inhomogeneous state of the formation of the oxide phase, and the value of the diffusion constant for oxygen in the zirconium oxide phase has been assumed to be equal to that in the perfect zirconium oxide phase. The deviation for 1.46×10^{-2} Pa was greater than that for 1.33×10^{-1} Pa: in the initial stage the state of the oxide layer in the former case is less complete than that in the latter case, as stated previously.

From the numerical computation we obtained appropriate values $c_e = 2.00$ and $c_e = 1.97$ for the experimental curves for 1.33×10^{-1} Pa and 1.46×10^{-2} Pa, respectively. The time necessary for the completion of the oxide film over the surface was estimated for each pressure of oxygen by calculation. We obtained 10 s for 1.33×10^{-1} Pa and 240 s for 1.46×10^{-2} Pa. For a pressure of 1.46×10^{-3} Pa we obtained the value of 1.08×10^{4} s, which is two orders of magnitude higher than the latter value indicated above. Under a pressure of 1.46×10^{-4} Pa the oxide film does not seem to be formed at the surface, since we obtained a small value for the surface oxygen concentration, *i.e.* 0.14 O/Zr over 8.64×10^{4} s, by computation. The value is sufficiently small in comparison with 0.40 O/Zr, which represents the boundary between Zr and $Zr\text{-}ZrO_2$ in the phase diagram. At a pressure of 1.46×10^{-5} Pa we obtained a far smaller surface oxygen concentration, 0.01 O/Zr, for the same time as above. These results obtained by calculation support the experimental conclusion that there is no evidence for formation of

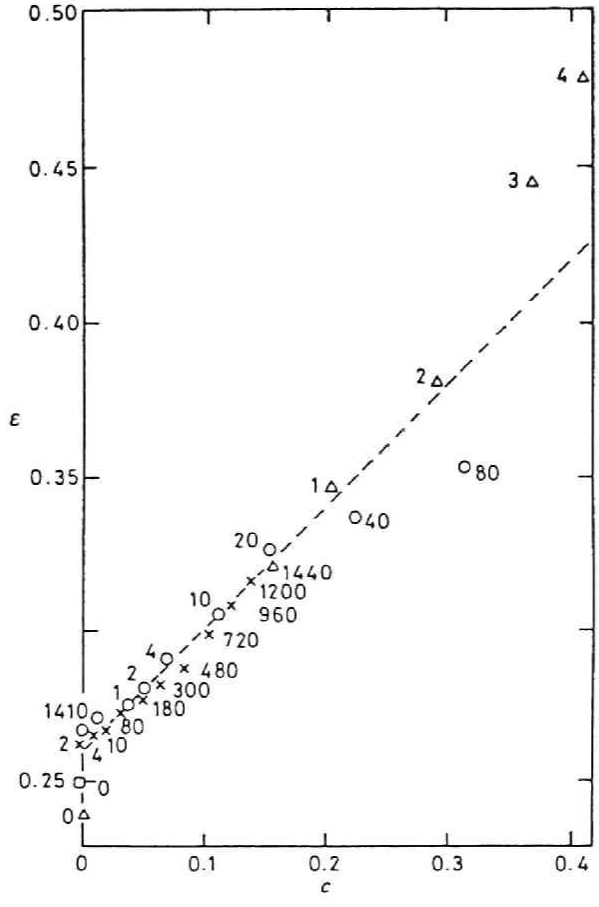

Fig. 1-9 Relationship between the effective emissivity, ε, and the surface concentration of oxygen, c. The situation in which oxide film was not formed on the surface was chosen. The figure indicated at each point is the duration t (in s) of the absorption of oxygen. △, 1.33×10^{-2}; ○, 1.46×10^{-3}; ×, 1.46×10^{-4}; □, 1.46×10^{-5} Pa.

the oxide film under the pressures $< 10^{-3}$ Pa. The above conclusion is also consistent with the results for the effective emissivity and from X-ray diffraction analysis.

The relationship between the electric resistivity and the oxygen concentration for α-zirconium at 1073K has been reported by Giam and Claisse.[15] By the use of this relation we calculated the electric resistivity of the specimen as a function of the oxygen concentration distribution determined from the above

computations. In the calculation of the electric resistivity of the specimen, the contribution of the oxide phase may be excluded if the metal phase has been converted into the oxide phase. The electric resistivity for the oxide phase, given as 10^2 Ω·m at 1073K, is greater by a factor of 10^8 than that for the metal phase. A comparison of the calculated result with the experimental result for the electric resistivity is indicated in Fig. 1-8, with good agreement for each pressure.

We obtained a linear relation by plotting the value of the effective emissivity observed in the experiment against the surface concentration determined by numerical calculation, as described in Fig. 1-9. The effective emissivity deviated upwards from linear as soon as the surface concentration of oxygen exceeded 0.35 O/Zr, and reached *ca.* 0.50 at 0.40 O/Zr. The concentration at which the change in the effective emissivity began to occur was equal to the boundary between the α-zirconium phase and the α-zirconium - zirconium oxide coexisting phase.[16] The transition in the effective emissivity from the straight-line value to 0.50 is attained by a gradual change rather than by an abrupt jump. The intermediate state specified by the concentration range 0.35-0.40 O/Zr, which corresponds to the transition, may be attributed to the occurrence of nucleation and growth of the oxide phase.

Conclusion

The rate of oxygen absorption by metallic zirconium with a clean surface at 1073K has been measured as a function of time by a volumetric

method in UHV apparatus under constant pressures of oxygen in the range of 10^{-1} Pa - 10^{-5} Pa. The electric resistivity, which is a measure of the oxygen concentration, and the effective emissivity, which is a measure of the degree of the surface coverage by oxygen, are observed in parallel with the rate of oxygen absorption of the specimen. Besides being determined experimentally, the absorption rate and the electric resistivity are evaluated by numerical calculation on the basis of an appropriate model constructed for the absorption process. Good agreement is obtained between the calculated and experimental results. At 1073K there is no evidence for formation of the oxide phase at the surface under pressures not higher than 10^{-4} Pa, whereas the oxide layer is formed promptly under pressures not lower than 10^{-1} Pa. The intermediate region between these two pressures represents the presence of a transient state, which would be characterized by the occurrence of the nucleation and growth of the oxide phase at the surface.

References for Chapter 1

1. C. J. Rosa, *J. Less-Common Met.*, 1968, 16, 173.
2. K. A. Sense, *J. Electrochem. Soc.*, 1969 , 109, 377.
3. R. J. Hussey and W. W. Smeltzer,
   J. Electrochem. Soc., 1964, 111, 564.
4. H. A. Porte, J. G. Schnizlein, R. C. Vogel and D. F. Fischer,
   J. Electrochem. Soc., 1975, 107, 1086.
5. J. Leviton, J. J. E. Draley and C. J. van Drunen,
   J. Electrochem. Soc., 1967, 114, 1086.
6. M. Dechamps and P. Lehr, *C. R. Acad. Sci., Ser. C,*

1970, 290, 169.

7. M. Nagasawa, E. Ueda and T. Yamashita, *Vacuum*, 1973, 23, 51.

8. G. B. Hoflund, D. F. Cox and R. E. Gilbert, *J. Vac. Sci. Technol. A*, 1983, 1, 1837.

9. D. A. King, in *Chemistry and Physics of Solid State Surface II*, ed. by R. Vanselow, (C.R.C., Press, Boca Raton FLA, 1979), pp.87-128.

10. I. G. Ritchi and A. Atrens, *J. Nucl. Mater.*, 1977, 67, 254.

11. H. Hahn and P. Ness, *Z. Anorg. Allg. Chem.*, 1959, 302, 37.

12. H. Hahn and P. Ness, *Z. Anorg. Allg. Chem.*, 1959, 302, 136.

13. H. Hahn and P. Ness, *Naturewissenschaften*, 1967, 54, 42.

14. W. B. Blumenthal, *The Chemical Behaviour of Zirconium*, (van Nostrand, London, 1958), pp.151-200.

15. T. M. Giam and F. Claisse, *J. Nucl. Mater.*, 1970, 34, 169.

16. P. Paetz and F. Sperner, in *Gase und Kohlenstoff in Metallen*, ed. by E. Fromm and E. Gebhardt, (Springer, Berlin, 1976), p.428

Chapter 2

Kinetics of Oxygen Absorption by α-Zirconium*

Introduction

Oxidation of zirconium has been experimentally studied over wide ranges of temperature and pressure by a number of authors.[1-35] Some of them[1-10] have observed a parabolic relation in the absorption of oxygen by zirconium at high oxygen pressures (10^{5} - 10^{-1} Pa, $T \geq 673$K)[1-7] and at low oxygen pressures (10^{-1} - 10^{-4} Pa) and low temperatures (*e.g.* < 873 K at 10^{-2} Pa).[9-10] The parabolic relation suggests that the absorption rate is limited by the diffusion of oxygen into zirconium, the surface of which is covered with an oxide film immediately after zirconium is exposed to oxygen.[36-37] The measurements under these conditions therefore cannot give any knowledge of processes in the early stage of oxidation. From measurements at low oxygen pressures and high temperatures (*e.g.* ≤ 10^{-2} Pa at 973 K) a few investigators[9-10] have obtained a linear relation, which suggests that the absorption rate is limited by surface reactions. Their experimental results, however, are inconsistent as to the temperature dependence of the absorption rate, and the sticking probabilities which

---

* Published in *J. Phys. Chem.*, 1989, 93, 5203.

they observed are about an order of magnitude smaller than that reported for the specimens with clean surfaces[15]. This may be because specimens prepared under UHV conditions were not used. In addition, the measurements[9-10] lack spectroscopic evidence for the absence of oxide films at the surface, which is crucial to interpret the experimental results.

It is well-known that metal oxidation occurs through the processes of dissociative adsorption of oxygen molecules, nucleation of oxide and growth of the oxide for many metals. Only the growth of oxide, however, has been discussed in the theory of metal oxidation, *e.g.* Wagner theory and Cabrera-Mott theory[36], in which the transport of oxygen through the oxide film is assumed to limit the rate. Detailed theoretical investigations of the absorption rate which is limited by the surface reactions (*e.g.* dissociative adsorption) have not been reported.

Surface spectroscopic studies (*e.g.* AES, XPS, UPS, LEED, ISS, EELS and ESD) have been recently reported for the static properties of adsorption of oxygen on zirconium at room temperature.[11-14,16-35] However, the dynamic properties of oxygen absorption at high temperatures under constant oxygen pressures, which are affected by processes both in the bulk and at the surface, have not been discussed in detail in these studies.

The purpose of this work is to investigate the rate of oxygen absorption under conditions where no oxide film is formed at the surface. We measure the absorption rate at low oxygen pressures and high temperatures using specimens prepared under UHV conditions. No transition of the metal phase to the oxide phase is found at the surface

by SIMS. Thus, under these experimental conditions we can measure the absorption rate that is directly related to the adsorption processes at the surface.

Rate theory is applied to describe the absorption rate experimentally obtained. We assume that the absorption process is comprised of three successive steps:[38] the dissociative adsorption of oxygen molecules on the zirconium surface, the transfer of adatoms at the surface sites to the outermost bulk sites and the diffusion of oxygen atoms into the bulk. A simple Langmuir model for adsorption and transfer is modified to explain the experimental results by incorporating an interaction between adatoms. It is known that this interaction makes an important contribution to the formation of ordered structures of oxygen adatoms on the surface.[39-40] We use the quasi-chemical approximation to introduce the interaction and to describe the contribution from the short-range configuration of adatoms. Diffusion is assumed to obey Fick's law. By coupling the equations of diffusion, transfer and adsorption, we numerically calculate the absorption rate. The calculated results are compared with the experimental results, and the parameters in these equations are determined.

Experimental

The change in the amount of absorbed oxygen with time (absorption curve) was measured volumetrically with a stainless steel UHV apparatus, which has a base pressure of 2.0×10^{-8} Pa. Fig. 2-1 schematically shows the apparatus. The pressure in a specimen chamber was measured with a Bayard-Alpert gauge, which had been calibrated by

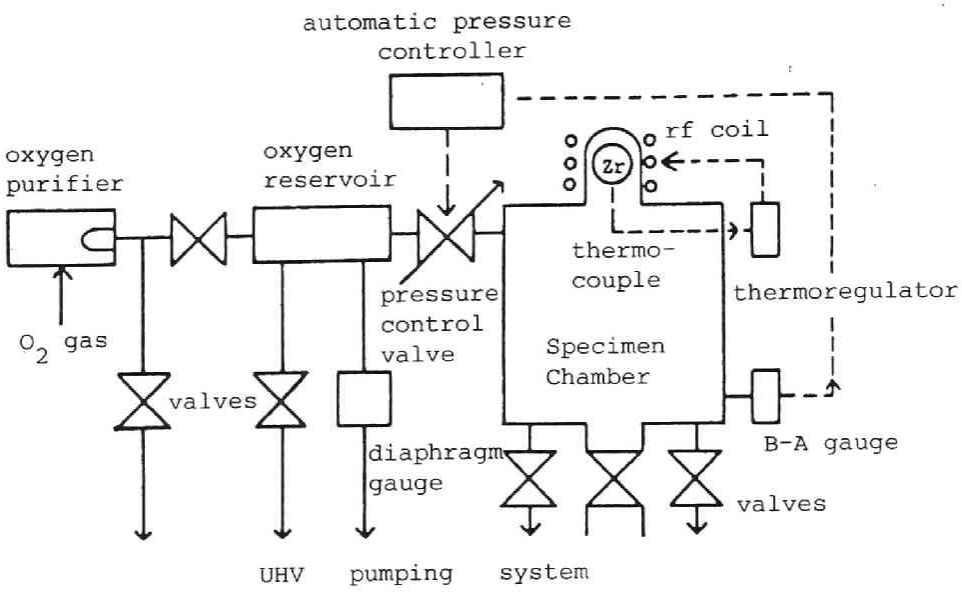

Fig.2-1. Schematic diagram of the apparatus for measuring the rate of oxygen absorption by zirconium.

using the sensitivity factor 0.9 for oxygen relative to nitrogen; the pressure in an oxygen reservoir was measured with a diaphragm gauge capable of measuring pressures between 10^{-1} and 10^{2} Pa. With valves between the specimen chamber and vacuum pumps closed and the specimen heated, the pressure in the specimen chamber could be kept below 7×10^{-7} Pa for a time long enough for one measurement to be completed. The specimen was heated inductively, and its temperature was measured with a Pt-PtRh13% thermocouple spot-welded to the specimen and controlled using a thermoregulator. The temperature fluctuation was kept within ± 1 K.

The specimen was of the form of a sphere (about 5.0 mm in diameter) machined from a polycrystalline zirconium bar of purity 99.8%. The machined specimen was mechanically polished, ultrasonically degreased in acetone and then heated in the specimen chamber to about

1070 K for 24 - 36 h at a pressure less than 10^{-7} Pa. In order to examine the effect of this heat treatment on the composition at the surface of the specimen and to ensure the absence of a surface oxide film during the absorption measurement, we duplicated the absorption experiment including the heat treatment in another vacuum chamber equipped with SIMS. SIMS measurements were made under the same conditions as those used in determining the absorption rates.

Oxygen gas was purified by permeation through a silver tube heated to 873 K and was then stored in the oxygen reservoir.

The measurement procedure was as follows. The specimen supported by a platinum wire was heated to a given temperature. The oxygen gas stored in the reservoir was then introduced into the specimen chamber. During the measurement the pressure in the specimen chamber was kept constant by means of an automatic pressure controller. The amount of oxygen supplied through the pressure control valve was recorded as a function of time. For the purpose of preventing impurities from accumulating in the specimen chamber, the two valves between the specimen chamber and the vacuum pumps were kept slightly open and a small amount of oxygen gas was leaked out at a constant rate. The leak rate was determined by the amount of oxygen supplied under the condition that the zirconium specimen was not placed in the chamber. The amount of oxygen absorbed by the specimen was determined by subtracting the amount of oxygen leaked from that supplied.

Results

Absorption curves were measured at constant pressures of 6.7 ×

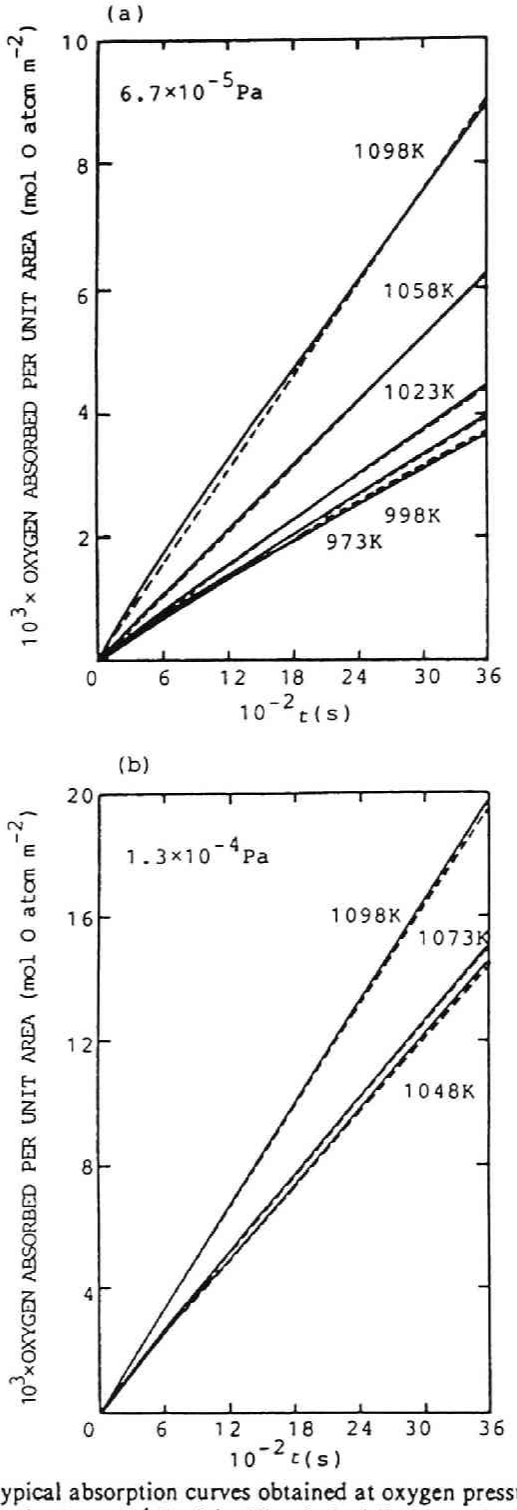

Fig.2-2. Typical absorption curves obtained at oxygen pressures of 6.7 $\times 10^{-5}$ (a) and 1.3 $\times 10^{-4}$ Pa (b). The dashed lines are the absorption curves computed by using the "best-fit" parameters.

10^{-5} and 1.3×10^{-4} Pa over the temperature range 973 - 1098 K. Reproducible data were obtained for different specimens, and the uncertainty of the experimental results is less than 10 %. Parts a and b of the Fig. 2-2 show the typical absorption curves obtained at oxygen pressures of 6.7×10^{-5} and 1.3×10^{-4} Pa, respectively.

The absorption curves show three characteristics. Firstly, the absorption rate is nearly constant with respect to time. This agrees with the results of measurements made at low pressures.[9-10] Secondly, the absorption rate decreases with a decrease in temperature. Nagasaka *et al.*,[10] however, have reported that it is independent of temperature over the range 973 - 1123 K at pressures between 5.3×10^{-2} and 5.3×10^{-4} Pa. This difference may be caused by the fact that their specimen was not prepared under UHV conditions. Thirdly, the absorption rate is almost directly proportional to the oxygen pressure. This suggests that the adsorption rate of oxygen onto the zirconium surface has an effect on the absorption rate.[41]

The SIMS measurements show that the heat treatment considerably decreases surface contaminant concentrations including that of oxygen, water, carbon monoxide, carbon and nitrogen. As shown in Fig. 2-3, the concentrations of these species at the surface were found to be comparable to their bulk concentrations after annealing. This result is in agreement with that obtained from AES measurements.[18]

Recently, Hoflund and co-workers found a low rate of oxygen adsorption at room temperature for specimens annealed above the h.c.p. - b.c.c. phase transition temperature of 1135 K in comparison with specimens annealed below the transition temperature.[21] They

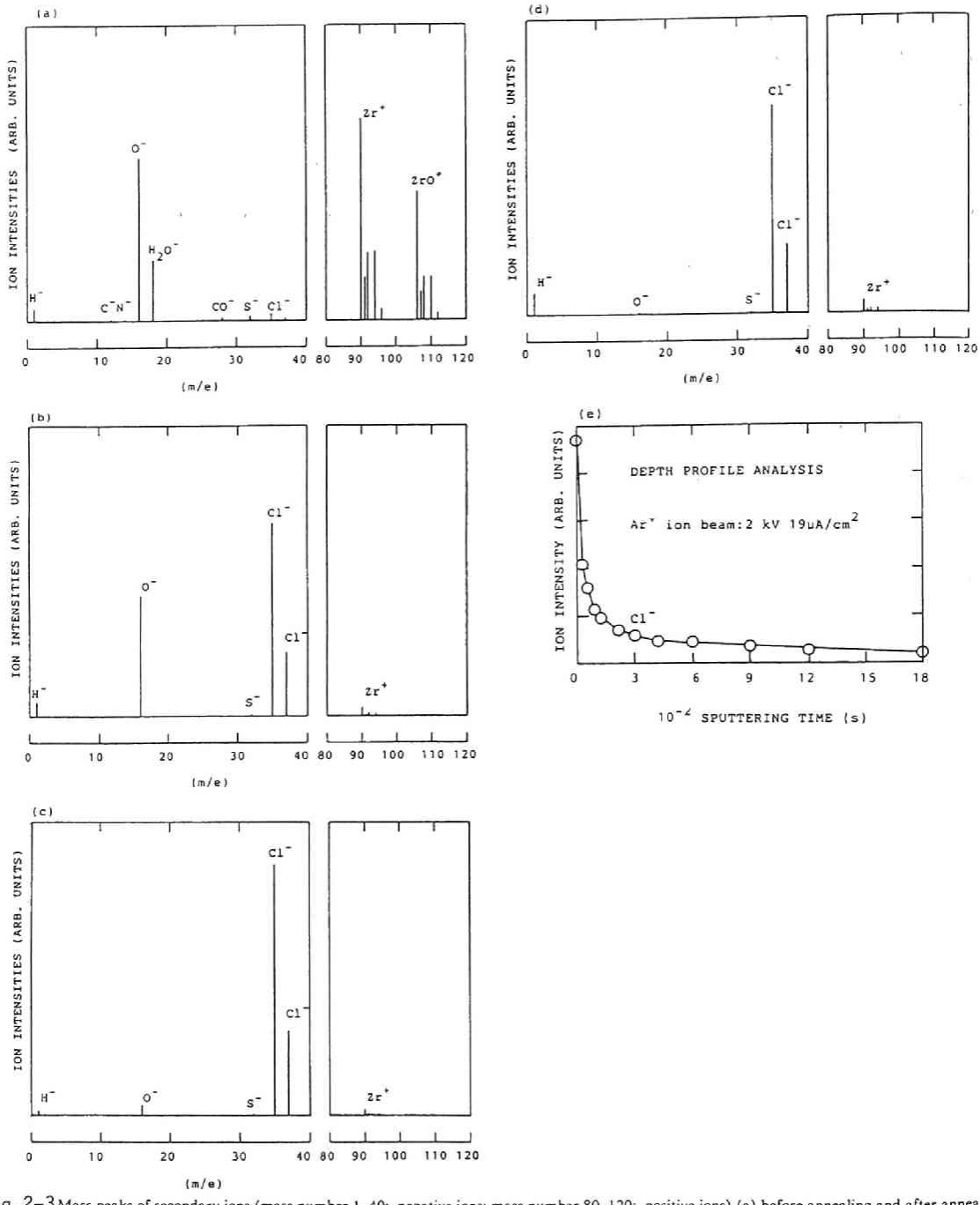

Fig. 2-3 Mass peaks of secondary ions (mass number 1–40: negative ions; mass number 80–120: positive ions) (a) before annealing and after annealing at 1023 K (b) for 60 min, (c) for 360 min, and (d) for 1440 min. The ion intensities in (a)–(d) are scaled relative to each other. (e) shows the depth profile analysis of Cl^- after annealing for 1440 min. All measurements were done under the condition that the specimen was heated at 1023 K.

reported that bulk impurities such as sulfur and chlorine segregate to the surface during annealing and suggested that the segregated impurities reduce the rate of adsorption.[29]

In our measurements of negative ions, it was found that chlorine segregates to the surface during annealing at 1023 K. The ion intensity of sulfur was much smaller than that of chlorine. A depth profile analysis showed that the intensity of chlorine was about 20-30 times as large as that in the bulk after annealing the specimen at 1023 K for 24 h as shown in Fig. 2-3(e). However, the effect of chlorine and sulfur on the rate of oxygen absorption at temperatures in our measurements is shown to be small. We duplicated the absorption measurement in the following way. A zirconium specimen of foil was heated at 973 K for 24 h. The oxygen gas was introduced into the chamber, and the pressure decrease in the oxygen reservoir was measured before and after the argon ion bombardment. After the argon ion bombardment the surface was demonstrated to be clean by SIMS. There were no significant differences in oxygen absorption between the two measurements. In addition, there is indirect evidence which supports the negligible effect of the impurities. Firstly, our measurements were done at temperatures of 973-1098 K and for specimens annealed at about 1070 K, *i.e.* below the transition temperature. On the other hand, Hoflund *et al.*[18,21,29] obtained the low adsorption rate at room temperature for specimens annealed above the transition temperature. The effect of chlorine and sulfur on the rate of oxygen adsorption, therefore, may be different in our measurements than their measurements. In our measurements at high temperatures the effect may be smaller than in their measurements at room temperature. In fact, the sticking probabilities in our measurement, 0.44-0.17 (defined as the

number of oxygen atoms adsorbed divided by the number of impinging oxygen atoms), are in good agreement with the values 0.2 ± 0.08 at 930 K and 0.45 ± 0.08 at 1050 K estimated from the report by Krishnan *et al.*, who used zirconium specimens cleaned by argon ion bombardment at 1000 K.[15] Secondly, the temperature dependence of the absorption rate is in good agreement with the result by Krishnan and coworkers. Thirdly, the rate of oxygen absorption at 1073 K by 99.8% zirconium specimens is almost the same as that by 99.98% zirconium specimens.[41] These facts support the negligible effect of chlorine and sulfur on the rate of oxygen absorption at the high temperatures used in our experiments.

The intensities of secondary positive ions are sensitive to the oxidation states at metal surfaces.[42] Our SIMS measurement showed that the positive ion intensities for ions such as Zr^+ and ZrO^+ are low for the zirconium surface and that they are increased by a factor of 10^2-10^3 for zirconium oxide. We found no significant increase in these intensities during the measurements made under the conditions used to determine the absorption rates. Therefore, we can regard the process of oxygen absorption by zirconium under our experimental conditions as that by α-zirconium. This SIMS result agrees with that from an AES measurement.[15]

Discussion

The adsorption and desorption of gases on metal surfaces have been interpreted on the basis of the simple Langmuir model modified by incorporating an interaction between adatoms or by

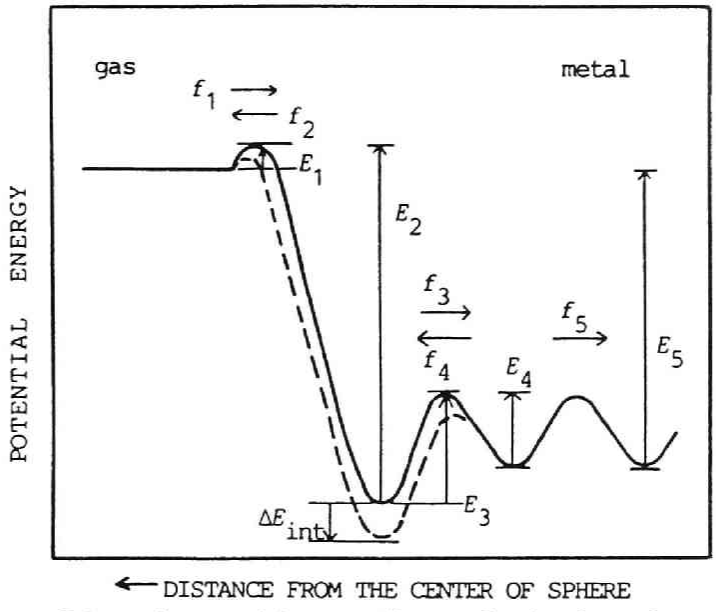

Fig.2-4. Schematic potential energy diagram for the absorption process. The dashed line indicates the potential variation due to the interaction between oxygen adatoms.

incorporating a distribution of binding energies between adatoms and substrate.[43] If we consider the fact that an indirect electronic interaction is important in the interaction between adatoms on a metal surface and that it is propagated via the valence band of the substrate,[44] then we cannot easily differentiate energy changes of surface sites caused by the two contributions; a change in the interaction energy implies a change in the binding energy. Thus, we adopt the interaction as a parameter to modify the simple Langmuir model. Actually, this interaction has been successfully used to interpret thermal desorption spectra[45] and the ordered structure of oxygen atoms on transition metals.[39-40]

Fig. 2-4 shows the schematic potential energy diagram for the

absorption process. The adsorption rate is calculated by using the expression for adsorption:

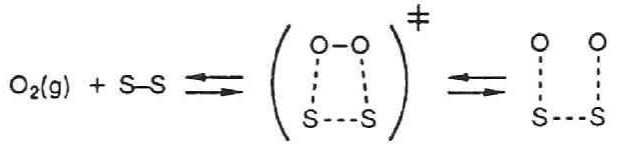

(2-1)

where S-S denotes a pair of two neighboring sites that can be occupied by adatoms and the index ‡ indicates an activated complex. The adsorption rate is assumed to be proportional to the probability that an oxygen molecule finds an empty neighboring pair of adsorption sites, because it has been believed that a transition (activated) state with both atoms bound to the surface is required to break the bond of the homonuclear diatomic molecule.[46] Foord *et al.* have also shown from the AES that the dissociative adsorption rate of oxygen on zirconium at room temperature is almost proportional to the probability that an oxygen molecule finds an empty pair.[13]

The quasi-chemical approximation gives the following expressions for the number of pairs per unit area:[47-49]

$$N_{11} = (1/2)qN_s\theta[1 - 2(1 - \theta)/(1 + \beta)] \tag{2-2}$$

$$N_{00} = (1/2)qN_s(1 - \theta)[1 - 2\theta/(1 + \beta)] \tag{2-3}$$

$$N_{10} = (1/2)qN_s\theta[2(1 - \theta)/(1 + \beta)] \tag{2-4}$$

where

$$\beta = \{1 - 4\theta(1 - \theta)[1 - \exp(-\omega/(kT))]\}^{1/2} \tag{2-5}$$

Here the subscripts 11, 00 and 10 indicate that the two neighboring sites

are both occupied by adatoms, they are both empty and one of them is occupied, respectively. Other symbols are as follows: q, the coordination number of the adsorption site; N_s, the number of the adsorption sites per unit area; θ, the surface coverage defined by N_1/N_s; N_1, the number of adatoms per unit area; T, the temperature of the metal; and ω, the interaction energy between adatoms (positive for repulsion, negative for attraction). Eqns. (2-2)-(2-5) imply that if the interaction is attractive, the adatoms take the possible lowest energy state by making clusters. The interaction energy corresponds to the energy change due to the reaction $2N_{10} \rightarrow N_{11} + N_{00}$, and the interaction energy per atom is given by

$$\Delta E_{\mathrm{int}} \equiv \partial(\omega N_{11})/\partial N_1 = (1/2)q\omega[1 + (2\theta - 1)/\beta] \tag{2-6}$$

The probability that an empty site is surrounded by j adatoms on the q nearest-neighbor sites is, from eqn. (2-3),

$$P(0;j) = \binom{q}{j}\left(\frac{2\theta}{1+\beta}\right)^{j}\left(1 - \frac{2\theta}{1+\beta}\right)^{q-j} \tag{2-7}$$

If $P(0;j)$ at site 0 is independent of $P(0';j)$ at another empty site 0' adjacent to site 0 and if the empty pair has Q nearest-neighbor sites, I of which are occupied by adatoms, then we have, for the required probability,

$$P(00;I) = \binom{Q}{I}\left(\frac{2\theta}{1+\beta}\right)^{I}\left(1 - \frac{2\theta}{1+\beta}\right)^{Q-I} \tag{2-8}$$

The absorption rate is affected by the interaction between adatoms as well as by this probability. If the change in the activation energy for adsorption is proportional to the number of adatoms surrounding the empty pair on which the oxygen molecule adsorbs, it is given by

$$\Delta E_{\mathrm{int}}(I) = 2(I/Q)\Delta E_{\mathrm{int}} \tag{2-9}$$

Assuming that the oxygen gas is ideal, we have, from eqns. (2-6) and (2-7). the adsorption rate[50]

$$\begin{aligned} f_1 &= \sum_{I=0}^{Q} P(00;I) \times \\ &\qquad (kT/h)z_1 P/(kT_g)N_{00} \exp[-(2E_1 + \Delta E_{\mathrm{int}}(I))/(kT)] \\ &= A(1-\theta)[1 - 2\theta/(1+\beta)]\sum_{I=0}^{Q} P(00;I) \exp[-\Delta E_{\mathrm{int}}(I)/(kT)] \end{aligned} \tag{2-10}$$

where

$$A = (1/2)qN_s PT/(hT_g)z_1 \exp[-2E_1/(kT)] \tag{2-11}$$

z_1 is the contribution of partition functions, and P and T_g are the pressure and the temperature of the oxygen gas, respectively. Desorption, *i.e.* the reverse step in eqn. (2-1), can be neglected because the oxygen pressure in equilibrium with zirconium is very small (*e.g.* 10^{-42} Pa at 1000 K)[8] and the desorption rate is very small.

The transfer step is expressed as

$$\mathrm{O\text{–}S + M \rightleftarrows (S\text{–}O\text{–}M)^{\ddagger} \rightleftarrows O\text{–}M + S} \tag{2-12}$$

where M denotes an outermost bulk site where the potential energy is

assumed to be the same level as in the bulk. We assume that the oxygen concentration at site M is small, and the interaction between oxygen atoms at the sites in the bulk is negligible. The forward rate can be written as

$$f_3 = (kT/h)z_3N_s\theta(1 - C_i)\sum_{j=0}^{q}P(1;j)\exp[-(E_3 + \Delta E'_{int}(j) - \Delta E_{int})/(kT)] \quad (2\text{-}13)$$

where C_i is the fraction of occupation by oxygen at site M. Here $P(1;j)$ is the probability that an adatom 1 is surrounded by j adatoms on the q nearest neighbor sites [see eqn. (2-2)]:

$$P(1;j) = \binom{q}{j}\left[1 - \frac{2(1-\theta)}{1+\beta}\right]^{j}\left[\frac{2(1-\theta)}{1+\beta}\right]^{q-j} \quad (2\text{-}14)$$

and

$$\Delta E'_{int}(j) = (j/q)\Delta E_{int} \quad (2\text{-}15)$$

The backward rate can be similarly written as

$$f_4 = (kT/h)z_4N_s(1 - \theta)C_i\sum_{j=0}^{q}P(0;j)\exp[-(E_4 + \Delta E'_{int}(j))/(kT)] \quad (2\text{-}16)$$

It is easily shown that eqns. (2-10), (2-13) and (2-16) lead to the simple Langmuir kinetic equations[38,50] when $\omega = 0$. Now we assume that the transfer step is in partial equilibrium. It has been shown that the assumption of such a partial equilibrium has no serious effect on the absorption rate except in the early stage of absorption.[38] Setting $f_3 = f_4$, we have

$$C_i = \theta/[\theta + BG(1-\theta)] \tag{2-17}$$

where

$$B = (z_4/z_3)\exp[-(E_4 - E_3)/(kT)] \tag{2-18}$$

$$G = \sum_{j=0}^{q} P(0;j)\exp[-\Delta E'_{\mathrm{int}}(j)/(kT)]/\sum_{j'=0}^{q} P(1;j')\times \exp[-(\Delta E'_{\mathrm{int}}(j') - \Delta E_{\mathrm{int}})/(kT)] \tag{2-19}$$

The diffusion of oxygen atoms into zirconium is described by the Fickean diffusion equation together with the flux at the adsorption site. For a sphere they are given by

$$\partial C/\partial t = D(1/r^2)\,\partial(r^2\,\partial C/\partial r)/\partial r \tag{2-20}$$

$$f_5 = -D\,\partial C/\partial(-r)|_{r=a} = D\,\partial C/\partial r|_{r=a} \tag{2-21}$$

where D is the diffusion coefficient for oxygen in α-zirconium, r is the distance from the center of the sphere, a is its radius, and C is the oxygen concentration in the bulk. Note that C_i is the concentration at $r = a$, at the site M.

We can now calculate the absorption rate by balancing the equations of adsorption, transfer and diffusion at the adsorption site. Thus, we can solve the diffusion equation with the boundary condition

$$f_1 = \mathrm{d}N_1/\mathrm{d}t + f_5 \tag{2-22}$$

which, because $dN_1/dt \ll f_5$ at temperatures in the present study, becomes

$$f_1 \simeq D\,\partial C/\partial r|_{r=a} \tag{2-23}$$

The amount of oxygen that has been absorbed up to the time t, *i.e.* the absorption curve, is given by

$$W(t) = \int_0^a 4\pi r^2 C(r,t)\,dr \tag{2-24}$$

or by integrating f_1 over the surface of the sphere from the time 0 to t.

We solve eqns. (2-20) and (2-23) numerically using the relation between θ and C_i [eqn. (2-17)]. By adjusting the values of A, ω and B considering the three characteristics mentioned in the Results section, we obtain the absorption curves which best fit the experimental data shown in Fig. 2-2. The values used for the numerical calculations include $D = 5.4 \times 10^{-4} \exp(-2.56 \times 10^4 T^{-1})$ $(m^2 \cdot s^{-1})$ [1] and $q = 6$. Analyzing the decays of the AES signal of oxygen by annealing, Foord *et al.* obtained the diffusion constant of oxygen.[13] Their data and the reported value for α-zirconium and zirconium oxide are

Foord *et al.*:[13]	$7.4\times10^{-16}\exp(-6060T^{-1})$	$/m^2s^{-1}$
α-Zr:[1]	$5.4\times10^{-4}\exp(-25600T^{-1})$	$/m^2s^{-1}$
ZrO_{2-x}:[1]	$1.1\times10^{-7}\exp(-14700T^{-1})$	$/m^2s^{-1}$

At the high temperatures used in our measurement their value is much smaller than the values of α-zirconium and oxide. The activation

energy 8.37×10^{-20} J per O atom obtained by them is also smaller than the value of α-zirconium, 3.53×10^{-19} J per O atom, and oxide 2.03×10^{-19} J per O atom. It seems that there are two reasons to explain why their diffusion constant is different from those in the bulk. Firstly, the surface effect on diffusion: their diffusion constant was determined by the contribution of oxygen transport within several layers at the surface. Secondly, the diffusion mechanism in their measurement at low temperatures (515 - 614 K) may be different from that at high temperatures; *i.e.* oxygen atoms diffuse along low-energy paths at low temperatures. If we use their small diffusion constant, the calculated concentration of oxygen at the surface would be increased more rapidly so as to form an oxide layer, and the experimental results could not be explained. Thereby, we used the diffusion constant of the α-zirconium. Our choice of the value $q = 6$ is based on the results of surface spectroscopic studies, particularly on those of LEED measurement,[22,25-27] dealing with the surface oxidation of zirconium[11-34] and of titanium.[51]

Fig. 2-5 shows computed curves of surface coverage θ at 6.7×10^{-5} Pa. The coverage rapidly increases with time as the temperature is lowered. This is consistent with the AES result obtained at low oxygen pressures and high temperatures.[15]

The interaction between adatoms ω was found to be attractive and to have the value -4×10^{-21} J per O-O pair. A theoretical study of the interaction between oxygen adatoms on the zirconium surface has not yet been published. The value -4×10^{-21} J per O-O pair seems reasonable if it is compared with that calculated by using indirect interaction models.[44] This magnitude is also similar to that

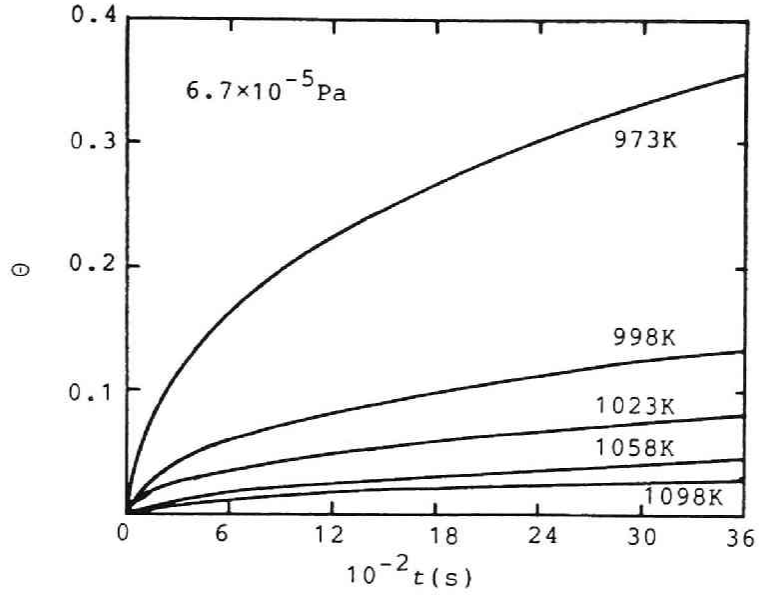

Fig.2-5. Computed surface coverage by oxygen atoms as a function of time for several temperatures.

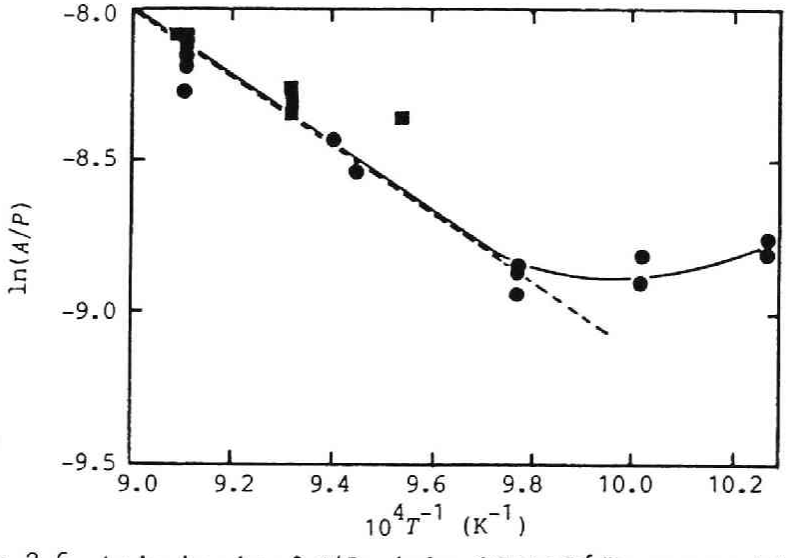

Fig.2-6. Arrhenius plot of A/P: circles, 6.7×10^{-5} Pa; squares, 1.3×10^{-4} Pa. The activation energy E_1 was evaluated from the straight dashed line.

calculated from the two-dimensional phase diagram of O/W(110).[52-54]

The activation energy for adsorption E_1 is obtained from the Arrhenius plot of A. Noting that the slope of the line is primarily determined by the exponential term, we obtain E_1 $(7.4 \pm 0.6) \times 10^{-20}$ J per O atom from the dashed line in Fig. 2-6. Krishnan and co-workers reported that when the rate of oxygen absorption is constant, the activation energy is $(6 \pm 3) \times 10^{-20}$ J per O atom.[15] Provided that the constant rate of absorption which they observed is limited by adsorption, the value of their activation energy is in good agreement with our result. The upward deviation of the solid curve from the straight line in Fig. 2-6 at low temperatures where θ rapidly increases may be interpreted as a sign implying an onset of changes in the surface structure. Surface spectroscopic studies have shown that the oxidation of zirconium occurs through the processes of dissociative adsorption of oxygen, reconstruction of surface, nucleation of nonstoichiometric oxides and growth of oxide.[15,19,22,25-29] Krishnan *et al.* have reported that the oxygen absorption curves at high temperatures of 773 - 1008 K obtained by AES indicate four steps: step 1, an initial period of rapid increase; step 2, a region of slow increase; step 3, a second period of further rapid increase where the nucleation of oxides occur; and step 4, a saturation region. They also reported that the rate at which oxygen accumulates on the surface increases with lowering temperatures during steps 1 and 3.[15] In fact, the step 3 was observed in our SIMS measured at 6.7×10^{-5} Pa and at lower temperatures than the temperatures used in our experiment. Thereby, the upward deviation may be a possible sign implying an onset of the change in the surface structure.

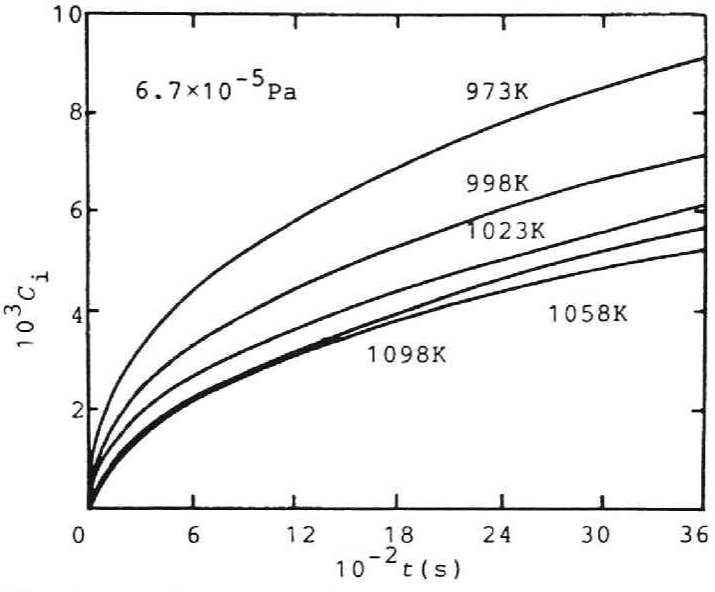

Fig.2-7. Computed occupation fraction of oxygen atoms at the outermost site in the bulk as a function of time. Note that the full occupation (C = 1) corresponds to O/Zr = 2.

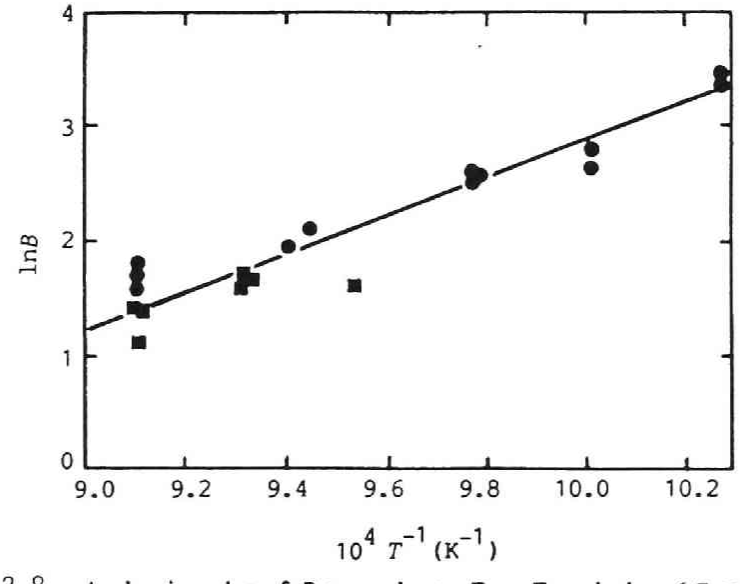

Fig.2-8. Arrhenius plot of B to evaluate $E_4 - E_3$: circles, 6.7×10^{-5} Pa; squares, 1.3×10^{-4} Pa.

Fig. 2-7 shows computed curves of oxygen concentration C_i at the outermost site in the bulk. C_i is much smaller than θ. This is consistent with the assumption that the interaction between oxygen atoms in the bulk is negligible. This could mean that diffusion into the bulk is very rapid enough to keep C_i small.

The energy difference ($E_4 - E_3$) in the transfer step (see Fig. 2-4) was estimated from the Arrhenius plot of B. From Fig. 2-8, $E_4 - E_3$ was found to be negative and to have the value $-(2.2 \pm 0.1) \times 10^{-19}$ J per O atom. This shows that the oxygen atom adsorbed is more tightly bound on the surface than in the bulk. The adiabatic potential energy for an oxygen atom moving onto a Ni(111) surface has been calculated by the use of effective medium theory.[55] The result shows that the oxygen atom is more stable on Ni(111) surface than at the outermost sites in the bulk and that the energy difference calculated is in the same order as our result.

Using the values of $E_4 - E_3$ and the value of the heat of absorption -1.0×10^{-18} J per O atom,[8] which corresponds to our E_5, we have $E_2 - E_1 = -1.2 \times 10^{-18}$ J per O atom for the adsorption heat. This value is in good agreement with the value -1.2×10^{-18} J per O atom calculated for oxygen adsorption on transition-metal surfaces using a simple quantum mechanical model.[56]

Conclusion

The model which is described by the modified Langmuir kinetics including the interaction between adatoms gives an explanation to the experimental results of the oxygen absorption by α-zirconium at

low oxygen pressures and high temperatures. The conclusions evaluated from the model are the following:

1. The activation energy for adsorption is $(7.4 \pm 0.6) \times 10^{-20}$ J per O atom.
2. The energy of the interaction, which is attractive, is -4×10^{-21} J per O-O pair.
3. The adsorption site has a potential energy lower by $(2.2 \pm 0.1) \times 10^{-19}$ J per O atom than the site in the bulk.
4. The adsorption step is the rate-limiting step. This conclusion may be easily understood by the following simple discussion. The reaction rate is given by the product (rate of collision) × (probability that collision carries enough energy to get over the potential energy barrier). The collision rate of oxygen molecules at low pressures ($\simeq 1\ s^{-1}$ per adsorption site at 10^{-4} Pa) is remarkably smaller than that of the transfer from the surface site to the outermost site in the bulk ($\simeq kT / h = 2 \times 10^{13}\ s^{-1}$ at 1073 K), although the exponential factor for adsorption [$\exp(-2 E_1 / kT) = 5 \times 10^{-5}$ at 1073 K] is much greater than that for transfer [$\exp(- E_3 / kT) = 2 \times 10^{-17}$)]. Thus, the adsorption rate f_1 given by the product is slower than the transfer rate f_3. Our experimental result that the adsorption rate is almost directly proportional to the pressure of oxygen supports this conclusion. Further spectroscopic studies seem necessary if we attempt to give a full explanation to the deviation as seen in Fig. 2-6.

References for Chapter 2

1. C. J. Rosa, *J. Less-Common Met.*, 1968, 16, 173.
2. H. A. Porte, J. G. Schnizlein, R. C. Vogel and D. F. Fisher, *J. Electrochem. Soc.*, 1960, 107, 506.
3. K. A. Sense, *J. Electrochem. Soc.*, 1962, 109, 377.
4. R. J. Hussey and W. W. Smeltzer, *J. Electrochem. Soc.*, 1964, 111, 564.
5. J. Levintan, J. E. Draley and C. J. Van Drunen, *J. Electrochem. Soc.*, 1967, 114, 1086.
6. C. J. Rosa, *J. Less-Common Met.*, 1968, 15, 35.
7. A. Madeyski, D. J. Poulton and W. W. Smeltzer, *Acta. Met.*, 1969, 17, 579.
8. P. Paetz and F. Sperner, in *Gase und Kohlenstoff in Metallen*, ed. E. Fromm and E. Gebhardt (Springer, Berlin, 1976), pp. 419-430.
9. M. Dechamps and P. Lehr, *C. R. Acad. Sci., Ser. C*, 1970, 270, 169.
10. M. Nagasaka, E. Ueda and T. Yamashina, *Vacuum*, 1973, 23, 51.
11. B. W. Veal, D. J. Lam and D. G. Westlake, *Phys. Rev. B*, 1979, 19, 2856.
12. J. Frandon, B. Brousseau and F. Pradal, *Phys. Stat. Sol. B*, 1980, 98, 379.
13. J. S. Foord, P. J. Goddard and R. M. Lambert, *Surf. Sci.*, 1980, 94, 339.
14. D. P. Valyukhov, M. A. Golubin, D. M. Grebenshchikov and V. I. Shestopalova, *Sov. Phys. Solid State*, 1982, 24, 1594.
15. G. N. Krishnan, B. J. Wood and D. J. Cubicciotti, *J. Electrochem. Soc.*, 1981, 128, 191.

16. R. L. Tapping, *J. Nucl. Mater.*, 1982, 10, 151.

17. L. R. Danielson, *J. Vac. Sci. Technol.*, 1982, 20, 86.

18. G. B. Hoflund, D. F. Cox and R. E. Gilbert,
J. Vac. Sci. Technol. A, 1983, 1, 1837.

19. P. Sen, D. D. Sarma, R. C. Budhani, K. L. Chopra and C. N. R. Rao,
J. Phys. F., 1984, 14, 565.

20. M. Y. Zhou, R. H. Milne, M. A. Karolewski, D. C. Frost and
K. A. R. Mitchell, *Surf. Sci.*, 1984, 139, L181.

21. G. B. Hoflund, D. A. Asbury and D. F. Cox,
Appl. Surf. Sci., 1985, 22/23, 252.

22. K. C. Hui, R. H. Milne, K. A. R. Mitchell, W. T. Moore, W. T.
and M. Y. Zhou, *Solid State Commun.*, 1985, 56, 83.

23. T. A. Sasaki and Y. Baba, *Phys. Rev. B*, 1985, 31, 791.

24. K. -O. Axelsson, K.-E. Keck and B. Kasemo,
Surf. Sci., 1985, 164, 109.

25. P. C. Wong and K. A. R. Mitchell, *Can. J. Chem.*, 1986, 64, 2409.

26. P. C. Wong, K. C. Hui, B. K. Zhong and K. A. R. Mitchell,
Solid State Commun., 1987, 62, 293.

27. P. C. Wong and K. A. R. Mitchell, *Can. J. Phys.*, 1987, 65, 464.

28. G. R. Corallo, D. A. Asbury, R. E. Gilbert and G. B. Hoflund,
Phys. Rev. B, 1987, 35, 9451.

29. G. B. Hoflund, G. R. Corallo, D. A. Asbury and R. E. Gilbert,
J. Vac. Sci. Technol. A., 1987, 5, 1120.

30. C. Palacio, J. M. Sanz and J. M. Martinez-Duart,
Surf. Sci., 1987, 189/190, 175.

31. C. Palacio, J. M. Sanz and J. M. Martinez-Duart,
Surf. Sci., 1987, 191, 385.

32. J. M. Sanz, C. Palacio, Y. Casas and J. M. Martinez-Duart, *Surf. Interface Anal.*, 1987, 10, 177.

33. P. Aebi, M. Erbudak, A. Leonardi and F. Vanini, *J. Electron Spectrosc. Relat. Phenom.*, 1987, 42, 351.

34. P. E. West and P. M. George, *J. Vac. Sci. Technol. A*, 1987, 5, 1124.

35. D. A. Asbury, G. B. Hoflund, W. J. Peterson, R. E. Gilbert and R. A. Outlaw, *Surf. Sci.*, 1987, 185, 213.

36. A. T. Fromhold, Jr., *Theory of Metal Oxidation*, (North-Holland, Amsterdam, 1976), Vol. I, II.

37. W. W. Jost, *Diffusion in Solids, Liquids, and Gases*, (Academic, New York, 1952), pp. 69-75.

38. S. Naito, *J. Chem. Phys.*, 1983, 79, 3113.

39. M. A. Van Hove, W. H. Weinberg and C. -M. Chan, *Low-Energy Electron Diffraction*, (Springer, Berlin, 1986).

40. M. G. Lagally, G. -C. Wang and T. -M. Lu, in *Chemistry and Physics of Solid State Surface II*, ed. R. Vanselow, (CRC, Florida, 1979), pp. 153-179.

41. H. Takeuchi, S. Naito, M. Yamamoto and T. Hashino, *J. Chem. Soc. Faraday Trans. 1*, 1988, 84, 4235.

42. W. N. Delgass, L. L. Lauderback and D. G. Taylor, in *Chemistry and Physics of Solid Surface IV*, ed. R. Vanselow and R. Howe, (Springer, Berlin, 1982) pp. 51-76.

43. F. C. Tompkins, *Chemisorption of Gases on Metals*, (Academic, London, 1978), pp.99-100.

44. T. L. Einstein, in *Chemistry and Physics of Solid State Surfaces II*, ed. R. Vanselow, (CRC, Florida, 1979),

pp. 181-208.

45. D. A. King, in *Chemistry and Physics of Solid State Surface II*, ed. R. Vanselow, (CRC, Florida, 1979), pp. 87-128.

46. B. I. Lundqvist, in *Many Body Phenomena at Surfaces*, ed. D. Lanfreth and H. Suhl, (Academic, Orland, 1984), pp. 93-144.

47. R. Fowler and E. A. Guggenheim, *Statistical Thermodynamics*, (Cambridge University, London, 1965), pp. 437-443.

48. R. Peierls, *Proc. Cambridge Phil. Soc.*, 1936, 32, 471.

49. D. A. Reed and G. Ehrlich, *Surf. Sci.*, 1981, 102, 588.

50. S. Glasstone, K. J. Laidler and H. Eyring, *The Theory of Rate Processes*, (McGraw-Hill, New York, 1941), pp. 347-366 and 516-544.

51. H. D. Shih and F. Jona, *Appl. Phys.*, 1977, 12, 311.

52. G. Ertl and D. Schillinger, *J. Chem. Phys.*, 1977, 66, 2569.

53. E. D. Williams, S. L. Cunningham and W. H. Weinberg, *J. Vac. Sci. Technol.*, 1978, 15, 417.

54. W. Y. Ching, D. L. Huber, M. Fishkis and M. G. Lagally, *J. Vac. Sci. Technol.*, 1978, 15, 653.

55. J. K. Nørskov, in *Dynamical Processes and Ordering on Solid State Surfaces*, ed. A. Yoshimori and M. Tsukada, (Springer, Berlin, 1985), pp. 94-103.

56. C. M. Varma and A. J. Wilson, *Phys. Rev. B*, 1980, 22, 3795 and 3805.

Chapter 3

Change in the Chemical Composition of Zirconium Surface by Oxidation: A SIMS Study on the Oxidation of Zirconium at High Temperatures and Low Oxygen Pressures*

Introduction

Zirconium and its alloys have considerable technological importance, and owing to their high affinity for oxygen it is of particular interest to study the surface oxidation of zirconium. Many investigators have recently reported surface spectroscopic studies (*e.g.* AES, EELS, XPS, UPS, LEED and ISS) of the initial oxidation of zirconium at room temperature.[1-23] However, these studies do not give a knowledge of the oxidation kinetics at high temperatures. The kinetics at high temperatures involve dynamic competition between the transport of oxygen at the surface and the diffusion of oxygen into the bulk. Few spectroscopic studies of the initial stage of the oxidation of the zirconium surface at high temperatures have been reported[24-25] whereas the rate of oxygen absorption by zirconium at high temperatures has been studied by several authors.[26-31]

---

* published in *J. Chem. Soc. Faraday Trans.*, 1990, 86, 157.

In the present study we have investigated the initial stages of oxidation of a clean polycrystalline zirconium surface at high temperatures(773 - 1073 K) and at low oxygen pressures (6.7×10^{-5} - 1.3×10^{-3} Pa) using a secondary ion mass spectroscopy (SIMS). The SIM spectra were sensitive to the oxidation state at the surface and provided information of the whole range of oxidation processes, *i.e.* adsorption of oxygen, nucleation of oxide and growth of oxide film. In order to identify the oxidation states at the surface we have compared the spectra with those obtained by other surface spectroscopic studies of the oxidation of zirconium at room temperature.

It is well known that the yield of the positive metal ion is increased by the oxide formation at the surface.[32-33] In most studies so far the change of the yield of the secondary ion has been explained by the change of the work function of the substrate. However, the increase of the yield of the positive metal ion by the oxide formation at the surface cannot be interpreted simply by the change of the work function, $\Delta\phi$, because it is widely different for different transition metals, {*e.g.* Zr($\Delta\phi$ = +0.6eV)[3], Fe(110) ($\Delta\phi$ = -0.1 eV)[34]}. We will explain the increase of the yield of the Zr^+ ion by assuming that the ionization probability of the sputtered atoms determines the ion yield uniquely and estimating the ionization probability of the zirconium atoms. Then we will show that the increase of the probability is due to the fact that the first ionization level of zirconium atom is below the Fermi level of the bulk metal[35] and the top of the oxygen 2p valence band of the oxide is below the ionization level of the metal atom.[4,36-37] We also measure the depth profile and discuss it briefly.

Experimental

All experiments were done in an ultra-high vacuum system which had a base pressure of the order of 10^{-8} Pa. The SIM spectra were obtained using a quadrupole mass spectrometer (ANELVA, AGA-360SIMS) and a 5 kV ion gun. The total pressure in the system was measured with a Bayard-Alpert gauge, and the partial pressures of gaseous components were determined with the quadrupole mass spectrometer.

Polycrystalline zirconium foils of dimensions 50 mm × 5mm × 0.025 mm and 99.99 % purity were used in this study. The specimen was mechanically polished, ultrasonically degreased in acetone, and then spot-welded onto two 0.8 mm platinum support wires. The specimen was heated resistively to 1023 K for 24 - 36 h. The temperature of the specimen was measured with a Pt-PtRh13% thermocouple spot-welded to the specimen and was controlled using a thermoregulator. The surface of the specimen was cleaned by Ar^+-ion bombardment at 1023 K. The SIMS measurements have shown that these treatments reduce surface contaminants such as oxygen, carbon, and chlorine segregated by annealing.[30]

After the surface of the specimen was cleaned, its temperature was adjusted to the desired value for measurement. Oxygen gas of 99.995% purity was admitted to the chamber. The leakage rate of the argon gas from the ion gun and the total pressure ($Ar + O_2$) in the chamber were controlled to be constant. The fluctuation of the partial pressure of oxygen was ± 10 %. Under the condition that the specimen was heated and the partial pressure of oxygen was constant, the specimen was bombarded for *ca.* 10 s on each occasion of the measurements with a beam energy of 2 keV and an ion current of 13

$\mu A \cdot cm^{-2}$. Secondary ions which have a kinetic energy of *ca.* 10 eV and an emission angle 45° to the surface normal were detected. The SIM spectra of the positive ions over the mass range 80 - 140 (*i.e.* Zr^+, ZrO^+ and ZrO_2^+ ions) were recorded on a digital voltmeter(Keithley model 194A). After the exposure to oxygen for 3600 s the specimen was cooled to room temperature and then the depth profile was measured with a 2 keV, 13 $\mu A \cdot cm^{-2}$ ion beam of argon.

The temperature of the specimen at the time of measurement may have an effect on the yields of the secondary ions or on the ratios of the yields. However, the effect of the temperature in the range 773 - 1073 K on the ion signal intensities was within ± 10 % in our measurement. Several investigators also observed no important effects on the SIM spectra of the clean or the oxidized polycrystalline metals as a function of specimen temperature.[32-33]

The change of the yields of the secondary ions due to the reaction between the ions and the oxygen molecule in the chamber would be negligible, because the mean free path of the oxygen molecule even at the highest pressure of oxygen in our measurement is much larger than the distance between the specimen and the mass spectrometer. The mean free path of oxygen is 10 m at 6.7×10^{-4} Pa and at 298 K.

In order to reduce perturbations such as a change of structure and chemical composition of the surface by argon ion bombardment in the so-called dynamic mode,[38] the surface was not bombarded continuously but for *ca.* 10 s on each separate occasion of the measurements (at 0, 300, 600, 1200, 1800, 2400, 3000 and 3600 s). It has been reported that the sputtering yield of zirconium is 1.2 atoms per ion

Table3-1. Differences in the intensities of the ion signals between the two measurement for an exposure of 3600 s at a constant oxygen pressure of 6.7×10^{-5} Pa[a]

	intensity difference (%)	
T/K	Zr^+	ZrO^+
973	0.0	−4.1
873	−8.1	−13.0
773	−4.2	−15.4

[a] The differences are shown by $100 \times [I(\text{blank}, t = 3600\ \text{s}) - I(\text{SIMS}, t = 3600\ \text{s})]/I(\text{SIMS}, t = 3600\ \text{s})$.

for 2 keV Ar^+-ion bombardment.[39] We can thus estimate that the 13 $\mu A \cdot cm^{-2}$ ion beam sputters one monolayer from the zirconium surface in *ca.* 10 s. The depletion of oxygen at the surface by Ar^+-ion bombardment could be compensated in a short time by the fast flow of oxygen from the gas phase.[30-31] In fact, as shown in Table 3-1, it was found that the difference between the ion-signal intensities I(SIMS, t = 3600 s) measured after argon-ion bombardment for 10 s on each separate occasion of measurements (at 0, 300, 600, 1200, 1800, 2400 and 3000 s) and the ion intensities I(BLANK, t = 3600 s) measured after the exposure of oxygen for 3600 s was *ca.* 15 % even at the lowest pressure of oxygen (6.7×10^{-5} Pa). This measurement supports the hypothesis that argon-ion bombardment causes little perturbation on the surface oxidation.

Results and Discussion

SIMS

The SIM spectra were measured at constant pressures of oxygen over the temperature range 773 - 1073 K. Reproducible spectra were obtained for different specimens. Fig. 3-1A, 3-1B and 3-1C show the typical change of the intensities of the secondary ion signals with time at constant pressures of oxygen (6.7×10^{-5} Pa, 1.3×10^{-4} Pa and 6.7×10^{-4} Pa, respectively).

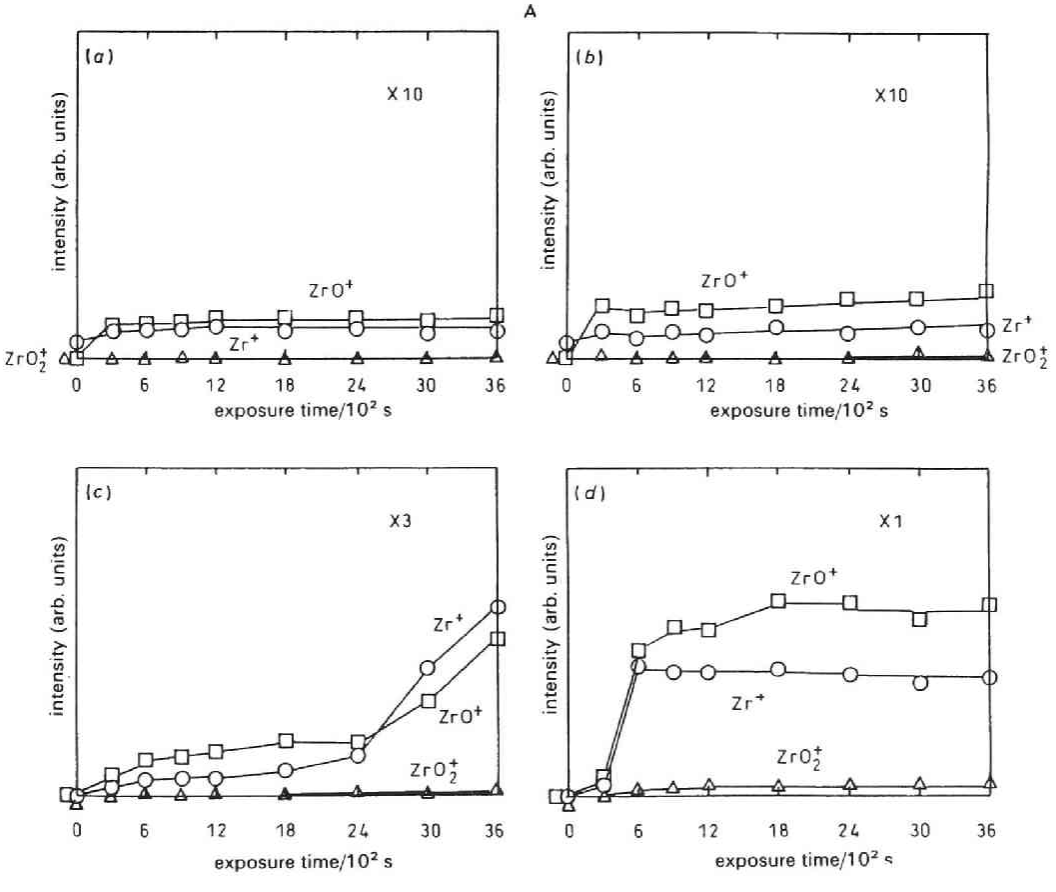

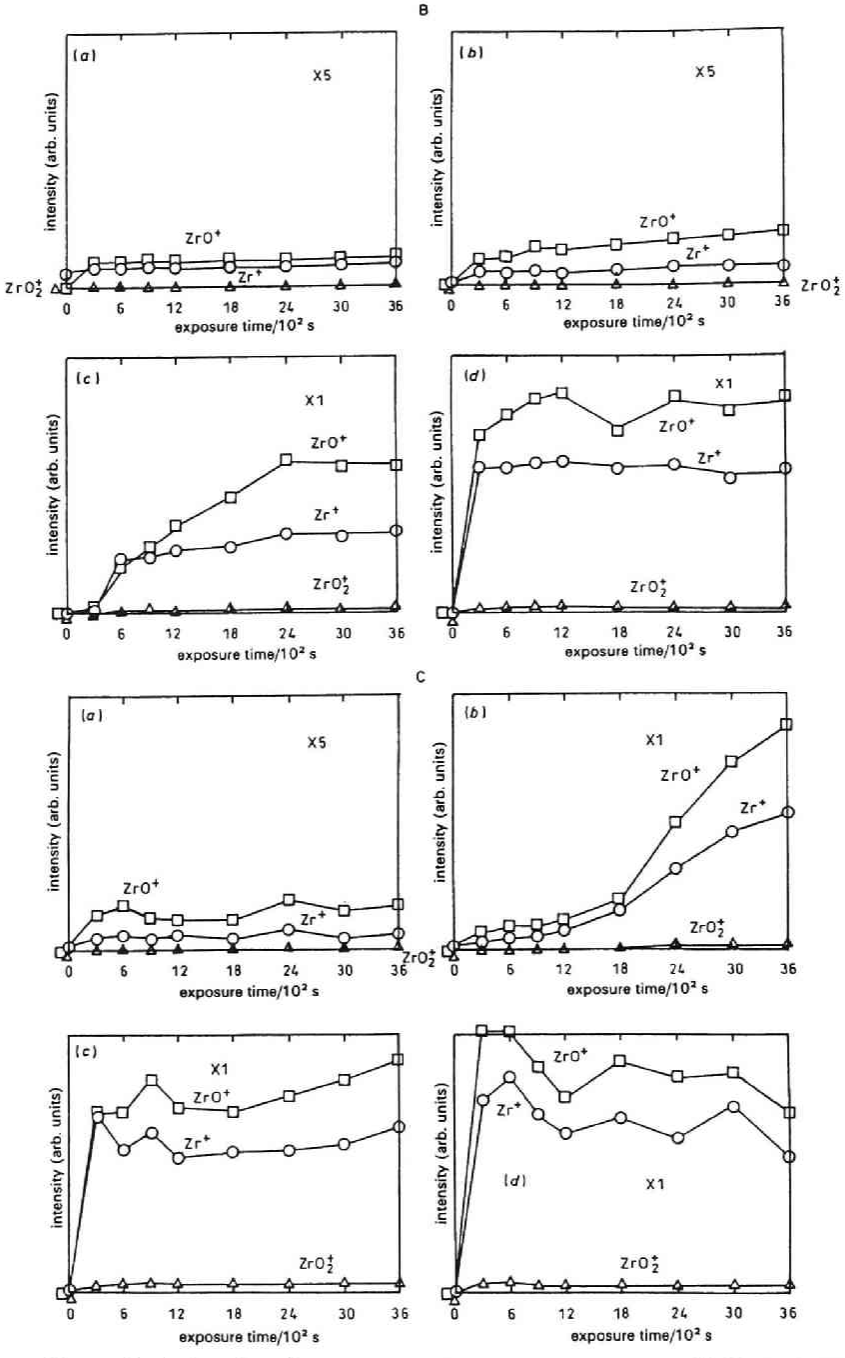

Fig. 3-1. Changes of the secondary ion intensities with oxygen exposure time at constant oxygen pressure: (A) 6.7×10^{-5}, (B) 1.3×10^{-4} and (C) 6.7×10^{-4} Pa. The amplification of intensity is shown in the top right hand corner of each graph. Since the rate of oxygen absorption at high temperatures depends on oxygen pressure and temperature, the abscissae are scaled by time of oxygen exposure rather than by Langmuir exposure (1 L = 10^{-6} Torr s): (*a*) 1073, (*b*) 973, (*c*) 873, (*d*) 773 K.

The change of the intensities of the secondary ion signals shows three characteristics. First, three distinct sequential stages of oxidation exist: (i) the first stage in which the intensities of the secondary ion signals of Zr^+, ZrO^+ and ZrO_2^+ increase slowly [see Fig. 3-1A at 1073 and 973 K, Fig. 3-1B at 1073 and 973 K and Fig. 3-1C at 1073 K.]; (ii) the second stage in which the intensities increase rapidly [see Fig. 3-1A at 873 K, Fig. 3-1B at 873 K and Fig. 3-1C at 973 K.]; (iii) the final stage in which the intensities show saturation [see Fig. 3-1A at 773 K, Fig. 3-1B at 773 K and Fig. 3-1C at 873 and 773 K]. Secondly, the rate of the increase of the intensities was lowered markedly at higher temperatures. Thirdly, the stages of the slow increase were prolonged at lower pressures of oxygen. [Compare Fig. 3-1A at 6.7×10^{-5} Pa with Fig. 3-1C at 6.7×10^{-4} Pa.]

Valyukhov and coworkers have investigated the surface oxidation of zirconium using SIMS and XPS.[24] They have measured the SIM and the XP spectra at room temperature after exposure of oxygen at 573 to 873 K. They have found characteristic sharp bends in the curves of changes of the intensity of the ZrO^+ ion signal with time, and that the sharp bend points extend to longer exposure with increasing temperature. Based on their XPS measurements, they suggested that islands of zirconium oxide form and grow in the linear increase stage of the ZrO^+ ion signal intensity, and that completion of surface coverage by a monolayer of the oxide was attained at the oxygen exposure of the bend points. The exposures at the bend points are roughly in agreement with those at the beginning of the saturation stage in our *in situ* measurement.

Three sequential stages in the increase of oxygen concentration at the zirconium surface (slow increase, rapid increase and saturation) were

found using AES measurements at high temperatures[25] and at room temperature[20] and by the ion-scattering measurements at room temperature[17]. The three stages reported are just the same behaviour as observed in our SIMS measurements. During the stage of rapid increase, energy shifts in zirconium[25] and oxygen AES peaks[20] have been observed. The shifts suggest the beginning of oxide nucleation at the surface.

Analysing the chemical shift of the 3d XPS peaks of zirconium by oxidation at room temperature, several investigators[7,22-23] have recently proposed that ZrO-like suboxides are formed on the zirconium surface in the oxide nucleation stage, and that with increasing oxygen exposure some of the ZrO-like suboxides are converted to the ZrO_2 oxide. Sen *et al.* have observed the three zirconium $M_{45}VV$ Auger peaks in the oxide nucleation stage :metal parent transition, interatomic [M_{45}(Zr 3d) V(O 2p) V(O 2p)] and intra-atomic [M_{45}(Zr 3d) V(Zr 4d) V(Zr 4d)] transition.[7] They have suggested that the appearance of the intra-atomic transition peaks in the nucleation stage indicates the existence of ZrO-like suboxides on the surface. It has been shown by Rao and Sarma that the interatomic Auger transition involving the oxygen 2p band occurs dominantly when the metal atom has no valence electrons in an oxide such as TiO_2, and that the intra-atomic transition in addition to the interatomic transition occurs when the metal atom in a suboxide such as TiO has some valence electrons.[40] Using the result of LEED measurement, Mitchell *et al.*[10,13-15] have proposed a possibility of the reconstruction of the Zr(0001) surface by oxidation. The reconstruction from the h.c.p. to the f.c.c. structure can occur even at oxygen exposures which correspond to the latter part of the

slow increase stage in our measurement. [See, for example, the curves at 873 K in Fig. 3-1A.]

From the above discussion, we can regard the rapid increase stage in our SIMS measurements as the nucleation stage in which the coexistence of the ZrO-like suboxides, the reconstructed surface, the zirconium dioxide and the metal phase occur on the surface.

It has been reported that the yield of the secondary positive ion of metal is sensitive to the oxidation states at the metal surface, *i.e.* the yield is low for the metal surface and the yield is increased by a factor of 10^2 - 10^3 for the oxide surface.[32-33] In our SIMS measurements the intensity of the Zr^+-ion signals increased *ca.* 300-fold at 773 K and at an oxygen pressure of 6.7×10^{-4} Pa, as shown in Fig. 3-1C. Therefore, we can regard the oxidation state at the surface in the saturation stage as the state of the surface covered by the oxide, and regard the oxidation state in the initial slow increase stage as the state of α-zirconium.

Increase in the Yield of Zr^+ Ion by Oxide Formation

Various models have been proposed for the emission mechanism of secondary ions.[36,41-46] In the present study, we assume that the ionization process of the sputtered atom has a dominant effect on the ion yield, and that the effect of the primary argon ion is to eject low-energy atoms from the surface.

Vasile[39] has observed a strong velocity dependence of the ionization probability of the secondary ions such as Zr^+, Ag^+, Cu^+ and

Cr^+ from their metal surfaces, and has suggested that the velocity dependence could be understood by a resonance tunnelling model or a model based on Auger processes. If the highest occupied level of the sputtered atom lies near the Fermi level of the bulk metal as in the case of zirconium,[35] resonance tunnelling is dominant for the electron transfer from the sputtered atom to the metal surface.[43,47] Therefore, we can neglect electron transfer based on Auger processes which require a core hole as an initial state.

The ionization probability of the zirconium atom from the metal surface may be given by the following approach discussed by Lang.[44] The time-dependent Anderson Hamiltonian of the electron system may be written (spin effects are neglected.)[43]

$$H = \sum_k \varepsilon_k C_k^+ C_k + \varepsilon_a(z(t)) C_a^+ C_a + \sum_k [V_{ak}(z(t)) C_a^+ C_k + h.c.] \quad (3\text{-}1)$$

where $V_{ak}(z(t))$ is the hopping matrix element between the non-degenerate atomic level a of energy ε_a and the metal state k of energy ε_k. C_a, C_k are the annihilation operators. Owing to the resonance tunnelling of the electron between the sputtered atom and the bulk metal the atomic level ε_a is broadened.[36] An exponential decay form for the half-width halh-maximum (HWHM) of the resonance level is assumed (interference effects are neglected):

$$\Delta(z(t)) = \pi \sum_k |V_{ak}(z(t))|^2 \delta(\varepsilon_k - \varepsilon_a(z(t)))$$

$$\simeq \Delta_0 \exp[-\gamma z(t)] \quad (3\text{-}2)$$

If the sputtered atoms are assumed to leave the surface at a constant velocity v, then

$$z(t) = tv\cos\Theta \tag{3-3}$$

where z is the distance from the surface, and Θ is the emission angle with the surface normal.

Hewson and Newns[48] have shown that if the energy of the surface plasmon is much greater than the energy of the lifetime broadening Δ of the atomic level, the effective atomic level can be written

$$\varepsilon_a(z) = -I + e^2/(16\pi\varepsilon_0 z) \tag{3-4}$$

where I is the ionization potential of the atom emitted (I = 6.84 eV for zirconium[35]) and the second term is due to the screening effect. The energy of the surface plasmon for zirconium(12 - 13 eV) [2,12,16,18-19,21] is much greater than the broadening Δ. (Δ_0 = 3.4 eV. Here Δ_0 is estimated by the calculation of the electronic structure of zirconium. [49-50]) So eqn. (3-4) can be applied. The energy levels of the zirconium atom and the metal are shown in Fig. 3-2. We suppose that the atomic level varies linearly with distance in the vicinity of the point z_c at which the atom level crosses the Fermi level. ($\varepsilon_F = -\phi = -4.05$ eV)[35]

$$\varepsilon_a(z) = \varepsilon_F + [d\varepsilon_a(z_c)/dz](z - z_c) \tag{3-5}$$

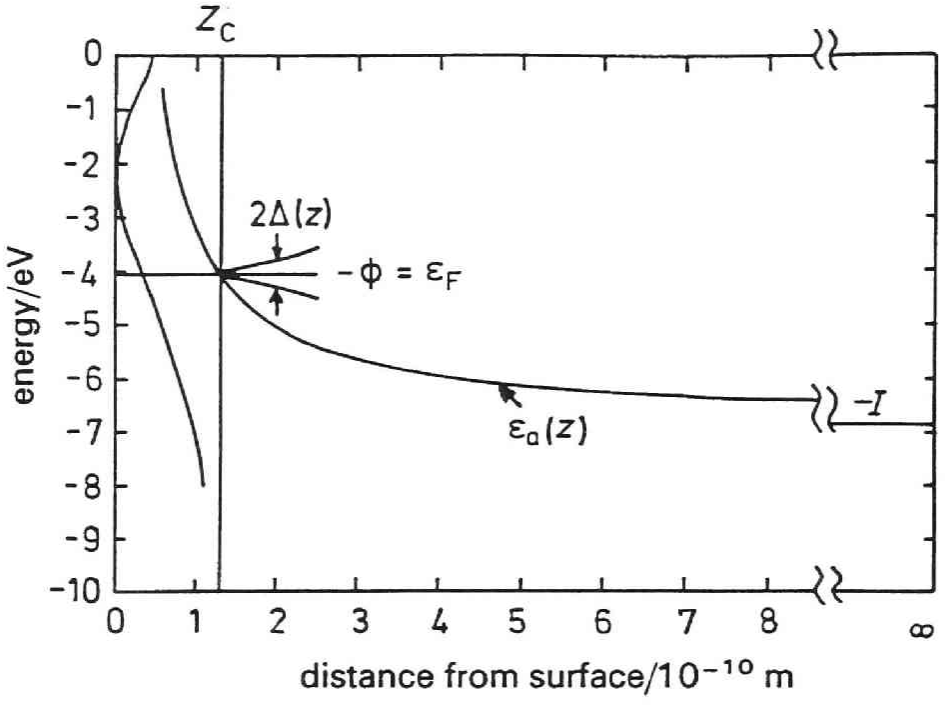

Fig. 3-2. Variation of the electronic level of the sputtered zirconium atom with distance from the bulk surface. The electronic state of the zirconium 4d band is approximated by $(1/\pi)\Delta_0/[(\varepsilon - \varepsilon_{centre})^2 + \Delta_0^2]$, where $\varepsilon_{centre} = -2.2$ eV and $\Delta_0 = 3.40$ eV.[49-50]

z_c is given to be 1.29×10^{-10} m by eqn. (3-4). Lang has obtained the electron occupation probability $\langle n_a(t)\rangle$ for $t \to \infty$: [44]

$$\langle n_a(\infty)\rangle = \langle n_a(0)\rangle \exp(-2G) + [1 - \exp(-2G)]/2 - (2G/\pi)\int_0^\infty dx \int_x^\infty dy \exp[-y - 2G\exp(-y)\cosh(x)]\sin[Ax(y - \gamma z_c)]/x \qquad (3\text{-}6)$$

where

$$G=\Delta_0/(\hbar\gamma v\cos\Theta) \tag{3-7}$$

and

$$A=2[d\varepsilon_a(z_c)/dz]/(\hbar\gamma^2 v\cos\Theta) \tag{3-8}$$

The probability that the sputtered zirconium atom becomes a positive ion is

$$P(Zr^+,E,\Theta) = N(Zr^+,E,\Theta)/N(Zr,E,\Theta) = 1-\langle n_a(\infty)\rangle \tag{3-9}$$

where

$$E=mv^2/2 \tag{3-10}$$

and $N(X,E,\Theta)$ is the rate at which the species X are emitted with the energy E and the angle Θ, and m is the mass of zirconium atom. It has been shown experimentally that the rate $N(Zr,E,\Theta)$ satisfies the Sigmund-Thompson relation:[51]

$$N(Zr,E,\Theta) = I_0 Y_{metal}(2E_b/\pi)E\cos\Theta/(E+E_b)^3 \tag{3-11}$$

where I_0, Y_{metal} and E_b are the primary ion current, the sputtering yield of zirconium and the surface binding energy, respectively. In this study, E_b is approximated by the cohesive energy of the solids (E_b = 6.31 eV per atom for zirconium metal).

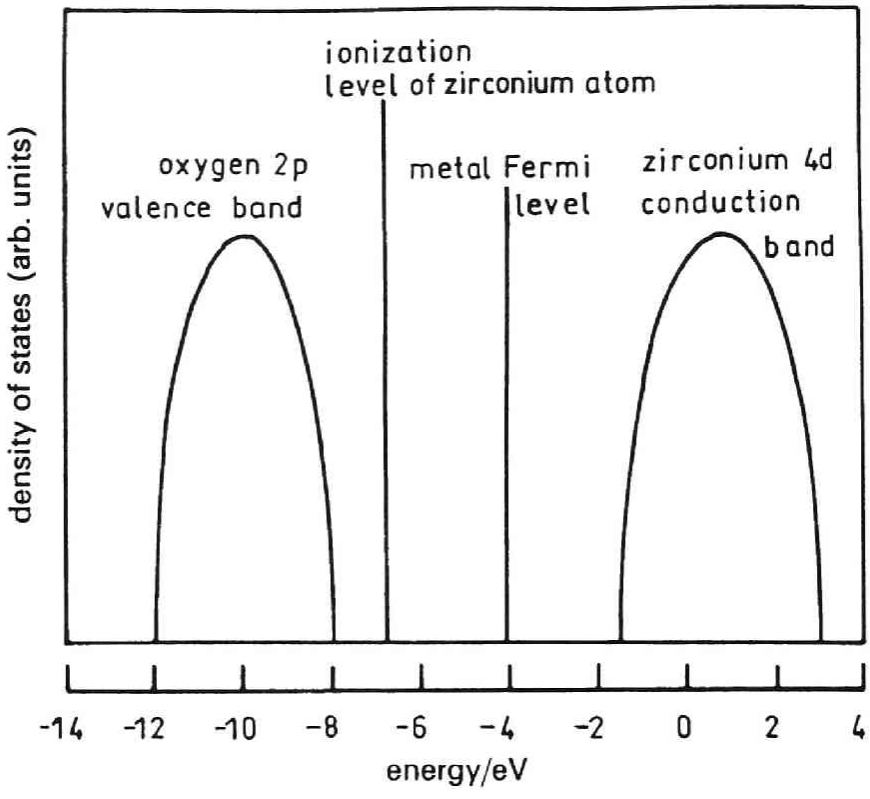

Fig. 3-3. Schematic diagram of the electronic state of zirconium oxide. The band of zirconium oxide is composed of an unoccupied Zr 4d conduction band and an occupied O 2p valence band. The energy zero is taken to be the vacuum level.

For the oxide surface of zirconium the emission mechanism may be different from that for the metal surface.[36] The electronic structure of zirconium oxide is schematically shown in Fig. 3-3. UPS measurements by Tapping have shown that the top of the oxygen 2p valence band is below the Fermi energy of the metal by 4 - 4.5 eV.[4] This result is in agreement

with the electronic structure calculated by Morinaga *et al.*, [37] who reported that the zirconium and the oxygen ion in the zirconium oxide have nearly three electronic units of positive charge and nearly two units of negative charge, respectively (in the cubic zirconium oxide the charge distribution is Zr : +3.12, O : -1.89).[37] When a zirconium ion leaves the surface, two electrons per particle can be transferred from the oxygen 2p valence band to the zirconium ion, because the atomic levels of Zr^{3+} and Zr^{2+} are far below the oxygen 2p valence band. The electronic energy levels of Zr^{2+} and Zr^{3+} are below the first ionization level by 13.1 and 36.1 eV, respectively.[35] Therefore, the Zr^{2+} and Zr^{3+} ions could not be detected in our SIMS measurement. On the other hand the first ionization level is above the oxygen 2p valence band, we can assume that the Zr^{+} ions are sputtered from the oxide surface, and that the number of sputtered neutral zirconium atoms is negligible.

Kelly and Lam have reported that the Sigmund-Thompson relation is valid for the total sputtering yield of the zirconium oxide surface.[52] By analogy with eqn. (3-11), we assume for the oxide that

$$N_{oxide}(Zr^{+}, E, \Theta) = I_{\theta} Y_{oxide} (2E_{b,oxide}/\pi) SE\cos\Theta/(E+E_{b,oxide})^{3} \quad (3\text{-}12)$$

where S is defined as the number of the emitted zirconium ions divided by the total number of sputtered atoms and $E_{b,oxide}$ is estimated to be 7.60 eV per atom.[27] The ratios of the intensities of the emitted positive and negative ion signal to the intensity of the Zr^{+} ion signal and to the ZrO_2^{-} ion signal were

$Zr^+ : ZrO^+ : ZrO_2^+ = 1 : 1.3 : 0.05$

$O^- : O_2^- : ZrO^- : ZrO_2^- : ZrO_3^- = 21.0 : 0.82 : 0.17 : 1 : 0.67$ (3-13)

Surfaces which have two or more components can be sputtered selectively. Contradictory observations have been reported on the selective sputtering of zirconium oxide. Kelly has reported that zirconium oxide is sputtered congruently;[53] on the other hand, a few investigators have reported that zirconium oxide preferentially loses oxygen.[54] If we assume that the effect of the selective sputtering is negligible, S is given to be 0.124. The sputtering yield Y_{oxide} is estimated by assuming that the ratio Y_{metal} / Y_{oxide} of the Ar^+-ion beam at 2 keV is the same for the Kr^+ ion beam at 10 keV.[52]

In our measurement the value $N_{oxide}(Zr^+, E=10eV, \Theta=45^\circ) / N(Zr^+, E=10eV, \Theta=45^\circ)$ is *ca.* 300 from the measurement at 773 K and 6.7×10^{-4} Pa. Then, using eqns. (3-11) and (3-12) we can estimate

$$P(Zr^+, E=10eV, \Theta=45^\circ) = 4.8 \times 10^{-4} \quad (3\text{-}14)$$

$P(Zr^+, E, \Theta)$ is given theoretically by eqn. (3-9). Assuming that $\langle n_a(0) \rangle = 1$, we have calculated the double integral of eqn. (3-6) numerically and estimated that $P(Zr^+, E=10eV, \Theta=45^\circ)$ is 5.1×10^{-4} for $\gamma = 2.25 \times 10^{10}$ m^{-1}. Several investigators have determined γ experimentally and theoretically. The values of γ are listed in Table 3-2. Lang and Nørskov have suggested[36] that the value of γ is nearly equal to the inverse of the Bohr radius (1.9×10^{10} m^{-1}). The value

Table3-2. Exponential decay coefficient of $\Delta(z)$

emitted particle/substrate	$\gamma/10^{10}\ m^{-1}$	ref.
Cu^+/Cu	2.3	42
Na/W(110)	1.74	43
Cs^+/Al	1.32	45
O^-/jellium	0.95–1.32	44

of γ estimated by us is in agreement with that value.

Vasile has determined the ionization probability of sputtered particles from the zirconium surface experimentally.[39] From his result the probability $P(Zr^+, E=10eV, \Theta=45°)$ is estimated to be *ca.* 1.2×10^{-3}, which is of approximately the same order as our value.

From the above discussion, we can explain the reason why the yield of the zirconium ion is increased by the oxide formation: since the Fermi level of the zirconium metal is above the ionization level, the ionization probability is very low. The vast majority of the sputtered species from the metal surface are neutral zirconium atoms.[55] On the other hand, the Zr^+ ions are sputtered from the oxide surface, because the top of the oxygen 2p valence band is below the ionization level and the zirconium ion in the oxide has the positive charges as an initial state.

Depth Profile Analysis

The depth profiles were measured at room temperature after the

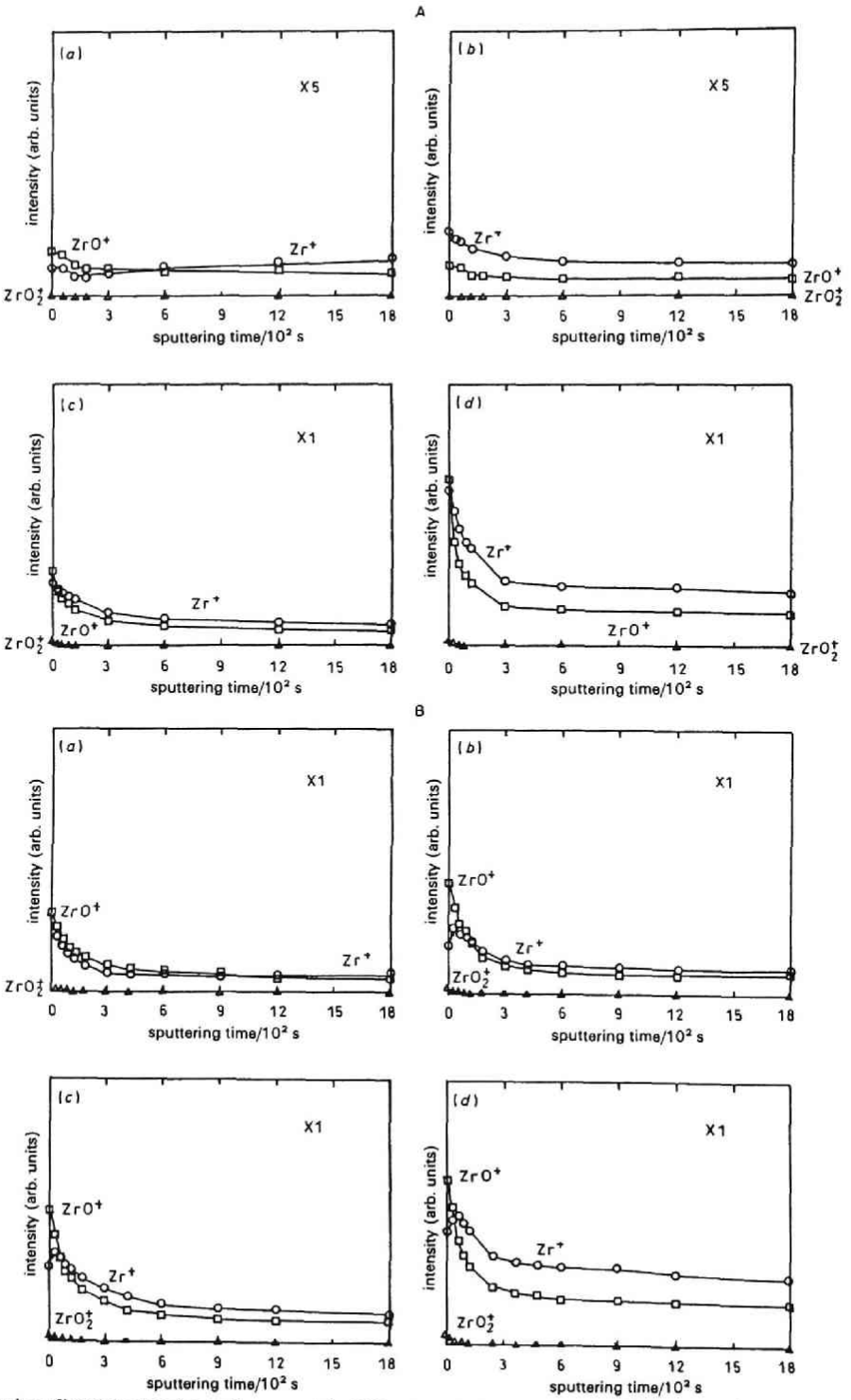

Fig. 3-4. Depth profiles of the zirconium surface exposed for 3600 s at constant oxygen pressures of (A) 1.3×10^{-4} and (B) 1.3×10^{-3} Pa at temperatures of: (*a*) 1073, (*b*) 973, (*c*) 873 and (*d*) 773 K.

exposure of oxygen for 3600 s at temperatures of 773 - 1073 K using a 2 keV argon-ion beam at a current of 13 $\mu A \cdot cm^{-2}$. Reproducible data were obtained for different specimens. Typical results of the depth profile measurements after the exposure of oxygen at 1.3×10^{-4} and 1.3×10^{-3} Pa are shown in Fig. 3-4A and Fig. 3-4B, respectively. Since atomic mixing by the ion bombardment may have an effect on the depth profile resolution,[24] the thickness of the surface oxide and the concentration profile of oxygen would not be exactly determined. However, it seems that the three characteristic properties are deduced from the measurement. First, the intensities of the Zr^+, ZrO^+ and ZrO_2^+ ion signals are generally decreased on going from the surface to the bulk, excepting that the intensity of the zirconium ion signal has a maximum at *ca.* 30-60 s at the high oxygen pressure of 1.3×10^{-3} Pa as shown in Fig. 3-4B. It cannot be unambiguously determined whether the maximum is due to a high concentration region in the subsurface[16] or due to experimental effects such as atomic mixing or the migration of oxygen when the specimen was cooled. Secondly, at higher temperatures the ion signal intensities are more uniformly distributed between the surface to the bulk, and at lower temperatures the region of the high ion signal intensities appears at the surface, which would suggest that the oxides are formed at the surface. Thirdly, the regions of the high ion signal intensities at higher pressures of oxygen are found deeper than at lower pressures.

The amount of oxygen at the surface is determined by the dynamic competition between the transport processes at the surface (*e.g.* the dissociative adsorption and the transfer process from the surface

into the bulk site) and the diffusion process in the bulk.[25,30-31] We have previously shown that the diffusion rate of oxygen into the bulk at higher temperatures (*e.g.* > 973 K at 6.7×10^{-5} Pa) is much faster than the rates of the surface processes and that diffusion rate would be slower at the lower temperatures.[30-31] Therefore, the ion signal intensities are uniformly distributed at a low level at high temperatures. The absorption rate would determine the pressure dependence of the depth profile, because the absorption rate on the metal surface is proportional to the pressure of oxygen and the rate on the oxide-covered surface is proportional to the square root of the oxygen pressure.[31]

Conclusion

An increase in the yield of the secondary ions Zr^+, ZrO^+ and ZrO_2^+ by oxidation of zirconium at oxygen pressures of 6.7×10^{-5} - 1.3×10^{-3} Pa and at temperatures of 773 - 1073 K has been measured using SIMS. Existence of three sequential stages of the increase in the yields has been found:(i) the first stage in which the surface remains as α-zirconium and the yields of the secondary ions increase slowly as a function of oxygen exposure time; (ii) the second stage in which nucleation of oxide causes rapid increase of the ion yields; (iii) the final stage in which the surface is covered with the oxide and the ion yields show saturation. The surface remains as α-zirconium longer at lower pressures of oxygen and at higher temperatures. An increase of the yield of the Zr^+ ions is explained by assuming that the ionization probability of the sputtered atoms determines the ion yield uniquely and estimating the ionization

probability of the zirconium atoms. The increase of the probability is due to the fact that the first ionization level of zirconium atom is below the Fermi level of the bulk metal and the top of the oxygen 2p valence band of the oxide is below the ionization level of the metal atom. Dynamic competition between transport of oxygen at the surface and diffusion of oxygen into the bulk determines the depth profile of oxygen.

References for Chapter 3

1. B. W. Veal, D. J. Lam and D. G. Westlake,
   Phys. Rev. B, 1979, 19, 2856.
2. J. Frandon, B. Brousseau and F. Pradal,
   Phys. Stat. Sol.(b), 1980, 98, 379.
3. J. S. Foord, P. J. Goddard and R. M. Lambert,
   Surf. Sci., 1980, 94, 339.
4. R. L. Tapping, *J. Nucl. Mater.*, 1982, 10, 151.
5. L. R. Danielson, *J. Vac. Sci. Technol.*, 1982, 20, 86.
6. G. B. Hoflund, D. F. Cox and R. E. Gilbert,
   J. Vac. Sci. Technol. A, 1983, 1, 1837.
7. P. Sen, D. D. Sarma, R. C. Budhani, K. L. Chopra and C. N. R. Rao,
   J. Phys. F., 1984, 14, 565.
8. M. Y. Zhou, R. H. Milne, M. A. Karolewski, D. C. Frost and K. A. R. Mitchell, *Surf. Sci.*, 1984, 139, L181.
9. G. B. Hoflund, D. A. Asbury and D. F. Cox,
   Appl. Surf. Sci., 1985, 22/23, 252.
10. K. C. Hui, R. H. Milne, K. A. R. Mitchell, W. T. Moore and M. Y. Zhou,
    Solid State Commun., 1985, 56, 83.

11. T. A. Sasaki and Y. Baba, *Phys. Rev. B*, 1985, 31, 791.

12. K.-O. Axelsson, K.-E. Keck and B. Kasemo,
Surf. Sci., 1985, 164, 109.

13. P. C. Wong and K. A. R. Mitchell, *Can. J. Chem.*, 1986, 64, 2409.

14. P. C. Wong, K. C. Hui, B. K. Zhong and K. A. R. Mitchell,
Solid State Commun., 1987, 62, 293.

15. P. C. Wong and K. A. R. Mitchell, *Can. J. Phys.*, 1987, 65, 464.

16. G. R. Corallo, D. A. Asbury, R. E. Gilbert and G. B. Hoflund,
Phys. Rev. B, 1987, 35, 9451.

17. G. B. Hoflund, G. R. Corallo, D. A. Asbury and R. E. Gilbert,
J. Vac. Sci. Technol. A., 1987, 5, 1120.

18. C. Palacio, J. M. Sanz and J. M. Martinez-Duart,
Surf. Sci., 1987, 189/190, 175.

19. C. Palacio, J. M. Sanz and J. M. Martinez-Duart,
Surf. Sci., 1987, 191, 385.

20. J. M. Sanz, C. Palacio, Y. Casas and J. M. Martinez-Duart,
Surf. Interface Anal., 1987, 10, 177.

21. P. Aebi, M. Erbudak, A. Leonardi and F. Vanini,
J. Electron Spectrosc. Relat. Phenom., 1987, 42, 351.

22. P. E. West and P. M. George,
J. Vac. Sci. Technol. A, 1987, 5, 1124.

23. C. O. De González and E. A. García, *Surf. Sci.*, 1988, 193 305.

24. D. P. Valyukhov, M. A. Golubin, D. M. Grebenshchikov and
V. I. Shestopalova, *Sov. Phys. Solid State*, 1982, 24, 1594.

25. G. N. Krishnan, B. J. Wood and D. Cubicciotti,
J. Electrochem. Soc., 1981, 128, 191.

26. C. J. Rosa, *J. Less-Common Met.*, 1968, 16, 173.

27. P. Paetz and F. Sperner, in *Gase und Kohlenstoff in Metallen*, ed. E. Fromm and E. Gebhardt (Springer, Berlin, 1976), pp. 419-430.
28. M. Dechamps and P. Lehr, *C. R. Acad. Sci., Ser. C*, 1970, 270, 169.
29. M. Nagasaka, E. Ueda and T. Yamashina, *Vacuum*, 1973, 23, 51.
30. M. Yamamoto, S. Naito, M. Mabuchi and T. Hashino, *J. Phys. Chem.*, 1989, 93, 5203.
31. H. Takeuchi, S. Naito, M. Yamamoto and T. Hashino, *J. Chem. Soc. Faraday Trans. 1*, 1988, 84, 4235.
32. W. N. Delgass, L. L. Lauderback, and D. G. Taylor, in *Chemistry and Physics of Solid State Surface IV*, ed. R. Vanselow and R. Howe (Springer, Berlin, 1982), pp. 51-76.
33. G. K. Wehner, in *Methods of Surface Analysis*, ed. A. W. Czanderna (Elsevier, Amsterdam, 1975), pp. 5-37, J. A. McHugh, in *Methods of Surface Analysis*, ed. A. W. Czanderna (Elsevier, Amsterdam, 1975), pp. 223-273.
34. T. Miyano, Y. Sakisaka, T. Komeda and M. Onchi, *Surf. Sci.*, 1986, 169, 197.
35. *Handbook of Chemistry and Physics*, 67th edition, ed. R. C. Weast, M. J. Astle, and W. H. Beyer (CRC, Florida, 1986), pp. E-76 - E-77 and pp. E-89 - E-90.
36. N. D. Lang and J. K. Nørskov, *Physica Scripta*, 1983, T6, 15.
37. M. Morinaga, H. Adachi and M. Tsukada, *J. Phys. Chem. Solids*, 1983, 44, 301.
38. A. Benninghoven, *Surf. Sci.*, 1975, 53, 596.
39. M. J. Vasile, *Phys. Rev. B*, 1984, 29, 3785.
40. C. N. R. Rao and D. D. Sarma, *Phys. Rev. B*, 1982, 25, 2927.
41. A. Benninghoven, F. G. Rudenauer and H. W. Werner,

Secondary Ion Spectrometry (Chemical analysis vol.86)
(John Wiley & Sons, New York, 1987), pp.296-328 and references therein.

42. J.K.NørskovandB.I.Lundqvist, *Phys.Rev.B*, 1979, 19, 5661.

43. R. Brako and D. M. Newns, *Surf. Sci.*, 1981, 108, 253.

44. N. D. Lang, *Phys. Rev. B*, 1983, 15, 2019.

45. M. L. Yu and N. D. Lang, *Phys. Rev. Lett.*, 1983, 50, 127.

46. E. R. Gagliano, E. C. Goldberg, M. C. G. Passegi and J. Ferron,
Phys. Rev. B, 1985, 31, 6988.

47. D. P. Woodruff and T. A. Delchar,
Modern Techniques of Surface Science,
(Cambridge Univ., Cambridge, 1986), pp.196-199.

48. A. C. Hewson and D. M. Newns,
Jpn. J. Appl. Phys. Suppl., 2, 121, 1974.

49. O. Jepsen, O. K. Andersen and A. R. Mackintosh,
Phys. Rev. B, 1975, 12, 3084.

50. Z. -W. Lu, D. Singh and H. Krakauer, *Phys. Rev. B*, 1987, 36, 7335.

51. R. B. Wright, M. J. Pellin and D. M. Gruen,
Surf. Sci., 1981, 110, 151.

52. R. Kelly and N. Q. Lam, *Radiation Effects*, 1973, 19, 39.

53. R. Kelly, *Nucl. Instr. Methods*, 1978, 149, 553.

54. L. I. Yin, S. Ghose and I .Adler, *Appl. Spectrosc.*, 1972, 26, 355.
T. Tanabe, M. Tanaka and S. Imoto, *Surf. Sci.*, 1987. 187. 499.

55. D. M. Gruen, A. R. Krauss, M. J. Pellin and R. B. Wright,
in *Chemistry and Physics of Solid State Surface IV*,
ed. R. Vanselow and R. Howe (Springer,Berlin, 1982), pp.107-122.

Chapter 4

Anomaly in the Rate of Oxygen Absorption by Zirconium due to the Formation of Oxide at the Surface·

Introduction

It is well known that metal oxidation occurs through the three stages of dissociative adsorption of oxygen molecules, nucleation of oxide and growth of the oxide for many metals. The adsorption rate at the growth stage of zirconium oxide was studied over wide ranges of temperature and pressure of oxygen by a number of authors in the 1960s.[1] The adsorption rate during dissociative adsorption of oxygen by α-zirconium has been investigated in our previous work.[2] However, few studies have been reported on the rate of oxygen absorption during the nucleation of oxide.

Recently, a number of surface spectroscopic studies (*e.g.* AES,[3] EELS,[4] XPS,[5-6] UPS,[6] LEED[7] and ISS[8]) have been reported on the surface oxidation of zirconium at room temperature. However, the dynamic properties of oxygen absorption at high temperature which depend on both temperature and oxygen pressure have not been discussed in detail in these studies.

· Published in *J. Chem. Soc., Faraday Trans.*, 1990, 86, 3797.

The purpose of this work is to investigate the rate of oxygen absorption during the nucleation and growth of oxide at high temperatures and low pressures of oxygen. An anomaly in the rate of oxygen absorption at the nucleation stage was observed: the rate was increased by the formation of oxide at the surface. A number of investigators have reported the anomaly in the rate of oxygen absorption during the nucleation of surface oxide[9-10] and the anomaly of the increase of the Auger electron intensity of oxygen on zirconium[11] and nickel surfaces[12] at the nucleation stage. In these studies it has been suggested that the anomaly is due to the preparation of adsorption sites by surface diffusion of oxygen adatoms to the nearest oxide nucleus.[9,12] In this model the transport of oxygen adatoms into the bulk and the adsorption of oxygen on the oxide island have been neglected. However, these two processes should be considered in the case of the absorption of oxygen by zirconium at high temperatures.

In the present study the rate of oxygen absorption at the nucleation stage is numerically evaluated on the following assumptions: (i)The surface of zirconium at the nucleation stage is composed of oxide and α-zirconium, (ii)the change in the coverage of oxide with time is evaluated by using a model in which nucleation and growth of surface oxide is approximated by an autocatalytic reaction,[12] and (iii) the absorption of oxygen by the α-zirconium surface[2] and by the oxide-covered surface[13] occurs simultaneously. The total rate of oxygen absorption at the nucleation stage is determined by the coverage of oxide and of α-zirconium. The change in the calculated coverage of oxide with time is compared with the results of the SIMS measurement.[14]

Experimental

The change in the amount of absorbed oxygen with time (absorption curve) was measured volumetrically with a stainless steel UHV apparatus, which has a base pressure of 2.0×10^{-8} Pa. Details of the experimental apparatus and procedure have been described previously.[2]

The specimen was of the form of a sphere (*ca.* 5.0 mm in diameter) machined from a polycrystalline zirconium bar of purity 99.8% (O 690 ppm, Fe 430 ppm, Cr 100ppm, Hf 80ppm and C 50 ppm). The specimen was mechanically polished, ultrasonically degreased in acetone and then heated inductively to 1070 K for 24 - 36 h in a vacuum chamber at a pressure less than 10^{-7} Pa. Using the results of the SIMS measurements we have previously shown[2] that the heat treatment considerably decreases surface contaminant concentrations including oxygen, water, carbon monoxide, carbon and nitrogen, and chlorine is segregated to the surface from the bulk during the heat treatment. The segregation of the other impurities such as iron and chromium was not found by our SIMS measurements. It has been shown that the effect of the segregated chlorine on the rate of oxygen absorption is within the limits of an experimental error under our experimental conditions.[2]

The specimen supported by a platinum wire was heated to a given temperature and the oxygen gas stored in the reservoir was then introduced into the specimen chamber. During the measurement the pressure in the specimen chamber was kept constant. The amount of oxygen absorbed by the specimen was determined by the amount of oxygen supplied.

Results

Absorption curves were measured at constant oxygen pressures of 1.3×10^{-3}, 1.3×10^{-4} and 6.7×10^{-5} Pa over the temperature range 743 - 1098 K. Reproducible data were obtained for different specimens, and the uncertainty in the experimental results is less than 10 %. Fig. 4-1(a), 4-1(b) and 4-1(c) show the typical absorption curves obtained at oxygen pressure of 1.3×10^{-3} Pa, 1.3×10^{-4} Pa and 6.7×10^{-5} Pa, respectively.

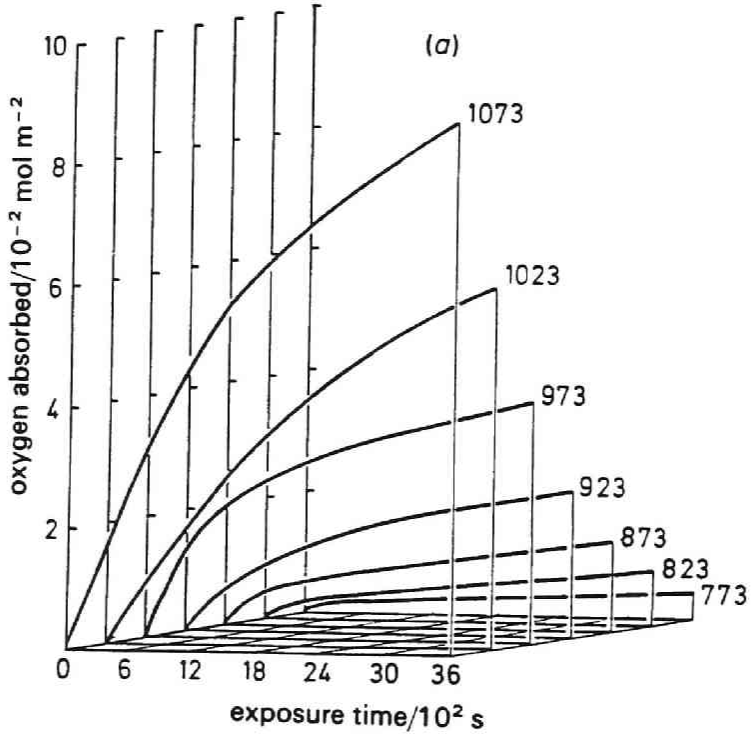

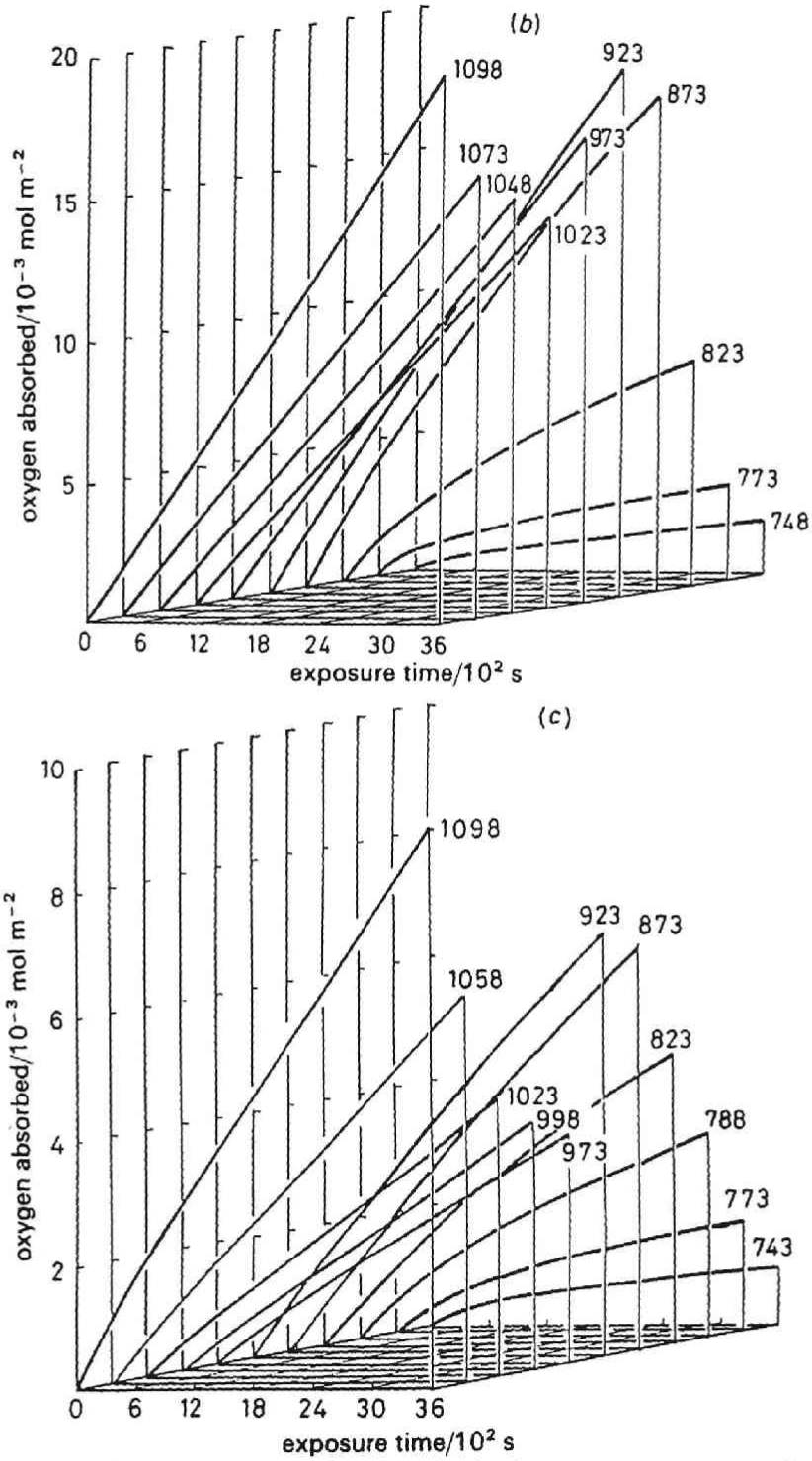

Fig. 4-1. Typical absorption curves obtained at oxygen pressures of 1.3×10^{-3} Pa (*a*), 1.3×10^{-4} Pa (*b*) and 6.7×10^{-5} Pa (*c*). Temperatures (in K) are indicated on the figure.

An anomaly in the rate of oxygen absorption has been observed at 973 K under a pressure of 1.3×10^{-4} Pa and at 923 K under a pressure of 6.7×10^{-5} Pa. That is, under these conditions, the rate is increased even though the temperature is decreased. The temperatures T_a at which the anomaly was observed decreased as the pressure of oxygen decreased.

It has been found that the rate is proportional to the square root of time (*i.e.* parabolic) at lower temperatures and higher pressures of oxygen (773 - 823 K, 1.3×10^{-3} Pa; 748 - 823 K, 1.3×10^{-4} Pa; 743 - 773 K, 6.7×10^{-5} Pa). We have previously reported that the rate of oxygen absorption at higher temperatures and lower pressures of oxygen (1098 - 1023 K, 1.3×10^{-4} Pa; 1098 - 973 K, 6.7×10^{-5} Pa) is nearly constant with respect to time (*i.e.* linear) and is almost directly proportional to the oxygen pressure.[2]

Discussion

Oxygen Absorption by Oxide-covered Zirconium

A parabolic rate of oxygen absorption has been observed when the surface of zirconium is covered by oxide.[1,13] The surface oxide formed at the early stage of oxygen exposure has been observed by SIMS measurements in conditions under which the parabolic absorption rate is observed, *i.e.* low temperatures and high pressures of oxygen.[14] The parabolic rate of oxygen absorption can be explained by

a model involving oxygen diffusion into the bulk with a moving boundary of oxide/metal interface.[1,13] The change in the electric resistivity caused by oxygen absorption, which is determined by the oxygen concentration calculated by the use of this model, is in agreement with the experimental results.[13] Electric-field and space-charge effects associated with the diffusion of charged oxygen atoms in the oxide may be included implicitly in this model, because we have used the diffusion constant[1] which was determined by fitting the oxide growth rate calculated by the present model of oxygen diffusion to the oxide growth rate measured.

The differential equations of oxygen diffusion through the oxide-covered substrate may be given by[1,13]

$$\partial C/\partial t = D(1/r^2)\partial(r^2\partial C/\partial r)/\partial r; \quad \text{for} \quad r=[0, x(t)] \tag{4-1}$$

$$\partial C/\partial t = D_{ox}(1/r^2)\partial(r^2\partial C/\partial r)/\partial r; \quad \text{for} \quad r=[x(t), \ell] \tag{4-2}$$

with the boundary conditions

$$(\partial C/\partial r)|_{r=0}=0 \tag{4-3}$$

$$D_{ox}(\partial C/\partial r)|_{r=\ell}=f[C_o-C(\ell)] \tag{4-4}$$

$$\partial x/\partial t = (C_o - C_m)^{-1}[D(\partial C/\partial r)|_{r=x-0} - D_{ox}(\partial C/\partial r)|_{r=x+0}] \tag{4-5}$$

Here C is the normalized concentration of oxygen, t is time of oxygen exposure, r is the distance from the centre of the

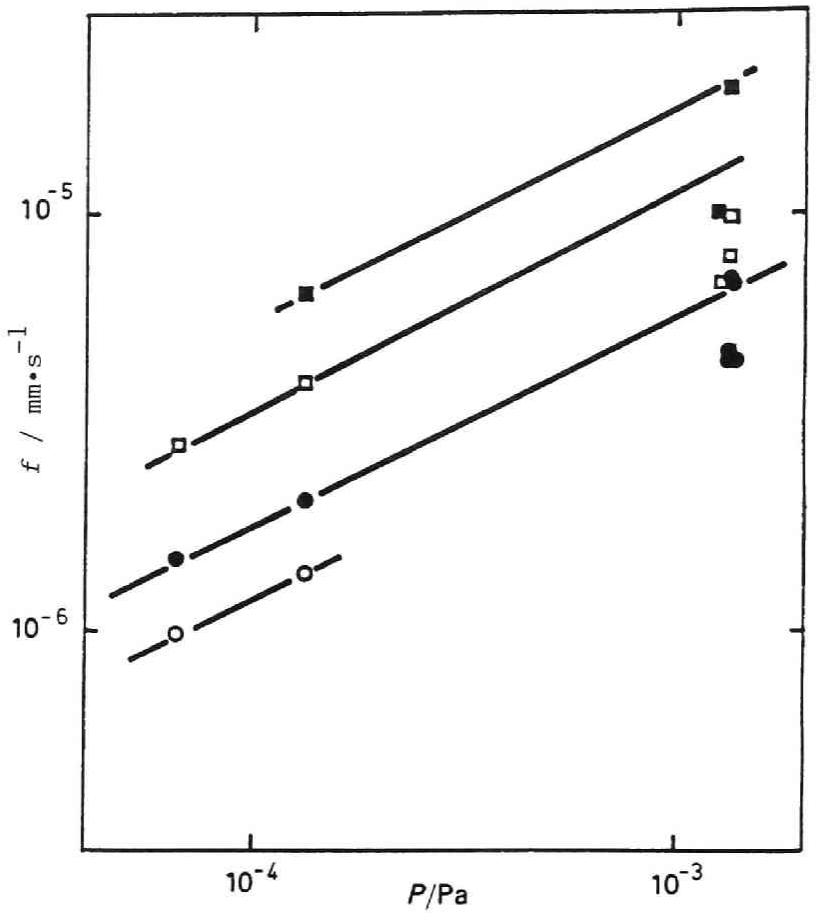

Fig. 4-2. Pressure dependence of the kinetic parameter f: (○) 743 and 748 K, (●) 773 K, (□) 823 K, (■) 873 K.

specimen with radius ℓ, D and D_{ox} are the diffusion constants of α-zirconium and oxide, [1,15] respectively, $x(t)$ is the boundary between oxide and α-zirconium and C_m and C_o indicate the concentration of oxygen in the state of maximum solubility in α-zirconium and the minimum concentration of oxygen in zirconium oxide, respectively. We used C_m = 0.20 (O/Zr = 0.40) and C_o = 0.98 (O/Zr = 1.96) obtained from the

phase diagram of the oxygen-zirconium system.[1,15]

We solve the diffusion equations numerically, and the amount of oxygen absorbed, $W(t)$, is determined by integrating the flux of oxygen at the surface [see eqn. (4-4)] from the time 0 to t. By adjusting the kinetic parameter, f, we obtain the absorption curves which best fit the parabolic absorption curves measured. As shown in Fig. 4-2, it has been found that f is proportional to the square root of the oxygen pressure. This means that the transfer of oxygen adatoms into the bulk sites of the oxide limits the flux of oxygen at the surface, if adsorption and desorption of oxygen on the oxide-covered surface are assumed to be in partial equilibrium.[13] From the temperature dependence of $(f/P^{1/2})$, as shown in Fig. 4-3, it has been found that the activation energy for the transfer of oxygen adatoms on the oxide-covered surface into the bulk sites is $(1.0 \pm 0.1) \times 10^{-19}$ J per O atom. Thus, we obtain the kinetic parameter f

$$f=2.7P^{1/2}\exp(-7.6\times10^{3}T^{-1}) \qquad /\mathrm{mm\cdot s^{-1}} \qquad (4\text{-}6)$$

The calculated rate of oxygen absorption by oxide-covered surface is greater than the calculated rate of oxygen absorption by α-zirconium under our experimental conditions. This may be due to the following: First, the activation energy for the transfer of oxygen adatoms on the oxide-covered surface into the bulk is *ca.* one half of the energy difference 2.2×10^{-19} J per O atom between the adsorption sites and the bulk sites of α-zirconium.[2] Secondly, the diffusion constant of oxygen in oxide [$(1.1 \times 10^{-7} \exp(-14700T^{-1})$ $/\mathrm{m^2 s^{-1}}$][1] is much greater than that in

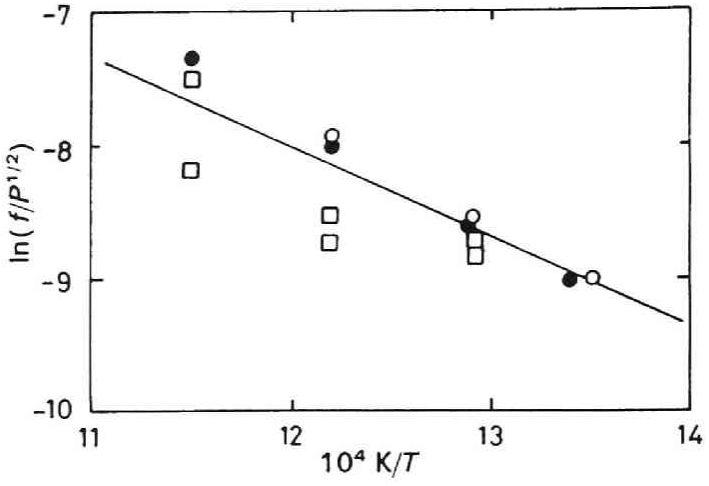

Fig.4-3. Arrhenius plot of ($f/P^{1/2}$) to evaluate the activation energy for the transfer of oxygen adatoms into the bulk oxide: (□) 1.3×10^{-3} Pa, (●) 1.3×10^{-4} Pa, (○) 6.7×10^{-5} Pa.

α-zirconium [$5.4 \times 10^{-4} \exp(-25600T^{-1})$ /$m^2 s^{-1}$][1] under our experimental conditions.

The calculated thicknesses of the oxide layer formed after exposure of oxygen for 3600 s are: 14.5 nm at 773 K and 6.8 nm at 823 K at 1.3×10^{-3} Pa; 6.5 nm at 748 K and 5.2 nm at 773 K at 1.3×10^{-4} Pa; and 1.8 nm at 743 K and 1.0 nm at 773 K at 6.7×10^{-5} Pa.

Oxygen Absorption by α-Zirconium

In previous work[2] we have shown that the rate of oxygen absorption at temperatures above T_a is limited by the dissociative adsorption of oxygen, and that no transition of the metal surface to the oxide surface is found above T_a by SIMS. Thereby, we can

identify the linear absorption of oxygen at high temperatures and lower pressures as the absorption by α-zirconium. The linear absorption rate has been explained by using a model in which the absorption process comprises three successive steps:[2] the dissociative adsorption of oxygen molecules on the zirconium surface with interaction between oxygen adatoms, the transfer of adatoms at the surface sites to the outermost bulk sites and the diffusion of oxygen atoms into the bulk. Kinetic parameters in the model have been determined:[2] the activation energy for adsorption is $(7.4 \pm 0.6) \times 10^{-20}$ J per O atom, the energy of the attractive interaction is -4×10^{-21} J per O-O pair and the adsorption site has a potential energy lower by $(2.2 \pm 0.1) \times 10^{-19}$ J per O atom than the site in the bulk.

Oxygen Absorption during the Oxide Nucleation Stage

The anomaly in the rate of oxygen absorption may be due to the nucleation of oxide at the surface, because the nucleation stage at which the intensity of the secondary ion Zr^+ increases rapidly was observed at 873 K under oxygen pressures of 1.3×10^{-4} Pa and 6.7×10^{-5} Pa in our SIMS measurement.[14] The anomaly at the nucleation stage was observed in other transition metal-oxygen systems.[9-12] The absorption rate observed at the nucleation stage is faster than the calculated rate of oxygen absorption by α-zirconium and is slower than the calculated rate of oxygen absorption by oxide-covered zirconium. This fact supports the conclusion that the oxidation at the surface is in the nucleation stage.

A number of investigators have studied theories of nucleation and growth, *e.g.* stochastic model,[16] the kinetic Ising model simulated by Monte Carlo methods[17] and the two-dimensional diffusion model.[9,12] The transfer of oxygen adatoms into the bulk as well as on the surface should be considered in the high-temperature oxidation of zirconium. We assume that nucleation and growth of quasi two-dimensional oxide islands by the transfer of oxygen from the perimeter of the islands is approximated by the autocatalytic chemical reaction.[12]

Although formation of surface suboxides of zirconium at the Zr/ZrO_2 interface[5] or surface reconstruction[7] at the early stages of oxidation have been reported recently, we assume that the surface of zirconium at the nucleation stage is composed of α-zirconium and oxide, and that the absorption of oxygen by α-zirconium and by the oxide-covered zirconium occurs simultaneously at the nucleation stage. We calculate the rates of oxygen absorption by α-zirconium and oxide-covered zirconium separately by using the kinetic parameters of the rate of oxygen absorption by α-zirconium[2] and the kinetic parameter , f, of the rate of oxygen absorption by the oxide-covered zirconium. The total rate of oxygen absorption is determined by the sum of the product of the absorption rate and oxide coverage for oxide-covered zirconium and the corresponding product for α-zirconium.

The coverage of oxide is evaluated by the use of the following autocatalytic nucleation model. The autocatalytic reaction of oxide island growth may be given by[18]

$$O(s) + O(ox) \underset{V_2}{\overset{V_1}{\rightleftharpoons}} 2O(ox) \qquad (4\text{-}7)$$

where (s) and (ox) indicate the α-zirconium and the oxide, respectively. The oxide nucleation reaction may be given by

$$O(s) + O(s) \underset{V_4}{\overset{V_3}{\rightleftharpoons}} 2O(ox) \qquad (4\text{-}8)$$

O(ox) and O(s) are approximated to the coverage of oxide, **a**, and the coverage of oxygen adatoms on α-zirconium, Θ, respectively. The coverage of oxygen adatoms, Θ, is calculated using a model of oxygen absorption by α-zirconium at oxygen pressures of 1.3×10^{-3} Pa, 1.3×10^{-4} Pa and 6.7×10^{-5} Pa.[2]

The time evolution of the oxide coverage, **a**, is given by

$$d\mathbf{a}/dt = V_1 \mathbf{a}\Theta - V_2 \mathbf{a}^2 + 2V_3\Theta^2 - 2V_4 \mathbf{a}^2$$

$$= -V_{24}\mathbf{a}^2 + V_1 \mathbf{a}\Theta + 2V_3\Theta^2 \qquad (4\text{-}9)$$

$$V_{24} = 2V_4 + V_2 \qquad (4\text{-}10)$$

In order to understand the dynamic quality of the solution of this non-linear equation intuitively, we consider the eqn. (4-9) an example of the equation of motion for an overdamped anharmonic oscillator.[18] The potential $V(\mathbf{a})$ of this system has the form

$$V(\mathbf{a}) = V_{24}\mathbf{a}^3/3 - V_1\Theta\mathbf{a}^2/2 - 2V_3\Theta^2\mathbf{a}. \qquad (4\text{-}11)$$

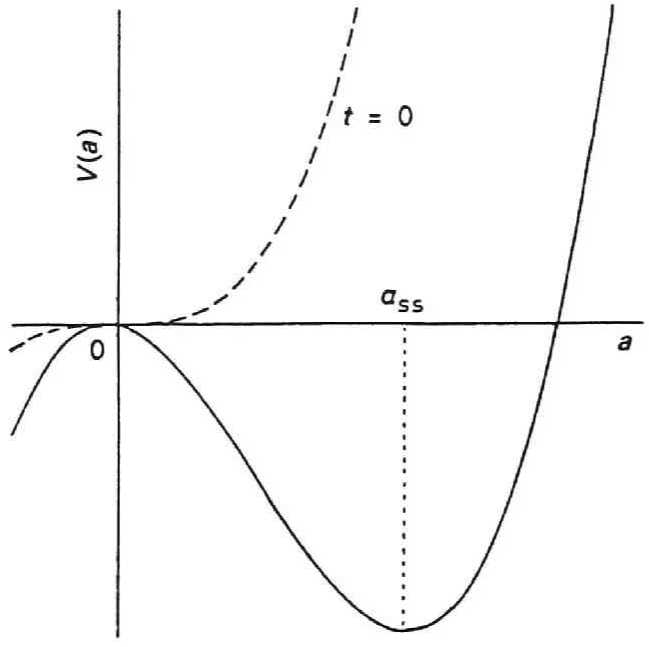

Fig. 4-4. Potential of the anharmonic oscillator given by a third-order polynomial (eqn. 4-11). (– – –) Potential at $t = 0$; a_{ss} indicates the stable steady state.

The potential is shown schematically in Fig. 4-4. We can expect that the coverage **a** increases from **a**=0 at t=0 to the coverage in the stable steady state, a_{ss}. Here, a_{ss} is given by

$$a_{ss} = \Theta[V_1 + (V_1^2 + 8V_{24}V_3)^{1/2}]/2V_{24} \qquad \leq 1. \qquad (4\text{-}12)$$

In the calculation of the time evolution of **a**, we approximate V_1 and V_3 to be constants. The temperature dependences of V_2 and V_4 are expected to be much greater than those of V_1 and V_3, because the oxide phase is stable thermodynamically and the activation energy for the decomposition of oxide should be greater than that of formation of

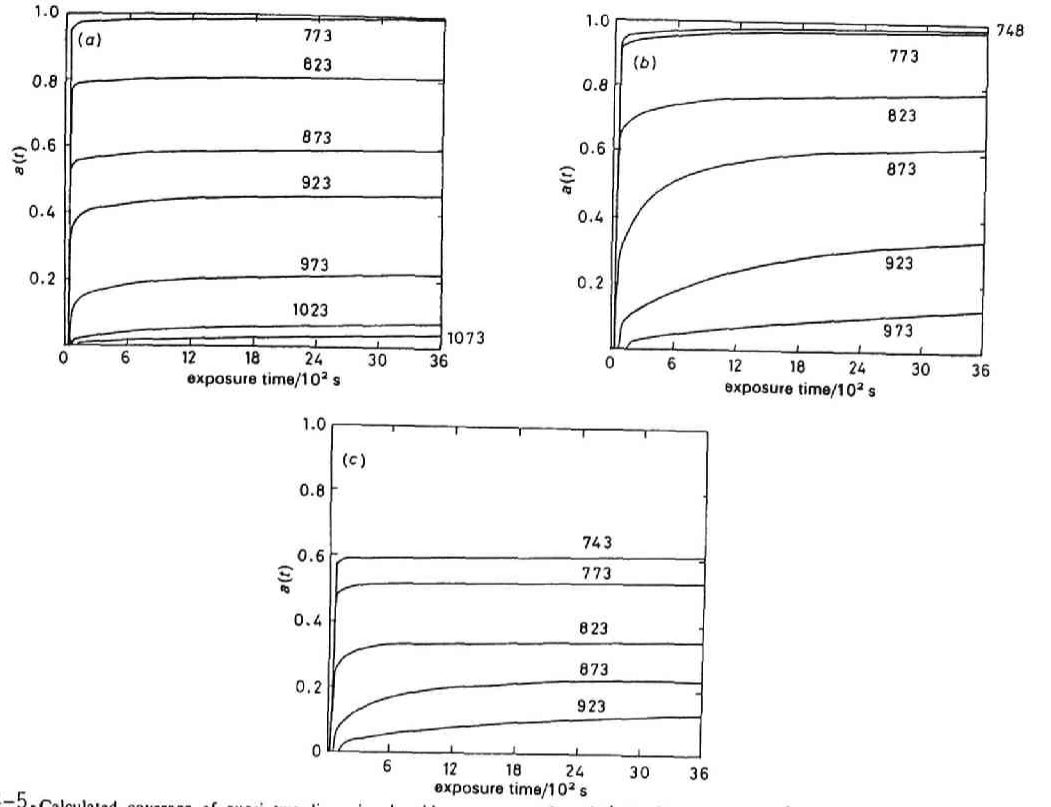

Fig. 4-5. Calculated coverage of quasi two-dimensional oxide as a function of exposure time at oxygen pressures of 1.3×10^{-3} Pa (*a*), 1.3×10^{-4} Pa (*b*) and 6.7×10^{-5} Pa (*c*). Temperatures (*in* K) are indicated on the figure.

oxide. By adjusting the kinetic parameter V_{24} we calculate the oxide coverage, **a** [see Fig. 4-5(a) - 4-5(c)], and obtain absorption curves which best fit the experimental absorption curves. Typical curves are shown in Fig. 4-6. The values used for the numerical calculations include $V_1 = 1.0$ and $V_3 = 1.0 \times 10^{-4}$.

At lower temperatures and higher pressures of oxygen, the oxide coverage calculated increases more rapidly and the saturation level of the oxide coverage is increased. We have recently

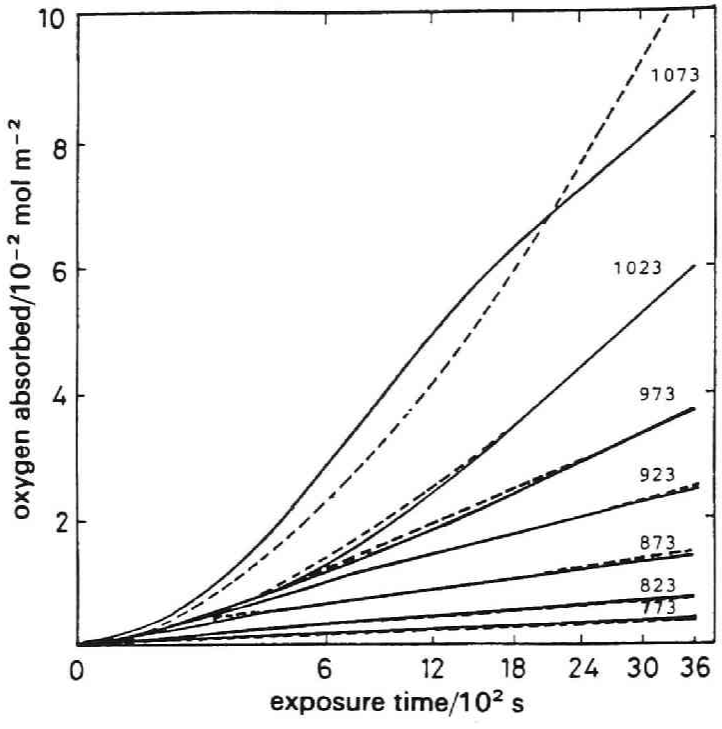

Fig.4-6. Absorption curves at oxygen pressures of 1.3×10^{-3} Pa. The solid and broken lines show the measured and calculated absorption curves, respectively. Temperatures (in K) are indicated on the figure. The abscissa is scaled by square root of the time of oxygen exposure.

reported SIMS measurements of oxidation of zirconium at high temperatures 773-1073 K and low oxygen pressures 6.7×10^{-5} - 6.7×10^{-4} Pa, and have shown that the yield of the secondary Zr^+ ion is increased *ca.* 300 times by oxide formation at the surface.[14] The increase in the yield gives information on the dynamics of the oxide nucleation. It can be seen from Fig. 4-7A and 4-7B that the dependence of the increase in the yield of Zr^+ ion on temperature and oxygen pressure is in good agreement with the temperature and pressure dependences of the increase in the oxide coverage, as shown in Fig. 4-5(b) and 4-5(c),

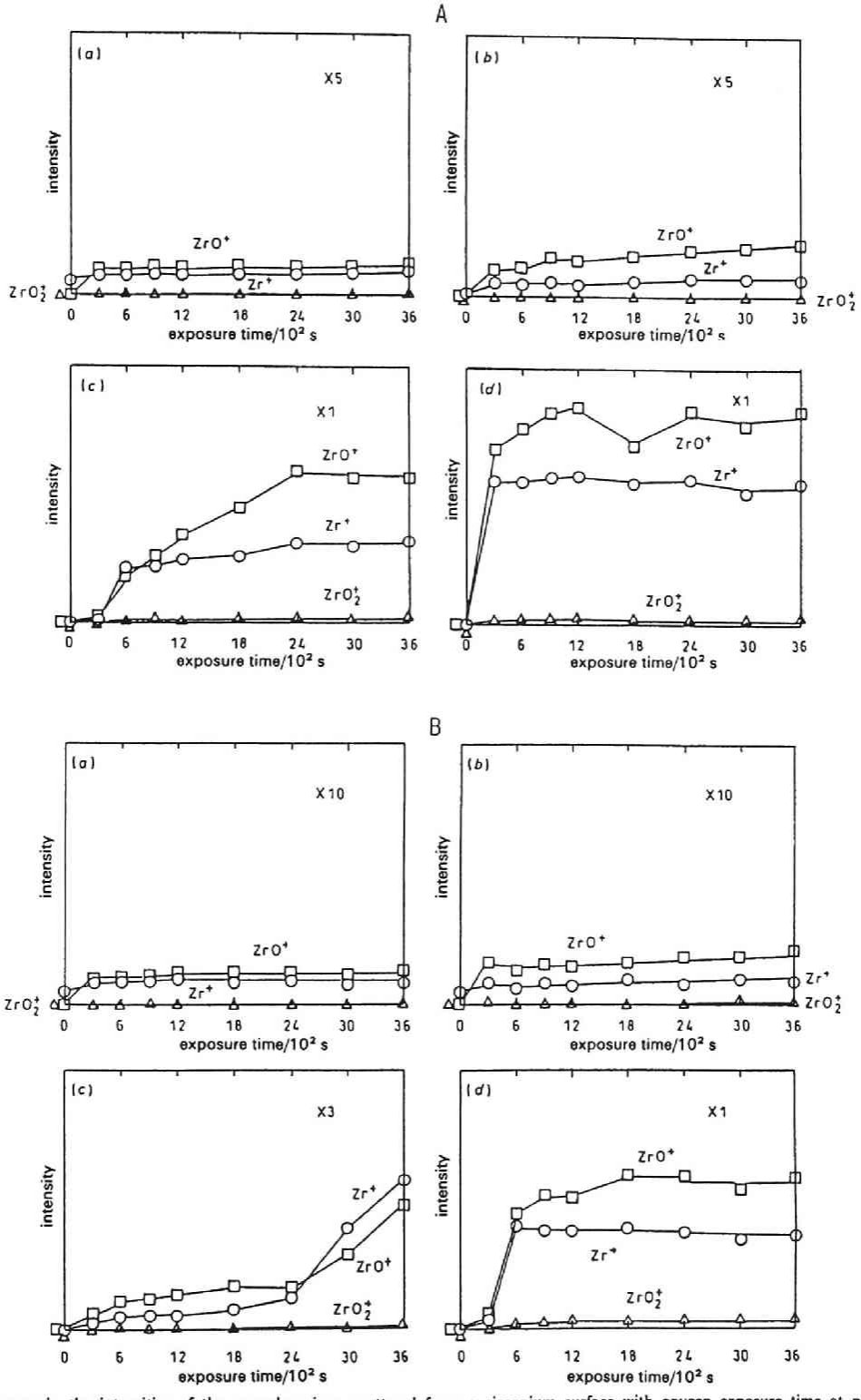

Fig. 4–7. Changes in the intensities of the secondary ions sputtered from a zirconium surface with oxygen exposure time at pressures of 1.3×10^{-4} Pa (A) and 6.7×10^{-5} Pa (B), and at temperatures of 1073 K (*a*), 973 K (*b*), 873 K (*c*) and 773 K (*d*). The amplification of intensity is shown in the top right-hand corner of each graph. The intensities in A and B are scaled relative to each other. [14]

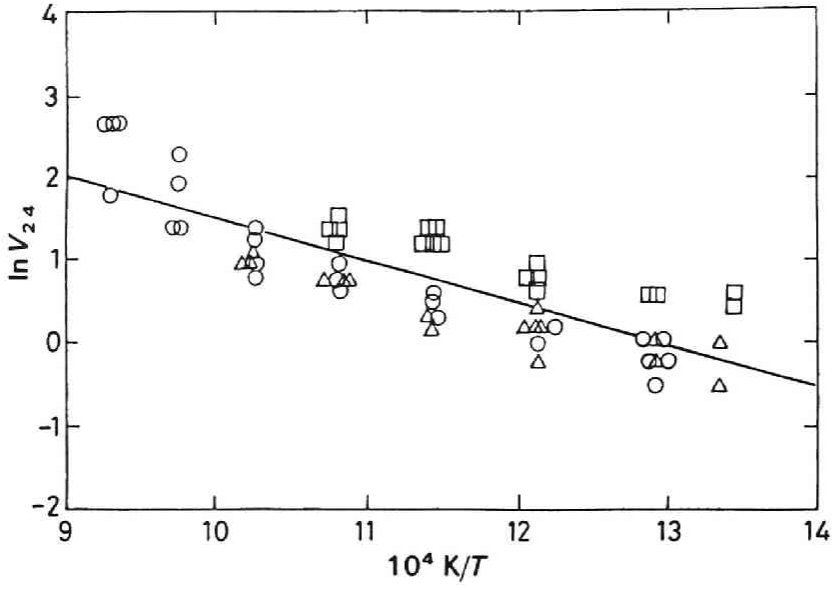

Fig. 4-8. Arrhenius plot of the kinetic parameter V_{24} to evaluate the activation energy of the oxide decomposition reaction: (○) 1.3×10^{-3} Pa, (△) 1.3×10^{-4} Pa, (□) 6.7×10^{-5} Pa.

respectively.

The calculated absorption curves for 873 K and 1.3×10^{-4} Pa, and 873-823 K and 6.7×10^{-5} Pa are not in good agreement with those obtained experimentally. This may be because the coalesce of the oxide nuclei was not taken into account in our autocatalytic nucleation model.

The Arrhenius plot of the kinetic parameter V_{24} is shown in Fig. 4-8. Assuming that the activation energies of the following reactions of oxide decomposition are almost the same,

$$2O(ox) \rightarrow O(s) + O(ox)$$

$$2O(ox) \rightarrow O(s) + O(s)$$

we can obtain the activation energy of oxide decomposition from the straight line in the Fig. 4-8. The activation energy of oxide decomposition is found to be $(7.0 \pm 0.5) \times 10^{-20}$ J.

Conclusion

An increase in the rate of oxygen absorption is observed during the oxide nucleation stage. The autocatalytic reaction model of the quasi two-dimensional nucleation and growth of oxide is used and the absorption rate at the nucleation stage is explained. The calculated oxide coverage is in good agreement with the SIMS measurement.

Two kinetic parameters in this model are evaluated: The activation energy for the transfer of oxygen adatoms on the oxide-covered surface into the bulk is $(1.0 \pm 0.1) \times 10^{-19}$ J per O atom and the activation energy of the decomposition of the quasi two-dimensional oxide is $(7.0 \pm 0.5) \times 10^{-20}$ J.

References for Chapter 4

1. C. J. Rosa, *J. Less-Common Met.*, 1968, 16, 173,
   and references are therein.
2. M. Yamamoto, S. Naito, M. Mabuchi and T. Hashino,
   J. Phys. Chem., 1989, 93, 5203.
3. J. M. Sanz, C. Palacio, Y. Casas and J. M. Martinez-Duart,
   Surf. Interface Anal., 1987, 10, 177.
   J. S. Foord, P. J. Goddard and R. M. Lambert,

Surf. Sci., 1980, 94, 339.

4. P. Aebi, M. Erbudak, A. Leonardi and F. Vanini,
J. Electron Spectrosc. Relat. Phenom., 1987, 42, 351.
G. R. Corallo, D. A. Asbury, R. E. Gilbert and G. B. Hoflund,
Phys. Rev. B, 1987, 35, 9451.
5. C. Moranto, J. M. Sanz, L. Galán, L. Soriano, and F. Rueda,
Surf. Sci., 1989, 218, 331.
P. Sen. D. D. Sarma, R. C. Budhani, K. L. Chopra and C. N. R. Rao,
J. Phys. F, 1984, 14, 565.
P. E. West and P. M. George,
J. Vac. Sci. Technol. A, 1987, 5, 1124.
C. O. De González and E. A. García, *Surf. Sci.*, 1988, 193, 305.
6. R. L. Tapping, *J. Nucl. Mater.*, 1982, 10, 151.
7. K. C. Hui, R. H. Milne, K. A. R. Mitchell, W. T. Moore
and M.Y. Zhou, *Solid State Commun.*, 1985, 56, 83.
P. C. Wong, K. C. Hui, B. K. Zhong and K. A. R. Mitchell,
Solid State Commun., 1987. 62, 293.
8. G. B. Hoflund, G. R. Corallo, D. A. Asbury and R. E. Gilbert,
J. Vac. Sci. Technol. A, 1987, 5, 1120.
9. F. Grønlund and P. J. Møller, *Surf. Sci.*, 1987, 184, 530.
10. D. F. Mitchell and M. J. Graham, *Surf. Sci.*, 1982, 114, 546.
11. G. N. Krishnan, B. J. Wood and D. Cubicciotti,
J. Electrochem. Soc., 1981, 128, 191.
12. P. H. Holloway and J. B. Hudson, *Surf. Sci.*, 1974, 43,
123 and 141, and references are therein.
13. H. Takeuchi, S. Naito, M. Yamamoto and T. Hashino,
J. Chem. Soc. Faraday Trans. 1, 1988, 84, 4235.

14. M. Yamamoto, S. Naito, M. Mabuchi and T. Hashino,
J. Chem. Soc. Faraday Trans., 1990, 86, 157.

15. P. Paetz and F. Sperner,
in *Gase und Kohlenstoff in Metallen*,
ed. E. Fromm and E. Gebhardt (Springer, Berlin, 1976), pp.419-430.

16. J. A. Venables and G. D. T. Spiller,
in *Surface Mobilities on Solid Materials*,
ed. Vu-T. Binh, (Plenum, New York, 1983), pp. 341-403.

17. H. Müller-Krumbhaar,
in *Monte Carlo Methods in Statisitical Physics*,
ed. K. Binder, (Springer, Berlin, 1979), chap. 7.

18. H. Haken, in *Synergetics: An Introduction*,
(Springer Verlag, Berlin, 1983), pp. 275-303.

Chapter 5

Change in the Work Function of Zirconium by Oxidation at High Temperatures and Low Oxygen Pressures*

Introduction

The work function of a metal, which is defined as the minimum energy required to remove an electron from the metal, is very sensitive to the state of the metal surface. The state of metal surface depends on existence of adsorbates on the metal surface, structure and imperfection of the metal surface, temperature of the substrate, mechanical stress on the metal and so on.[1]

The changes in the work function induced by oxidation of transition metal surface have been studied by a number of investigators.[1] A few investigators have studied the change in the work function of polycrystalline zirconium by oxidation at room temperature[2] and that of the zirconium (0001) surface at near-liquid-temperature.[3] Physical origins of the change of the work function have not been discussed in detail, and these studies do not give a knowledge of the kinetics of the surface oxidation of zirconium at high temperatures. The oxidation kinetics at high temperatures involves the dynamic competition between

---

* Accepted for publication in *J. Chem. Soc., Faraday Trans.*

the adsorption of oxygen at the surface and the diffusion of oxygen into the bulk.[4-7]

In the present study we have investigated the change in the work function induced by oxidation of a clean polycrystalline zirconium surface at temperatures 426 - 765 K and at oxygen pressures 3.0×10^{-6} - 3.0×10^{-4} Pa. It has been found that there are three stages of the change in the work function: decrease at the initial stage, increase at the second stage and saturation at the final stage. It is well known that metal oxidation occurs through the three successive steps which represent the dissociative adsorption of oxygen molecules, the nucleation of oxide and the growth of oxide for many metals. The oxidation states at the zirconium surface were identified using the secondary ion mass spectroscopy (SIMS). It has been found that the three stages of the change in the work function correspond to the three processes of metal oxidation respectively.

A few investigators have proposed that the initial decrease in the work function is due to the incorporation of oxygen adatom into the subsurface.[2-3] Using the results of LEED measurements, Mitchell *et al.* have suggested that oxygen atoms occupy octahedral subsurface sites of a reconstructed f.c.c. zirconium.[8] In the present study we will discuss the physical origin of the incorporation of oxygen adatom to the subsurface on the basis of a calculated oxygen potential for adsorption on Zr(0001) surface. The positive change in the work function by the oxide formation and the pressure and temperature dependence of the change in the work function are explained qualitatively.

Experimental

All experiments were done in a UHV system which had a base pressure of 2×10^{-8} Pa. A Kelvin-Zisman vibrating capacitor method was employed for the measurement of the change in the work function ($\Delta\phi$). A Kelvin probe similar to that designed by Saito *et al.*[9] was used. A gold electrode was chosen as the reference electrode. The difference of the contact potential between the reference electrode and the specimen is continuously followed by using a feedback detection system. The detection system was tested by applying a given voltage externally on the specimen and we confirmed the fact that the potential difference detected holds constant with the error of ± 5% of the test voltage. The SIM spectra were observed by using a quadrupole mass spectrometer (ANELVA, AGA-360SIMS) and a 5 kV ion gun.

Polycrystalline zirconium disks of 0.5 mm thick and 12 mm in diameter and of 99.99 % in purity were used as a specimen. The specimen was mechanically polished, ultrasonically degreased in acetone and then fixed onto a ceramic heater wrapped in a gold foil. The specimen was heated by thermal conduction from the heater. The temperature of the specimen was measured with a W5%Re-W26%Re thermocouple spot-welded and was controlled using a thermoregulator. The surface of the specimen was cleaned by the cyclic Ar^+-ion bombardment at 873 K and the annealing at 1073 K. The results of the SIMS measurement have shown that this treatment remarkably reduces the surface contaminants such as oxygen, carbon and chlorine segregated onto the surface by annealing.[5]

The oxygen gas of 99.995% in purity was introduced. The oxygen

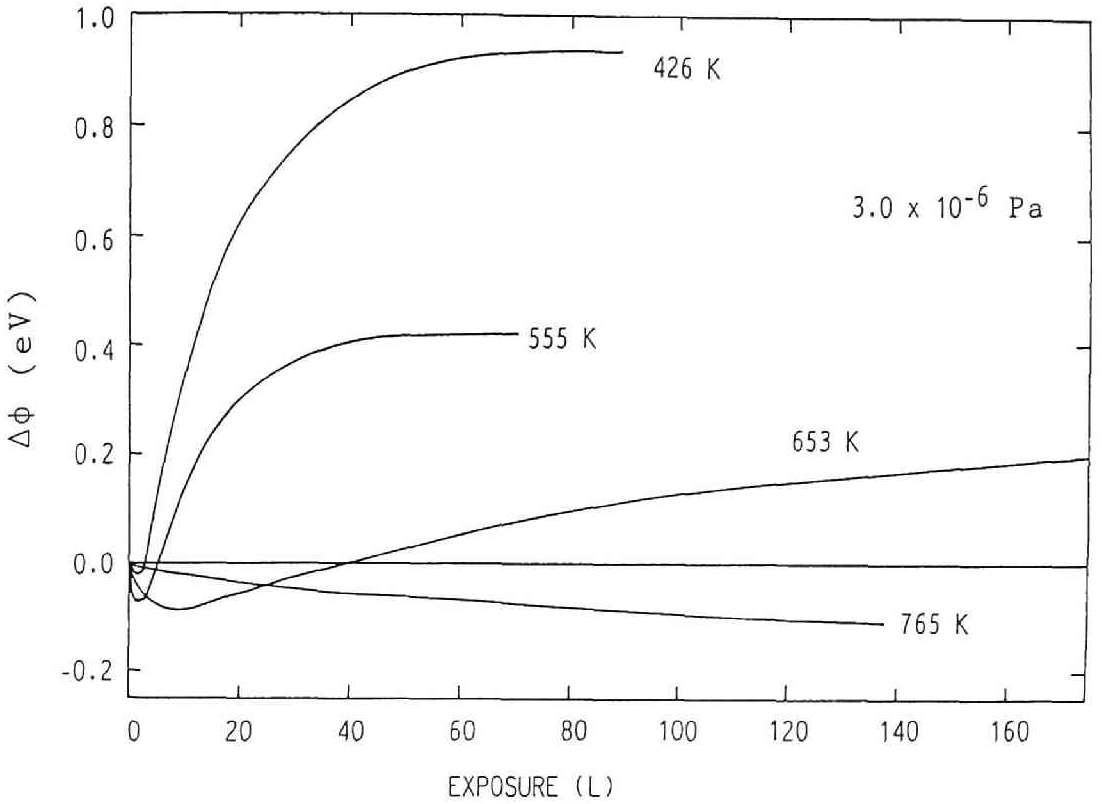

Fig. 5-1. Change in the work function $\Delta\phi$ as a function of oxygen exposure at an oxygen pressure 3.0×10^{-6} Pa. Exposure in Langmuir unit is used. 1 L corresponds to 10^{-6} Torr·s.

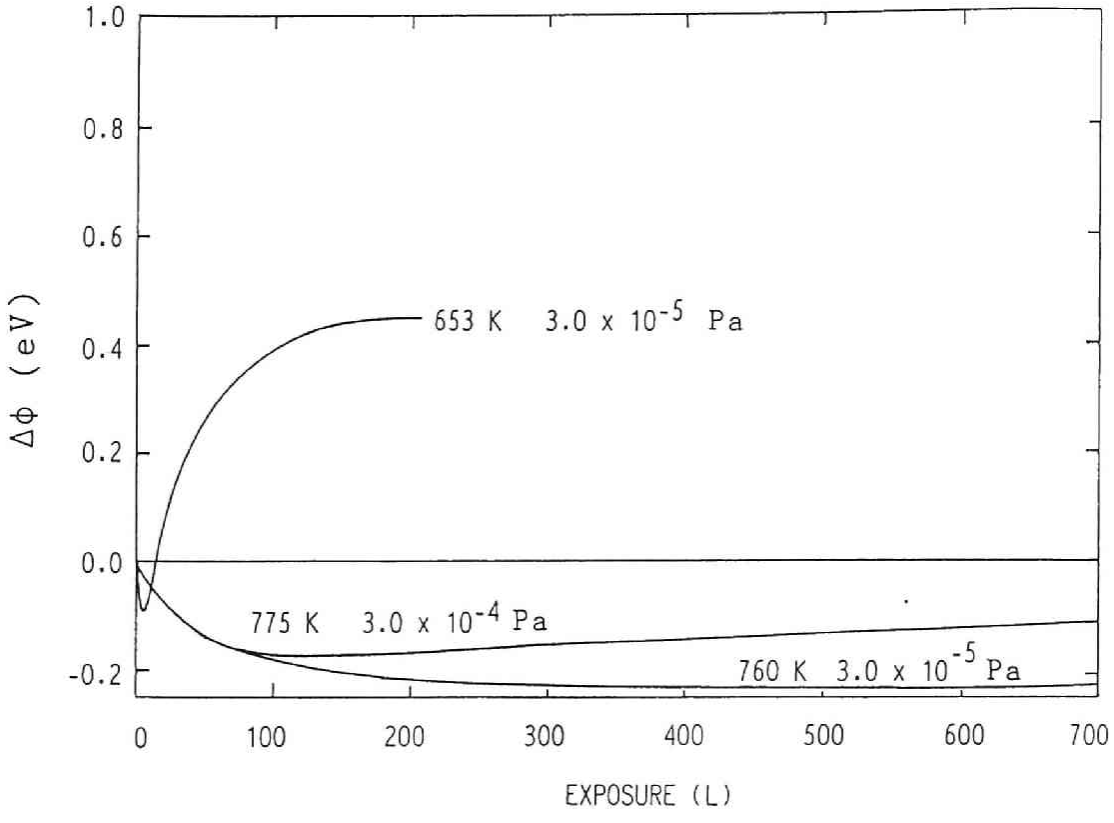

Fig. 5-2. Change in the work function $\Delta\phi$ as a function of oxygen exposure at oxygen pressures 3.0×10^{-5} Pa and 3.0×10^{-4} Pa.

pressure in the specimen chamber was kept constant by using an automatic pressure control valve.

Results

The changes in the work function by oxidation of zirconium have been measured at oxygen pressures 3.0×10^{-6} Pa - 3.0×10^{-4} Pa and at temperatures 426 - 775 K. The results of the measurements at a oxygen pressure 3.0×10^{-6} Pa and at oxygen pressures 3.0×10^{-5} Pa - 3.0×10^{-4} Pa are shown in Fig. 5-1 and Fig. 5-2, respectively.

The change in the work function shows the five characteristics: (i)The change in the work function were composed of three stages: decrease in the work function at the first stage, increase at the second stage and saturation at the final stage. The three stages have been also observed in the measurements of the change in the work function of zirconium by oxidation at room temperature[2] and at near-liquid-nitrogen temperatures.[3] (ii) The first stages were prolonged to higher exposures at high temperatures and lower pressures of oxygen. (iii)The minima of the work function were reduced at lower temperatures. (iv)The rate of increase in the work function at the second stage is decreased at high temperatures and at lower pressures. (v)The saturation levels of the work function were lowered at higher temperatures and at lower pressures. The temperature dependence of the work function change is in good agreement with that for the titanium oxidation at high temperatures.[10]

The oxidation states at the surface have been identified by using SIMS measurements done after the exposure of oxygen for 100 L at an oxygen

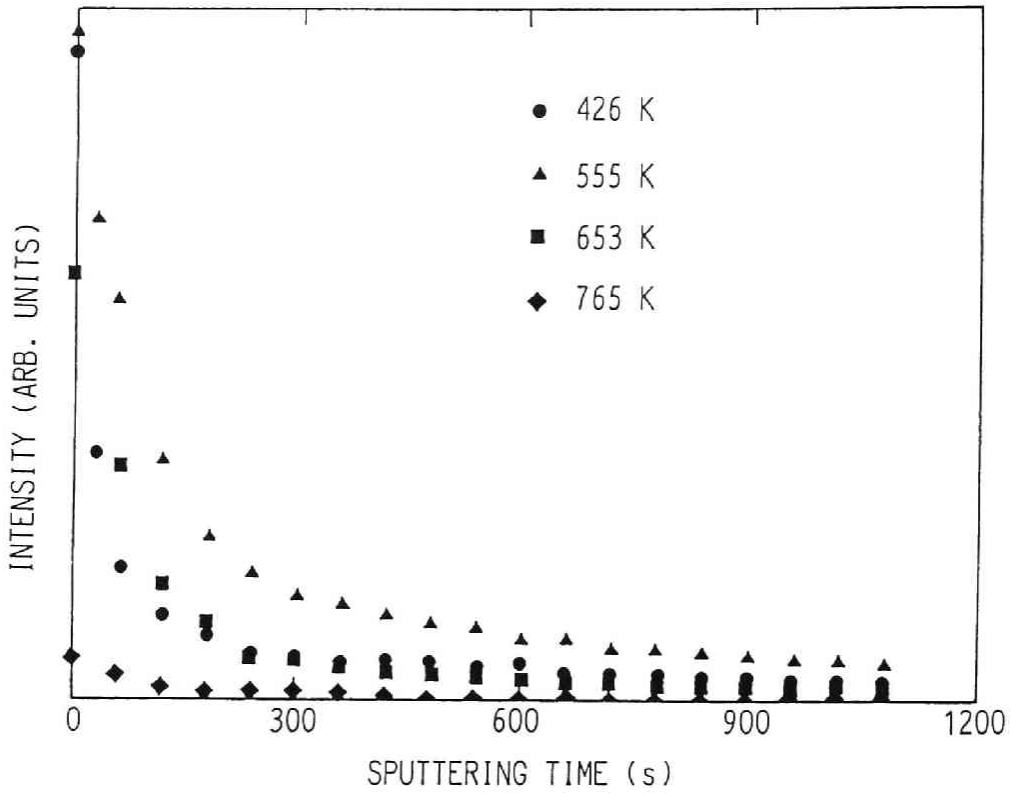

Fig. 5-3. Intensities of the Zr^+ secondary ion sputtered from the oxidized zirconium surface after the exposure of oxygen for 100 L at an oxygen pressure 3.0×10^{-6} Pa.

pressure 3.0×10^{-6} Pa. The stages of the work function change at 100 L exposure are at the final stage of saturation at temperatures of 426 K and 555 K, at the second stage of increase at 653 K and at the initial stage of decrease at 765 K, respectively. The specimen cooled to room temperature was bombarded with a beam energy of 2 keV and an ion current of *ca.* 10 $\mu A \cdot cm^{-2}$. Secondary ions which have a kinetic energy of *ca.* 10 eV and an emission angle 45° to the surface normal were detected. The sputtering yield of zirconium is reported to be 1.2 atoms per ion for 2 keV Ar^+-ion bombardment.[11] The 10 $\mu A \cdot cm^{-2}$ ion current is estimated to sputter one monolayer from the zirconium surface in *ca.* 15 s.

It is well known that the yield of the secondary positive ion of metal is low for the metal surface and the yield is increased by a factor of 10^2-10^3 for the oxide surface.[12] We have previously shown that the yield of the Zr^+ secondary ion sputtered from the oxide surface is increased by *ca.* 300 times as compared to that from the clean surface, and that the increase in the yield is caused by the downward energy shift of the highest occupied electronic level of the substrate by the oxide formation.[6] From the yield of the Zr^+ secondary ion as shown in Fig. 5-3, it has been found that the surface is covered by oxide at 426 K and 555 K (the stage of oxide growth), α-zirconium at 765 K (the stage of oxygen adsorption) and at the intermediate stage of oxidation at 653 K (the stage of nucleation). Hence we can regard that the three stages of the work function change observed correspond to the three stages of oxidation of zirconium, *i.e.* the initial stage of decrease is at the stage of oxygen adsorption, the second stage of increase is at the oxide nucleation stage and the final stage of saturation is at

the stage of oxide growth.

Discussion

Initial Decrease in the Work Function

The work function of a metal is composed of a surface-dependent part of the surface dipole and a bulk dependent part of the chemical potential of the electron in the metal (the Fermi energy). Glötzel *et al.* have reported that the bulk-dependent part of the work function of zirconium metal (in the fcc phase) is 1.62 eV and the surface-dependent part is 3.4 eV.[13]

The work function of the transition metals such as Ni,[1,14] Cr,[15] Fe,[16,] Cu,[1] W,[1] Pd[17] and Ru[18] is generally increased by oxidation at the early stage, *i.e.* at the oxidation stage of oxygen adsorption, and decreased in metals such as Ti,[10] Zr,[2-3] Nb[1] and Mo.[1,19] It has been suggested that the increase or the decrease in the work function depends on whether the oxygen atoms are adsorbed on the surface or at the subsurface. The oxygen adatom has a strong electronegative properties and the surface dipole barrier increases by the existence of oxygen adatoms on the surface and reduces by the existence of oxygen adatoms at the subsurface. Freeman *et al.*[20] have determined the electronic structure of the clean and oxidized Al(001) and Al(111) surface by means of a self-consistent calculation. They have shown that the work function is increased for the Al(111) surface by the existence of oxygen adatom outside the surface and decreased for the open structure Al(001) surface because the oxygen adatom incorporates to

the coplanar site. The oxygen adatom at the coplanar site attracts the electronic charge from the neighboring Al atoms. An outward dipole moment localized on the surface Al atom is formed and the work function is reduced.

In order to explain a physical origin of the decrease in the work function of zirconium at the initial stage of oxidation, we will consider the chemisorption potential of oxygen on the zirconium surface. The chemisorption potential of adatom such as hydrogen, nitrogen and oxygen has been obtained by a modified Newns-Anderson model and a self-consistent calculation using a cluster model, a jellium model and a slab model.[21] In the present study we will calculate the potential by an effective medium theory.[22] It has been shown that adsorption site, binding energy and ground state frequency of hydrogen adatom on transition metal surfaces calculated by the effective medium theory are in good agreement with the experiment results.

There are the four significant contributions to the oxygen chemisorption potential $E(\boldsymbol{r})$ calculated by the effective medium theory:[22] (i)interaction of oxygen atom with a homogeneous electron gas. (ii)hybridization of oxygen 2p level with the homogeneous electron gas. (iii)interaction of oxygen atom with core states of metal atom. (iv)large lattice relaxation around oxygen atom.[23] We will evaluate the oxygen chemisorption potential in the 0th order approximation by calculating the interaction energy given by (i). Nordlander *et al.* have suggested that the contributions (ii)-(iii) are relatively small in comparison with the contribution (i), and shown that the contribution (iv) for the energy barrier of oxygen incorporation is less than 0.1 eV in the oxygen-titanium system.[23]

In the 0th order approximation the chemisorption potential $E(r)$ is given by

$$E(r)=E[\bar{n}_0(r)] \tag{5-1}$$

The interaction energy $E[\bar{n}_0(r)]$ has been given by Chakraborty *et al.*[22] $\bar{n}_0(r)$ is the weighted average of the electron density $n_0(r)$ of metal with the oxygen induced potential $v(r)$ of electron.

$$\bar{n}_0(r)=\int_a dr'\, n_0(r')\,v(r'-r)/\int_a dr'\, v(r') \tag{5-2}$$

The average has been done over a sphere of radius 2.5 a_0, which is almost of the same radius as oxygen ion 2.6 a_0. Here a_0 is the Bohr radius. $v(r)$ is chosen as the oxygen atomic potential.[22] The electron density of metal is approximated to be a superposition of atomic electron density.

$$n_0(r)=\sum_{R_i} n_{atom}(r-R_i) \tag{5-3}$$

The atomic density of zirconium is calculated self-consistently using a modified Herman-Skillman computer program.[24] We use the Perdew-Zunger local density approximation for the electron exchange and correlation.[25] Latter's modification for the electron is not performed in the numerical calculation.[26] The configuration of the valence electron of h.c.p. zirconium metal is chosen as $4d^3 5s^1$. Sharma and Ahuja have shown that the

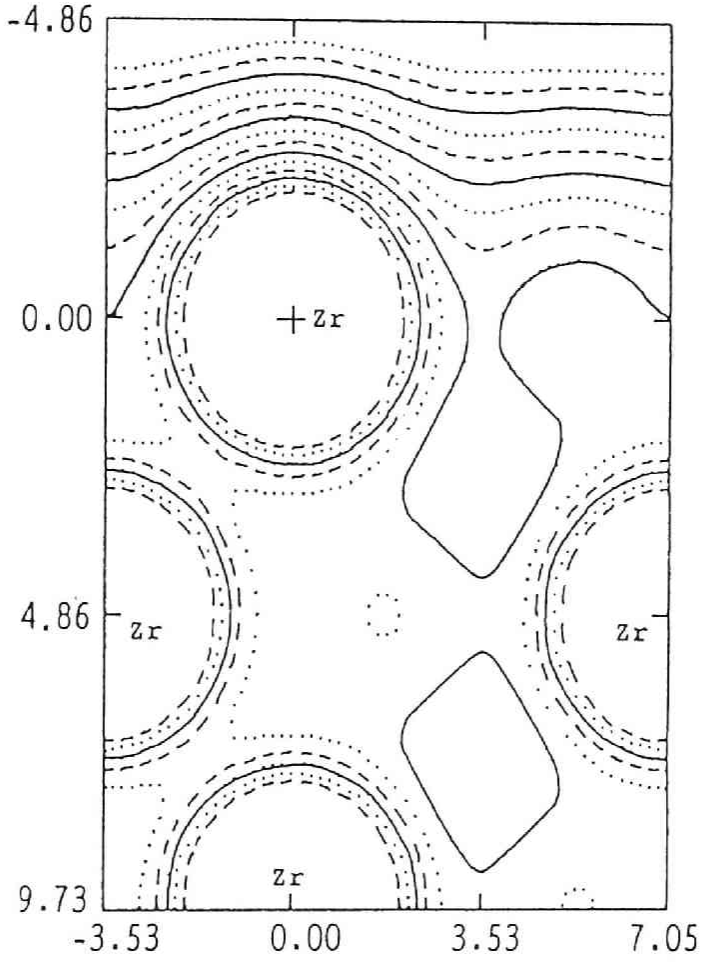

Fig. 5-4. Contour plot of the electron density of the Zr(0001) surface on a vertical-cut plane passing through a line connecting a surface atom with one of its nearest neighbors at the second layer. The distances are given in a.u. The outermost contour is 2.0×10^{-3} a.u. Charge densities on successive contours are in the ratio 1.3.

electron-momentum distribution calculated on the basis of this configuration is in best agreement with the electron-momentum distribution determined by their Compton-scattering measurement.[27]

The electron density of zirconium (0001) surface is calculated as shown in Fig. 5-4. The electron density calculated is analogous to the electron density of Ti(0001) surface calculated self-consistently by Feibelman *et al.*[28] (No self-consistent calculation of the electron density of zirconium surface has been reported within our knowledge.) Existence of a low electron density channel is found along a vertical line passing through an octahedral site between the surface layer and the second layer. This channel may provide an interstitial site for oxygen with a low potential energy and a low barrier of oxygen incorporation to the bulk site of zirconium. The effective medium theory predicts that the oxygen chemisorption potential estimated from the interaction energy between electron gas and oxygen atom gives a minimum at the electron density 0.013 a.u.[22] It is expected that the incorporation barrier for the close-packed (0001) surface is greater than the barrier for the other surface with open structure. Hence the incorporation barrier of polycrystalline zirconium used in our measurement would be lower than that of (0001) surface.

The calculated oxygen potential along the path vertical to the (0001) zirconium surface is shown in Fig. 5-5. The incorporation barrier of oxygen from the surface to the octahedral site at the subsurface is found to be 0.5 eV. The incorporation barrier of oxygen on nickel, whose work function is increased by the adsorption of oxygen atom outside the surface, is 4.1 eV in the 0th order approximation, and is 1.7 eV in the approximation including the effect of lattice relaxation.[23] It seems that

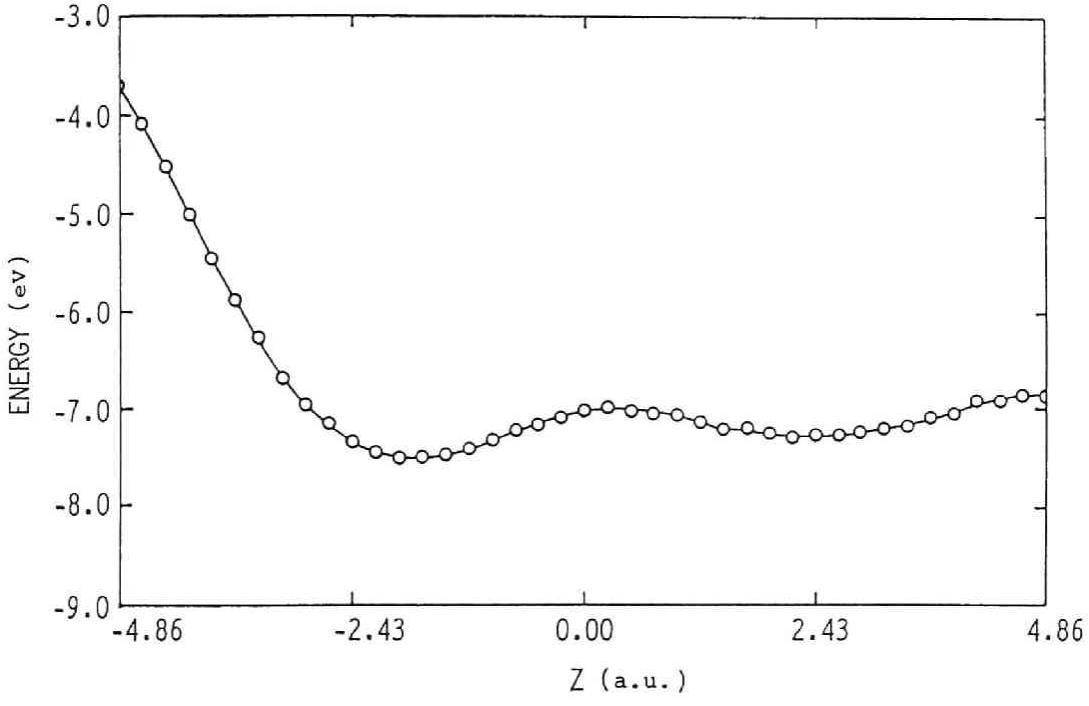

Fig. 5-5. Potential of oxygen along a vertical line passing through an octahedral site between the surface layer and the second layer of zirconium (0001) surface. The positive sign of the distance corresponds to the interior of the metal.

the incorporation barriers of the other transition metals whose work function is increased by oxygen adsorption are greater than that of the transition metals such as Zr and Nb[23] whose work function is decreased by the initial oxidation. A low electron density channel such as in the case of zirconium is not found in the contour of the nickel electron density.[29] Thus the fact that metallic zirconium has the lower incorporation barrier of oxygen may be one of the causes of the incorporation of oxygen to the subsurface at the initial oxidation of zirconium. The effect of lattice relaxation may reduce the incorporation barrier.

The chemisorption energy obtained is 7.5 eV and the value corresponds to the minimum interaction energy between the oxygen atom and the homogeneous electron gas. We have previously reported that the experimental chemisorption energy of oxygen by zirconium is 10.1 eV.[5] The difference 2.6 eV between the calculated value and the measured one may mainly arise from the hybridization energy of oxygen 2p level with the valence electron gas. The minimum of the oxygen potential is located at 1.8 a.u. outside the surface. The octahedral site between the surface layer and the second layer is the second minimum of the oxygen potential. The potential energy at the outside site is lower by 0.2 eV than the octahedral site because of the presence of the kinetic energy repulsion[22-23] at the interstitial site which has a higher electron density. The above results support the fact that the oxygen atom is adsorbed mainly on the site located outside the surface. However, the effect of hybridization energy[22] which is expected to be greater at a nearer distance between zirconium atom and oxygen atom may cause to provide the adsorption site close to the surface, and the interaction between two oxygen adatoms produced by the dissociative

adsorption of oxygen molecule will have a remarkable effect on the chemisorption potential.

Increase in the Work Function by Oxide Formation

The work function of zirconium is increased going beyond the minimum, as shown in Fig. 5-1 and 5-2. Our SIMS measurement suggests that the second increase stage of the work function corresponds to the stage of oxide nucleation.

In the present study we will try to explain a physical origin of the increase in the work function in terms of the contribution of the bulk-dependent part of the work function. The UPS measurement of the valence band of the oxide-covered surface of zirconium has shown that the oxygen 2p band was formed at the energy level below the Fermi level of metallic zirconium by 6 eV and the density of state from the Fermi level of the metal to the top of the oxygen 2p band was remarkably reduced.[30] The electronic structure of the bulk zirconium oxide in monoclinic phase was calculated by Zandiehnadem *et al.*[31] They have shown that the band gap between the oxygen 2p valence band and the zirconium 4d conduction band is 4.5 eV. The chemical potential of semiconductor may be approximated to be located in the middle of the band gap at high temperatures. (The chemical potential corresponds to Fermi level in the case of metal.) Provided that the energy of the oxygen 2p band measured is in agreement with that of the valence band calculated, the chemical potential of the electron in zirconium oxide is lowered by *ca.* 1 eV than the Fermi energy of the metallic zirconium. Thereby the downward

energy shift of the chemical potential may be the origin of the increase of the work function of zirconium by the oxide formation at the surface.

The surface-dependent part of the work function of metal oxide has not been determined unambiguously because existence of oxygen adatoms and the point defects of oxygen ion at the oxide surface affect not only the surface dipole moment of the electron density but also on the band bending at the surface. The amount of the point defects of oxygen ion and the adatoms may depend on the pressure of oxygen and the temperature of substrate.

Temperature and Pressure Dependences of the Change in the Work Function

The depth profile of the Zr^+ secondary ion is a measure of the concentration distribution of oxygen. As shown in Fig. 5-3, the depth profile at 765 K shows the intensity uniformly distributed in the region from the surface to the bulk. The uniform distribution may be caused by the faster diffusion rate of oxygen into the bulk than the adsorption rate at the surface. The region of the higher intensity at lower temperatures would be due to the oxide formation at the surface. The region of high intensity at 426 K becomes shallower than that at higher temperatures, because the total absorption rate of oxygen by zirconium becomes slower at lower temperatures.[4-5,7]

We have previously shown that the concentration of oxygen at the surface is determined by the dynamic competition between the transport processes at the surface(*e.g.* the dissociative adsorption and the transfer process from the surface to the outermost bulk site) and the

diffusion process in the bulk.[4-7] Since the rate of oxygen diffusion is faster than the rate of surface processes at higher temperatures and lower pressures of oxygen (*e.g.* > 973 K at 6.7×10^{-5} Pa),[5] the first stage of the decrease in the work function (α-zirconium surface) is prolonged with increase in temperature and with decrease in oxygen pressure.(See Fig 5-2.) The rate of transport processes at the surface becomes greater than that of diffusion with decrease in temperature (*e.g.* < 923 K at 6.7×10^{-5} Pa),[7] because the activation barrier of oxygen diffusion in the bulk is greater by 1.7 eV per O atom than that of dissociative adsorption of oxygen molecule.[5] The accumulation of oxygen onto the surface and the subsequent nucleation of oxide occurs. Thereby the decrease in minima of the work function and the greater rate of the increase in the work function at the second stage may be explained by the earlier beginning of oxide nucleation and the greater rate of oxide formation at lower temperatures, respectively.

The absorption rate which is determined by the adsorption rate at low pressures as in our measurement is proportional to the pressure of oxygen in the case of metal surface, and proportional to the square root of the pressure in the case of oxide-covered surface.[4-5] The pressure dependence of the change in the work function can be explained by the greater rate of oxide formation as a natural consequence of the greater total rate of oxygen absorption at higher pressures.

The temperature and pressure dependences of the saturation level of the work function change at the final stage may be caused by the following: (i)the difference of the amount of the oxygen adsorbates or the oxygen point defects on the oxide surface (ii)the difference of the depth of the

oxide film. These differences are expected to cause a change of the electronic dipole at the surface and the band bending at the surface. Surface spectroscopic measurements and calculation of the electronic structure of the surface should be needed to discuss the dependence in detail.

Conclusion

The changes in the work function of zirconium by oxidation have been measured at oxygen pressures 3.0×10^{-6} - 3.0×10^{-4} Pa and at temperatures 426 - 775 K. Three stages of the change in the work function are found: decrease at the initial stage, increase at the second stage and saturation at the final stage. By using the secondary ion mass spectroscopy(SIMS), it is shown that the three stages of the change in the work function correspond to the oxidation stage of oxygen adsorption, the stage of oxide nucleation and the stage of oxide growth, respectively. The initial decrease in the work function of zirconium is caused by the incorporation of oxygen adatoms into the subsurface. The oxygen adsorption potential of zirconium is evaluated by the effective medium theory, and we conclude that one of the reasons of the incorporation of oxygen adatom is the low incorporation barrier of oxygen from the surface site to the subsurface site. The positive change in the work function by the oxide formation is explained by the formation of oxygen 2p band at energy lower by several electron volts below the Fermi energy of metal. It has been found that the temperature and pressure dependences of the change in the work function by oxidation is closely correlated with the dynamic competition between the surface processes and the diffusion process.

References for Chapter 5

1. J. Hölzl and F. K. Schulte, in *Solid-Surface Physics*, (Springer, Berlin, 1979), pp. 1-150, and references are therein.
2. J. S. Foord, P. J. Goddard and R. M. Lambert, *Surf. Sci.*, 1980, 94, 339.
3. K. Griffiths, *J. Vac. Sci. Technol. A*, 1988, 6, 210.
4. H. Takeuchi, S.Naito, M. Yamamoto and T. Hashino, *J. Chem. Soc. Faraday Trans. 1*, 1988, 84, 4235.
5. M. Yamamoto, S. Naito, M. Mabuchi and T. Hashino, *J. Phys. Chem.*, 1989, 93, 5203.
6. M. Yamamoto, S. Naito, M. Mabuchi and T. Hashino, *J. Chem. Soc. Faraday Trans.*, 1990, 86, 157.
7. M. Yamamoto, S. Naito, M. Mabuchi and T.Hashino, *J. Chem. Soc. Faraday Trans.*, in press.
8. K. C. Hui, R. H. Milne, K. A. R. Mitchell, W. T. Moore and M. Y. Zhou, *Solid State Commun.*, 1985, 56, 83.
   P. C. Wong and K. A. R. Mitchell, *Can. J. Chem.*, 1986, 64, 2409.
   P. C. Wong, K. C. Hui, B. K. Zhong and K. A. R. Mitchell, *Solid State Commun.*, 1987, 62, 293.
   P. C. Wong and K. A. R. Mitchell, *Can. J. Phys.*, 1987, 65, 464.
9. S. Saito, T. Soumura and T. Maeda, *J. Vac. Sci. Technol. A*, 1984, 2, 1389.
10. J. B. Bignolas, M. Bujor and J. Bardolle, *Surf. Sci.*, 1981, 108, L453.
11. M. J. Vasile, *Phys. Rev. B*, 1984, 29, 3785.

12. W. N. Delgass, L. L. Lauderback and D. G. Taylor, in *Chemistry and Physics of Solid State Surface IV*, ed. R. Vanselow and R. Howe (Springer, Berlin, 1982), pp.51-76.
G. K. Wehner, in *Methods of Surface Analysis*, ed. A. W. Czanderna (Elsevier, Amsterdam, 1975), pp.5-37,
13. M. Cardona and L.Ley, in *Photoemmision in Solids I*, ed. M. Cardona and L.Ley (Springer, New York, 1978), p.19, and reference is therein.
14. P. H. Holloway and J. B. Hudson, *Surf. Sci.* 1974, 43, 123.
K. Akimoto, Y. Sakisaka, M. Nishijima and M. Onchi, *Surf. Sci.* 1979, 82, 349.
S. Masuda, M. Nishijima, Y. Sakisaka and M. Onchi, *Phys. Rev. B.* 1982, 25, 863.
D. F. Mitchell and M. J. Graham, *Surf. Sci.*, 1982, 114, 546.
15. Y. Sakisaka, H. Kato and M. Onchi, *Surf. Sci.* 1980, 120, 150.
16. Y. Sakisaka, T. Miyano and M. Onchi, *Phys. Rev. B*, 1984, 30, 6849.
Y. Sakisaka, T. Komeda and M. Onchi, *Surf. Sci.*, 1986, 169, 197.
17. L. Surnev, G. Bliznakov and M. Kiskinova, *Surf. Sci.*, 1984, 140, 249.
18. T. E. Madey, H. A. Engelhardt and D. Menzel, *Surf. Sci.*, 1975, 48, 304.
19. R. Riwan, C. Guillot and J. Paigne, *Surf. Sci.* 1975, 47, 183.
20. H. Krakauer, M. Posternak, A. J. Freeman and D. D. Koelling, *Phys. Rev. B*, 1981, 23, 3859.
D. S. Wang, A. J. Freeman and H. Krkauer, *Phys. Rev. B*, 1981, 24, 3092, and 3104.
21. K. Christmann, *Surf. Sci. Reports*, 1988, 9, 1,

and references are therein.

22. J. K. Nørskov, *Phys. Rev. B*, 1982, 26, 2875.
P. Nordlander, S. Holloway and J. K. Nørskov,
Surf. Sci., 1984, 136, 59.
B. Chakraborty, S. Holloway and J. K. Nørskov,
Surf. Sci., 1985, 152/153, 660.
23. P. Nordlander and M. Ronay, *Phys. Rev. B*, 1987, 36, 4982.
24. F. Herman and S. Skillman, *Atomic Structure Calculations*,
(Prentice-Hall, Elgelwood Cliffs, N.J., 1963)
25. J. P. Perdew and A. Zunger, *Phys. Rev. B*, 1981, 23, 5048.
26. J. C. Slater, in *The Calculation of Molecular Orbitals*,
(John Wiley & Sons, New York, 1979)
27. B. K. Sharma and B. L. Ahuja, *Phys. Rev. B*, 1988, 28, 3148.
28. P. J. Feibelman, J. A. Appelbaum and D. R. Hamann,
Phys. Rev. B, 1979, 20 , 1433.
29. C. S. Wang and A. J. Freeman, *Phys. Rev. B*, 1980, 21, 4585.
30. R. L. Tapping, *J. Nucl. Mater.*, 1982, 10, 151.
31. F. Zandiehnadem, R. A. Murray and W. Y. Ching,
Physica B, 1988, 150, 19.

Chapter 6

Change in the Electronic Structure of Zirconium by Oxidation: AES, EELS and SES Studies on the Oxidation of Zirconium at High Temperatures and Room Temperature*

Introduction

In the 1980s a number of surface spectroscopic studies on the oxidation of zirconium have been reported. These studies involve Auger electron spectroscopy(AES),[1-7] low energy electron diffraction(LEED),[8-10] X-ray photoelectron spectroscopy(XPS),[11-17] ultraviolet photoelectron spectroscopy (UPS),[12] electron energy loss spectroscopy(EELS),[4,18-22] secondary electron emission spectroscopy(SES),[19-20] secondary ion mass spectroscopy(SIMS)[13,23] and change in work function.[1,24-25] These studies have been mainly concerned with the oxidation of zirconium at room temperature, but a knowledge of dynamic properties of the oxidation of zirconium at high temperatures has not been given.

A Dynamic competition between the surface processes (*i.e.* the dissociative adsorption of oxygen molecules and the transfer of oxygen adatoms into the bulk) and the diffusion process of oxygen in the bulk

---

* Accepted for publication in *J. Chem. Soc., Faraday Trans.*

determines the oxygen concentration at the surface in the oxygen absorption by transition metal at high temperatures. In our previous works[26-28] we have investigated the rate of oxygen absorption by zirconium at high temperatures of 743-1098 K and at low oxygen pressures of 6.7×10^{-5} - 1.3×10^{-3} Pa. It has been found that the rate of oxygen absorption by α-zirconium is linear with time and that the rate is limited by the adsorption process of oxygen.[27] The linear rate has been explained by a model based on three successive steps of the oxygen absorption: dissociative adsorption, transfer of oxygen adatoms into the bulk sites and diffusion of oxygen in the bulk. The rate of oxygen absorption by oxide-covered surface has been found to be parabolic.[26,28] The rate is limited by the diffusion of oxygen in the bulk and the rate has been explained by a model involving oxygen diffusion with a moving boundary of oxide/metal interface. An anomaly in the rate of oxygen absorption is observed, *i.e.* the rate is increased anomalously by the oxide nucleation at the surface. Although some kinetic parameters have been determined from the absorption measurements, a knowledge of the oxidation state of zirconium surface at high temperatures has not been given in the absorption measurements.

Few studies on the oxidation of zirconium at high temperatures by using *in situ* surface spectroscopic measurements have been reported.[2,7,23,25] In these studies the change in the electronic structure by oxidation at high temperatures has not been discussed. The purpose of the present study is to investigate the change in the electronic structure of the surface by oxidation and the dynamic properties of the oxidation of zirconium at high temperatures by using the AES, EELS and SES measurements. First we will investigate the change in the spectra by

oxidation at room temperature, and then the results are used to analyse the change by oxidation at high temperatures.

Experimental

All experiments were done in a UHV system which had a base pressure of the order of 10^{-8} Pa. Auger electron, electron energy loss and secondary electron emission spectra were obtained by the use of a Varian single-pass cylindrical mirror analyzer with resolution ($E/\Delta E$) of *ca.* 200. The derivative Auger electron spectra ($dN(E)/dE$) and the second-derivative energy loss and secondary electron emission spectra ($-d^2N(E)/dE$) were measured with the electron beams at primary energies of 3000 eV, 500 eV and 500 eV, respectively, with its axis at 30° to the normal of the specimen surface. The electron currents of 0.3, 0.05 and 0.3 μA were used for the AES, EELS and SES measurement, respectively. A modulation voltage of 1 V_{pp} was supplied to the cylindrical mirror analyzer.

Polycrystalline zirconium foils of dimensions 25 mm × 5 mm × 0.025 mm and 99.99 % purity were used in this study. The specimen was mechanically polished, ultrasonically degreased in acetone, and then spot welded onto two tantalum support wires of 0.8 mm in diameter. The specimen which was on the ground electric potential was heated resistively by passing a 60 Hz alternative electric current. The ac voltage across the specimen was less than 1 V. No significant changes were observed in the Auger electron, the electron energy loss and the secondary electron emission spectra of the clean and the oxidized surface between room temperature and high temperatures at 773 - 1073 K. The temperature of the

specimen was measured with a Pt-PtRh13% thermocouple spot welded to the specimen and was controlled using a thermoregulator. The surface of the specimen was cleaned by the cyclic Ar^+-ion bombardment (2 keV, 10 $\mu A \cdot cm^{-2}$) at 773 K and by the annealing at 1073 K. No impurities were detected within the detection limit of the AES. Our previous SIMS measurements have shown that these treatments reduce the surface contaminants such as oxygen, carbon and chlorine segregated by annealing.[27]

After the surface of the specimen was cleaned, the temperature of the specimen was adjusted to the desired value for a measurement. The oxygen gas of 99.995% purity was admitted to the chamber, and the oxygen pressure in the specimen chamber was kept constant by using an automatic pressure control valve. The fluctuation of the partial pressure of oxygen was within ± 5 %. In order to reduce the perturbation of the surface such as an electron stimulated desorption of oxygen by the electron bombardment, the surface was not bombarded continuously but bombarded for *ca.* 80 s on each separate occasion of the measurements (at 0, 300, 600, 1200, 1800, 2400, 3000 and 3600 s). The decrease of the peak-to-peak height of the oxygen Auger electron by the electron bombardment for *ca.* 80 s was confirmed to be less than 5 %. In the oxidation of zirconium at room temperature the spectra were measured under the condition that the specimen was not exposed to oxygen gas.

Results and Discussion

AES

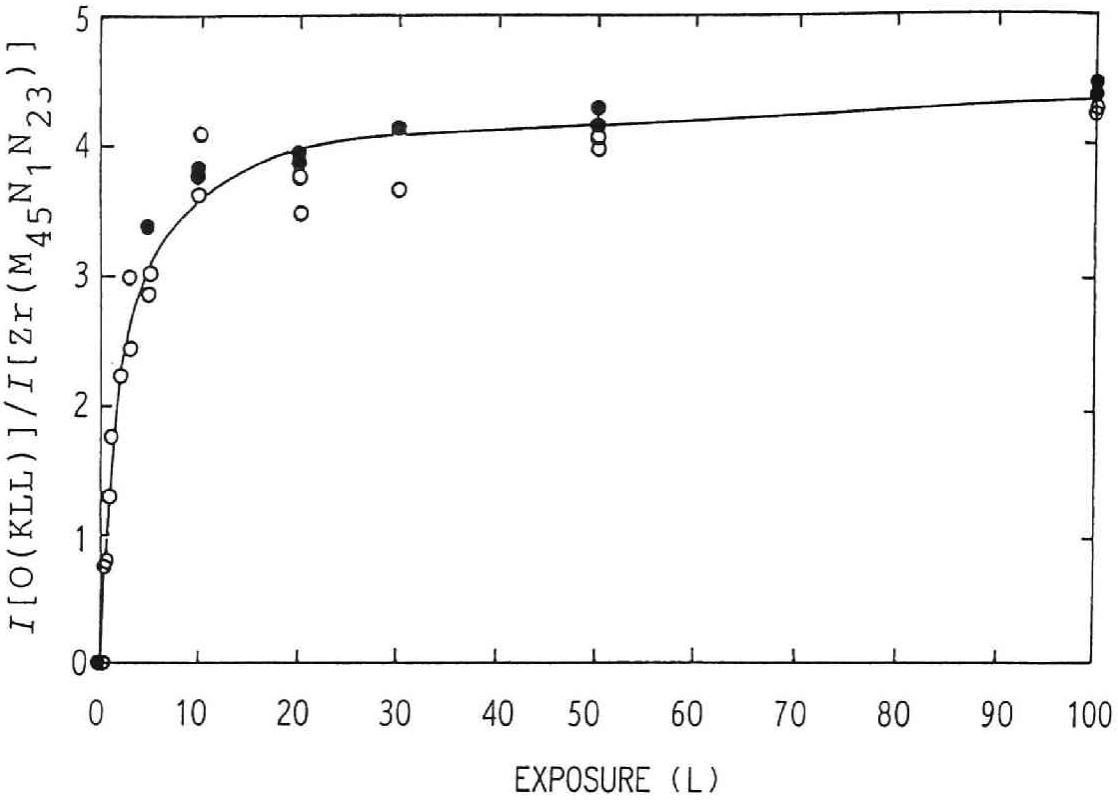

Fig. 6-1. Relative peak-to-peak height of the oxygen KLL Auger transition and of the zirconium $M_{45}N_1N_{23}$ transition as a function of oxygen exposure in Langmuir (1 L ≡ 10^{-6} Torr·s). Metallic zirconium with a clean surface was oxidized at room temperature under constant oxygen pressures of 1.3 × 10^{-6} (○) and 1.3 × 10^{-5} Pa (●).

Oxidation at Room Temperature

Metallic zirconium with a clean surface was exposed to oxygen at room temperature and under oxygen pressures of 1.3×10^{-5} and 1.3×10^{-6} Pa. Fig. 6-1 shows the typical change in the relative peak-to-peak height of the oxygen KLL Auger transition (510 eV for the clean surface) and of the zirconium Auger $M_{45}N_1N_{23}$ transition (90 eV for the clean surface) as a function of oxygen exposure. The relative height may be a measure of the surface concentration of oxygen, because the above-mentioned Auger processes involve only the electron transitions among the core states. The relative height was increased rapidly up to 20 L (1L $\equiv 10^{-6}$ Torr·s) and remained almost constant to 100 L. This behaviour is in good agreement with that reported previously.[1,4-5] It has been reported that the relative height is scarcely increased by the further exposure of oxygen > 100 L.[4-5] As the results at 1.3×10^{-6} Pa are compared with the results at 1.3×10^{-5} Pa, the change of the relative height has been found to depend on the exposure scaled in the unit of Langmuir.

The Feynman diagram of the Auger processes and the kinetic energy of the Auger ABC transition E(ABC) are given by

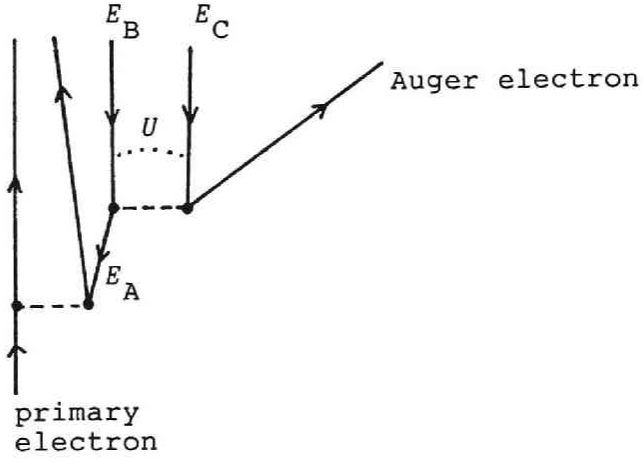

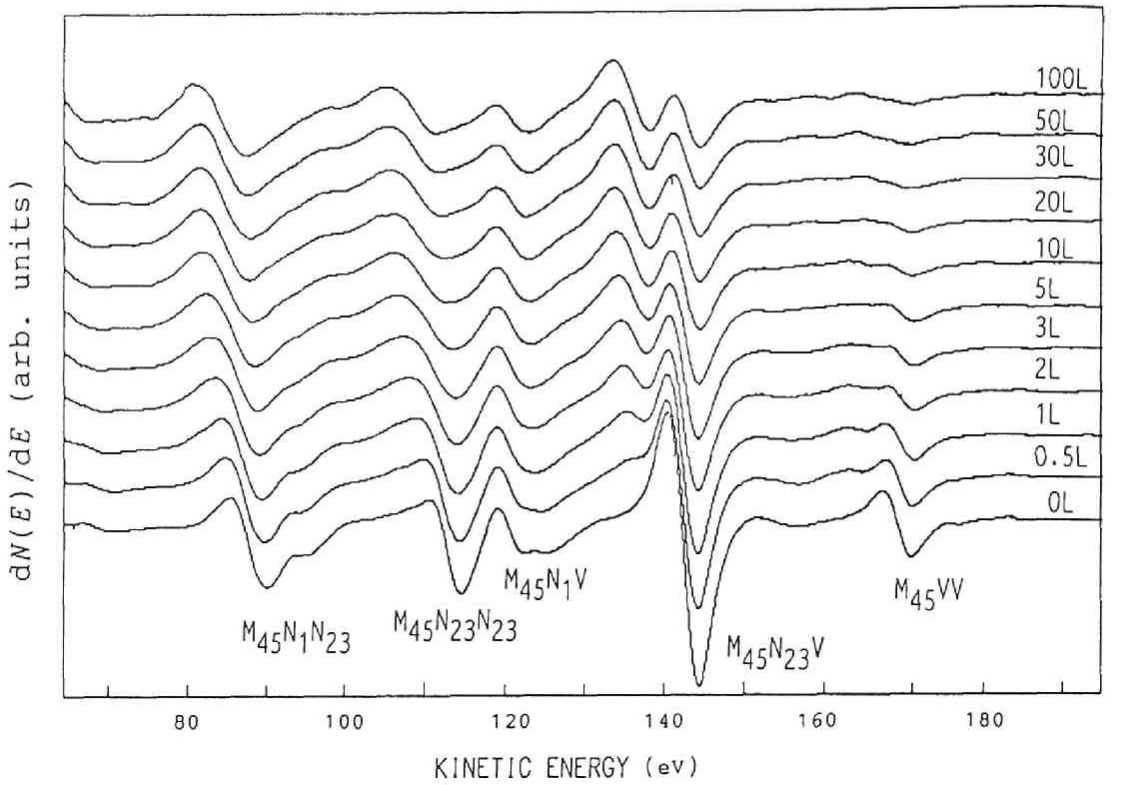

Fig. 6-2. Change in the Auger electron spectra of zirconium by oxidation at room temperature as a function of oxygen exposure in Langmuir.

$$E(ABC) = E_A - E_B - E_C - U - \Phi_S \quad (6\text{-}1)$$

$$U = H - P \quad (6\text{-}2)$$

where E_A, E_B and E_C are the one-electron binding energies of A, B and C level, respectively, and are normally taken to be those measured in X-ray photoelectron spectroscopy, which include one-hole relaxation effect. U is the repulsive hole-hole interaction energy which decreases the kinetic energy of Auger electron. H is the hole-hole interaction energy in the free atom and may have a correlation with the second ionization energy of zirconium atom 13 eV. P is the effect of relaxation by the solid environment and is expected to reduce the interaction energy U. Φ_S is the work function of the spectrometer and the reference level of the energies E_A, E_B and E_C is chosen as the Fermi energy. The value of Φ_S is approximated to be 5 eV.[29]

Fig. 6-2 shows the change in the Auger spectra of zirconium by oxidation at room temperature in the 70-190 eV energy range as a function of oxygen exposure. The assignments of the Auger peaks for the clean surface are as follows: the peaks for the clean surface at the kinetic energy of 90.0, 114.7, 125.3, 145.0 and 172.0 eV correspond to the $M_{45}N_1N_{23}$, $M_{45}N_{23}N_{23}$, $M_{45}N_1V$, $M_{45}N_{23}V$, $M_{45}VV$ transition, respectively. The above assignments are in agreement with those reported previously.[1-7] If the hole-hole interaction energy U is negligible, the kinetic energies are given by using the values of the electronic levels determined by XPS[11-17,30] and UPS[12];

$E(M_{45}N_1N_{23})$ = 94.7 - 97.8 eV (measured value 90.0 eV)
$E(M_{45}N_{23}N_{23})$ = 116.8 - 120.7 eV (measured value 114.7 eV)

$E(M_{45}N_1V)$ = 122.3 - 124.6 eV (measured value 125.3 eV)
$E(M_{45}N_{23}V)$ = 144.3 - 147.4 eV (measured value 145.0 eV)
$E(M_{45}VV)$ = 171.8 - 174.1 eV (measured value 172.0 eV)

where the level V is chosen as the level of the maximum of density of states (1 eV below the Fermi level).[12] The calculated energies except for the $M_{45}N_1N_{23}$ transition are in good agreement with those measured, then the assumption that U is negligible may be justified. This fact suggests that the relaxation P is comparable to the energy H.

As shown in Fig. 6-3, as a result of the oxidation of zirconium the kinetic energies of the Auger electron were decreased by 2.6 eV in the $M_{45}N_1N_{23}$ transition, 3.2 eV in the $M_{45}N_{23}N_{23}$ transition and 2.1 eV in the $M_{45}N_1V$ transition. In the $M_{45}N_{23}V$ transition a new peak at the energy lower by 6.4 eV was observed from the exposure at 1 L and no change in energy of the peak at 145 eV was found. In the $M_{45}VV$ transition a new peak at the energy lower by 5 - 6 eV appeared from oxygen exposure 1 L to 10 L and this peak disappeared at exposure of 20 L and a new peak at the energy lower by *ca.* 10 eV appeared.

Several investigators have studied the energy shift of the Auger peak of zirconium by the oxide formation at the surface.[4-6] However, the energy shift has not been discussed by using the results of the energy shift both of the core levels and of the valence band by the oxide formation. The energy shift of the core levels is due to the chemical shift, which is caused by a change in the electron configuration surrounding the zirconium atom in the oxide and a change in the relaxation of the core holes in the final state. The energy shift of the valence band is due to the formation of oxygen 2p band below the Fermi level by the oxide formation. It has been shown from the results of the XPS[11-17,30] and the UPS[12] that the downward energy shift of the M_{45}, N_1, N_{23} and the

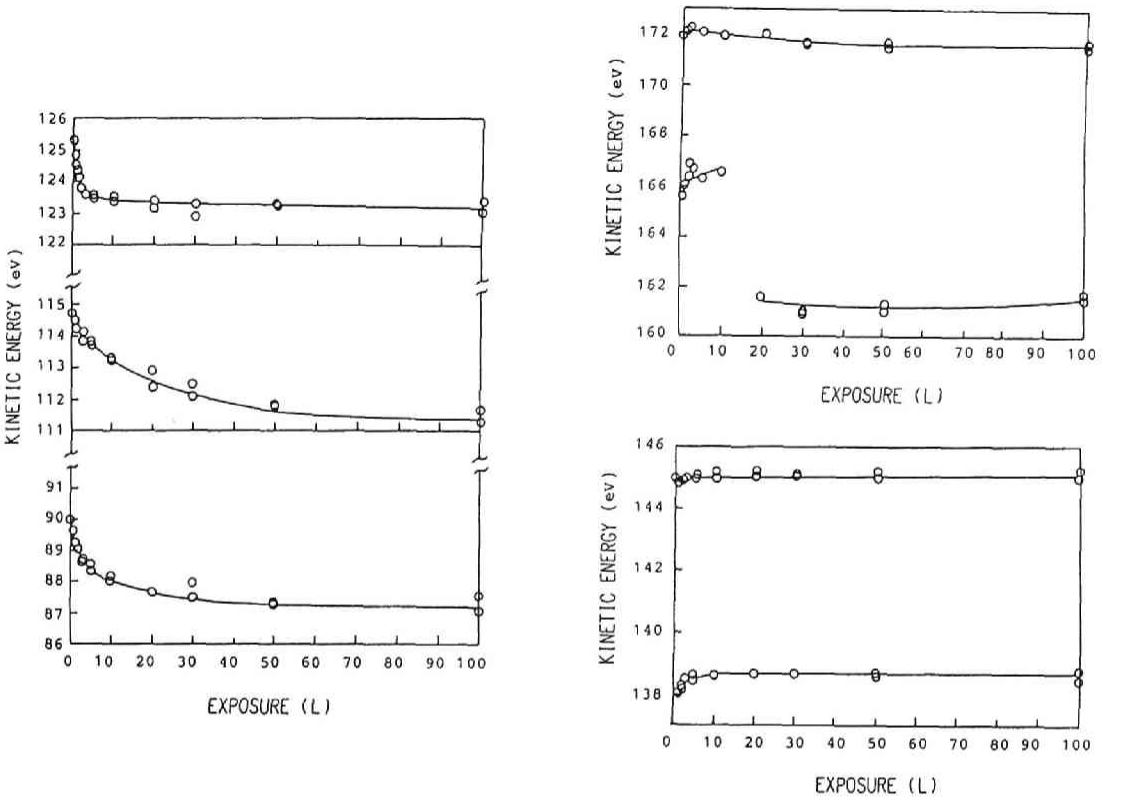

Fig. 6-3. Changes in the kinetic energies of the Auger electron of zirconium by oxidation at room temperature as a function of oxygen exposure in Langmuir.

valence level are 4.3 eV, 1.1 eV, 4.1 eV and 5 eV, respectively. The energy shift of the Auger peak is given by eqn.(6-1), if we assume that hole-hole interaction is negligible.

$*\Delta E[M_{45}(O)N_1(O)N_{23}(O)] = 4.3 - 1.1 - 4.1 = -0.9$ eV
(measured value -2.6 eV)

$*\ \Delta E[M_{45}(O)N_{23}(O)N_{23}(O)] = 4.3 - 4.1 - 4.1 = -3.9$ eV
(measured value -3.2 eV)

$*\ \Delta E[M_{45}(O)N_1(O)V(O)] = 4.3 - 1.1 - 5 = -1.8$ eV
$\Delta E[M_{45}(O)N_1(O)V(M)] = 4.3 - 1.1 - 0 = +3.2$ eV
$\Delta E[M_{45}(M)N_1(M)V(O)] = 0.0 - 0.0 - 5 = -5.0$ eV
(measured value -2.1 eV)

$*\ \Delta E[M_{45}(O)N_{23}(O)V(O)] = 4.3 - 4.1 - 5 = -4.8$ eV
$\Delta E[M_{45}(O)N_{23}(O)V(M)] = 4.3 - 4.1 - 5 = +0.2$ eV
$\Delta E[M_{45}(M)N_{23}(M)V(O)] = 4.3 - 4.1 - 5 = -5.0$ eV
(measured value -6.4 eV)

$*\ \Delta E[M_{45}(O)V(O)V(O)] = 4.3 - 5 - 5 = -5.7$ eV
$\Delta E[M_{45}(O)V(O)V(M)] = 4.3 - 5 - 0 = -0.7$ eV
$\Delta E[M_{45}(O)V(M)V(O)] = 4.3 - 0 - 5 = -0.7$ eV
$\Delta E[M_{45}(O)V(M)V(M)] = 4.3 - 0 - 0 = +4.3$ eV
$\Delta E[M_{45}(M)V(O)V(O)] = 0 - 5 - 5 = -10$ eV
$*\ \Delta E[M_{45}(M)V(M)V(O)] = 0 - 0 - 5 = -5$ eV
$*\ \Delta E[M_{45}(M)V(O)V(M)] = 0 - 5 - 0 = -5$ eV
(measured value -5 - -6 eV from 1 - 10 L and *ca.* -10 eV after 20L)

Here M and O indicate the electronic levels in the metallic zirconium and in the zirconium oxide, respectively. An interatomic transition between the core levels cannot occur because the overlap of the wave functions of the core states between the neighboring atoms is negligible. The asterisk * in the first column indicates the most probable transition.

The kinetic energies of the Auger transitions which involve only those among the core levels are in agreement with the kinetic energies calculated by the change in energy of the relevant core states of the oxide. The Auger transitions which involve the valence band have a possibility that an interatomic and a cross transition occur.[5-6] The change in energy of the $M_{45}N_1V$ transition may be caused by the 000

transition among the levels in the oxide. The change in energy of the $M_{45}N_{23}V$ transition may be explained by either the 000 transition or the interatomic MM0 transition. However, the change may be caused by the 000 transition, because the transition probability of the 000 transition is greater than that of the interatomic transition. The kinetic energy of the core-valence-valence $M_{45}VV$ transition at the energy lower by 5 - 6 eV may be explained by the MM0 interatomic and the M0M cross transition, because the peak appeared at initial oxidation stage of 1 - 10 L and the new peak at the energy lower by *ca.* 10 eV appeared at the further exposure > 20L. The peak at the energy lower by *ca.* 10 eV can not be explained by the 000 transition on the assumption that the hole-hole interaction is negligible. It seems that the transition is caused by the M00 interatomic transition at the energy lower by *ca.* 10 eV. However, we can not conclude that the transition is caused by the interatomic transition or the 000 transition which include the hole-hole interaction of several electron volts. The probability of the occurrence of the M00 interatomic transition may be low at the oxide-covered surface in comparison with that of the 000 transition.

By oxidation of zirconium the peak-to-peak height are decreased in comparison with those for the clean surface: 20 % decrease in the $M_{45}N_1N_{23}$ transition, 50 % decrease in the $M_{45}N_{23}N_{23}$ transition and 40 % decrease in the $M_{45}N_1V$ transition. The concentration of zirconium is decreased by *ca.* 30 % from the metal to oxide surface. The decrease in the heights of the $M_{45}N_1N_{23}$ transition may be explained by the decrease in the concentration of zirconium. The decrease in the height of the $M_{45}N_{23}N_{23}$ transition may be caused by the decrease in the concentration of zirconium and the peak broadening. The lower kinetic energy part of the $M_{45}N_1V$

transition overlaps the peak of the $M_{45}N_{23}N_{23}$ transition, and the decrease in the height can not be discussed in detail. The heights in the $M_{45}N_{23}V$ and $M_{45}VV$ transitions were decreased and the new split peaks were observed at the lower kinetic energy. As shown by Axelsson *et al.*[4] the peak broadening of the metallic peaks of the $M_{45}N_{23}V$ and the $M_{45}VV$ transition and the peak split may cause the decrease in the peak-to-peak heights by 80 %.

By using the result of the decrease in the peak-to-background height of the Auger $M_{45}N_{23}V$ transition we will estimate the oxide thickness on the metal zirconium.[5] The assumptions made to estimate of the oxide thickness are: (i)a homogeneous oxide layer grows on the metallic zirconium surface and (ii) the signal of the $M_{45}N_{23}V$ transition at 145 eV is the signal of the electron emission from the metallic zirconium under the oxide layer. The decay of the signal of the normal emission through the oxide layer of thickness d is given by

$$I(\text{Zr under oxide layer}) / I(\text{Zr clean surface}) = \exp(-d / \lambda) \quad (6\text{-}3)$$

where λ is the electron inelastic mean free path. λ, which has a uncertainty of *ca.* 30 %, is determined for inorganic compounds by Seah and Dench.[31] For zirconium oxide λ is estimated to be 0.982 nm for the electron of the $M_{45}N_{23}V$ transition. By correcting factors of the emission and the detection angle of the electron measured in our experimental arrangement, we have determined the oxide thickness as a function of oxygen exposure. As shown in Fig. 6-4, the growth of the oxide thickness after the exposure of oxygen for 100 L is almost completed and

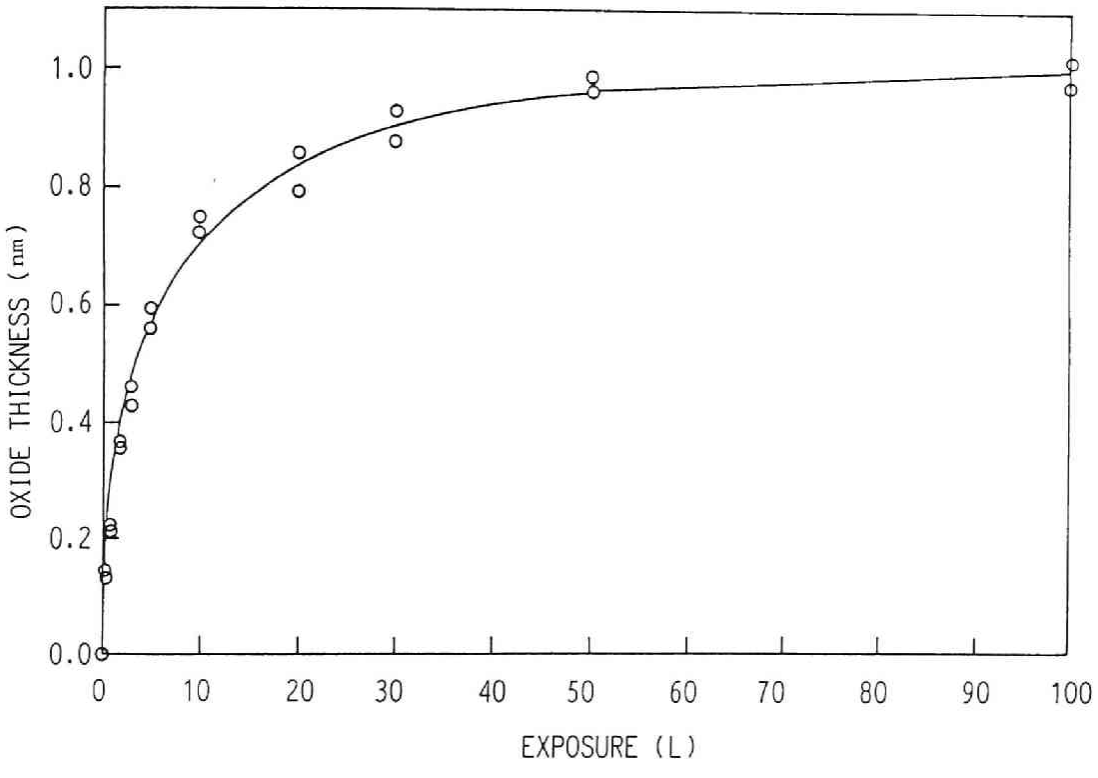

Fig. 6-4. Growth of the oxide film by oxidation at room temperature as a function of oxygen exposure in Langmuir.

the thickness is estimated to be *ca.* 1 nm. In the previous studies[5,6-17] the oxide thickness on metallic zirconium at room temperature is reported to be *ca.* 1-1.5 nm at the exposure of 100 L. The oxide thickness estimated in the present study is in good agreement with those reported previously.

Oxidation at High Temperatures

Metallic zirconium with a clean surface was exposed to oxygen at temperatures of 773 - 973 K and under constant oxygen pressures of 1.3×10^{-5} - 1.3×10^{-3} Pa. Auger spectra were measured *in situ* at oxygen pressures of 1.3×10^{-5} - 6.7×10^{-5} Pa. The specimen oxidized at pressures of 1.3×10^{-4} - 1.3×10^{-3} Pa and at 873 K was cooled down to room temperature and Auger spectra were measured at pressures less than 4×10^{-7} Pa. Fig. 6-5 and Fig. 6-6 show the temperature and pressure dependences of the typical change in the relative peak-to-peak height of the oxygen KLL transition (510 eV for clean surface) and of the zirconium $M_{45}N_1N_{23}$ transition (90 eV for clean surface) as a function of exposure time. The temperature dependence of the change in the relative height at a constant oxygen pressure of 1.3×10^{-5} Pa and the pressure dependence at 873 K are shown in Fig. 6-5 and Fig. 6-6, respectively.

Recently we have shown that the oxygen concentration at the surface is determined by the dynamic competition between the rate of the surface processes such as the adsorption of oxygen gas and the transfer of oxygen adatoms to bulk sites and the rate of the oxygen diffusion into the bulk.[23,26-28] As shown in Fig. 6-5, the low relative height at 873 - 973

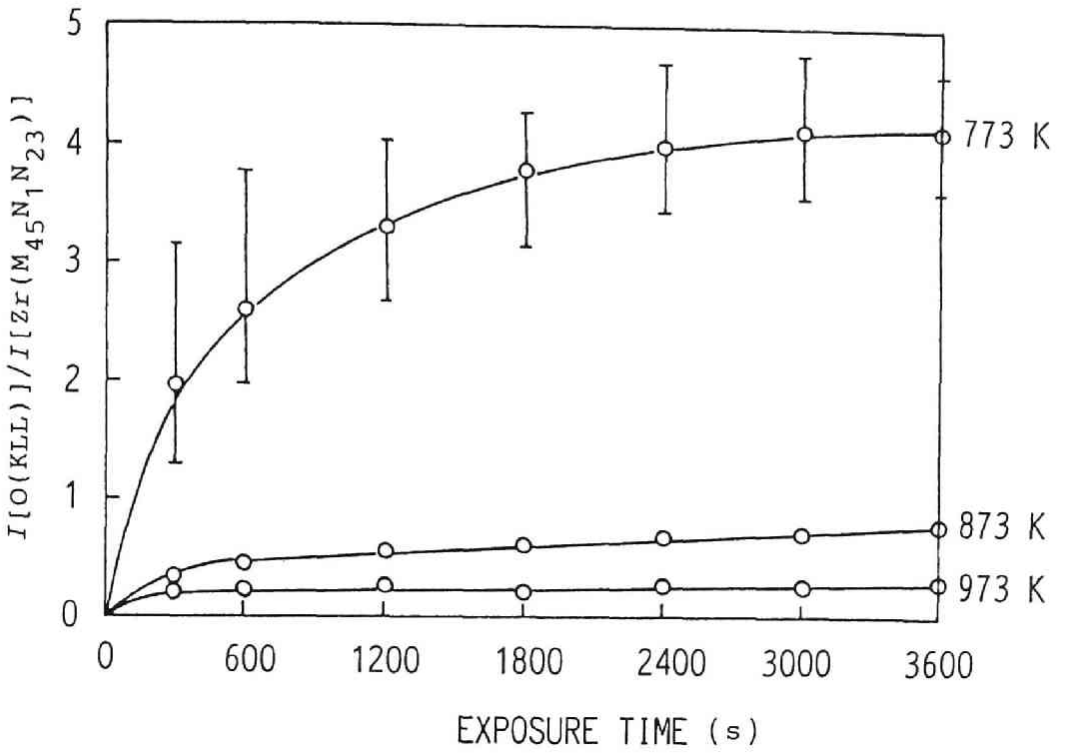

Fig. 6-5. Temperature dependence of the increase in the relative peak-to-peak height of the oxygen KLL transition and of the zirconium $M_{45}N_1N_{23}$ transition as a function of oxygen exposure in time. Metallic zirconium with a clean surface was oxidized under a constant oxygen pressure of 1.3×10^{-5} Pa.

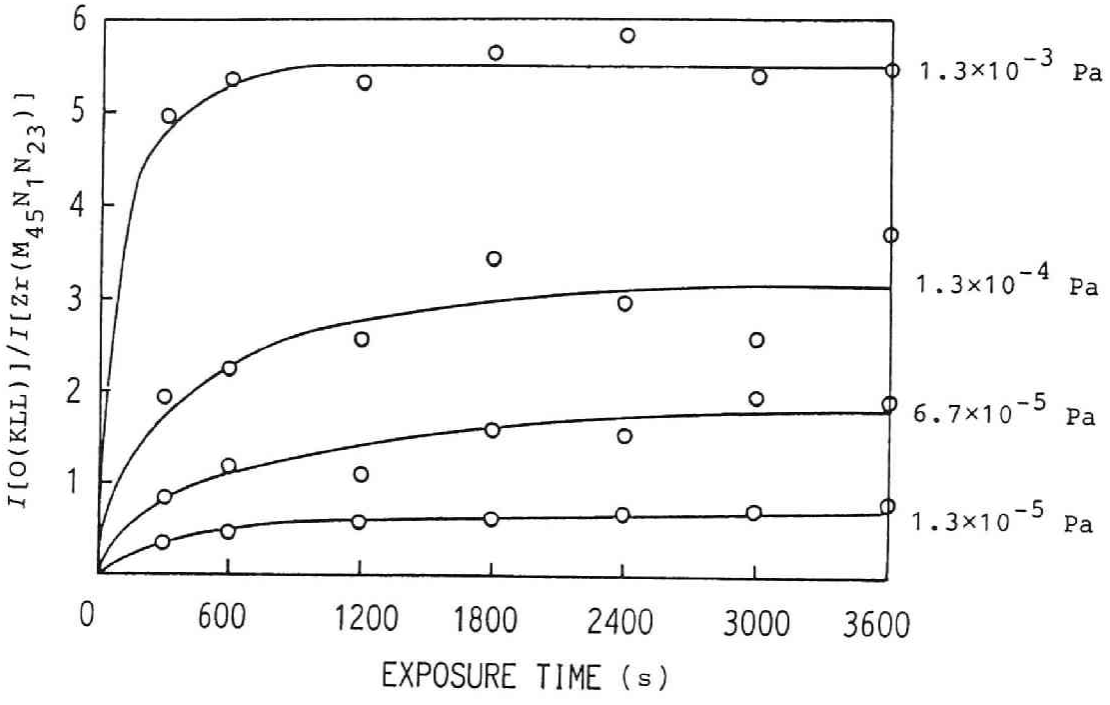

Fig. 6-6. Pressure dependence of the increase in the relative peak-to-peak height of the oxygen KLL transition and of the zirconium $M_{45}N_1N_{23}$ transition as a function of oxygen exposure in time. Metallic zirconium with a clean surface was oxidized at 873 K.

K may be caused by the slow accumulation rate of oxygen at the surface due to the faster diffusion rate at high temperatures. By the slower diffusion rate at 773 K the relative height is increased rapidly and saturated to the value 4 at *ca.* 1800 s (180 L). However, the exposure at which the relative height showed saturation at 773 K was prolonged in comparison with that at room temperature because of the diffusion of oxygen into the bulk.

In our previous study[26-28] the rate of oxygen absorption by α-zirconium at high temperatures is found to be proportional to the pressure of oxygen and the rate of oxygen absorption by the oxide-covered surface is proportional to the square root of the pressure of oxygen. As shown in Fig. 6-6, the relative height was increased with the pressure of oxygen. However, the increase in the relative heights did not simply depend on the oxygen exposure represented by the product of the oxygen pressure and the exposure time, *i.e.* exposure in Langmuir. This fact supports that the concentration of oxygen at the surface is determined by the dynamic competition between the surface processes and the diffusion process. The change of the relative height at room temperature depends on the exposure scaled in the unit of Langmuir, because the rate of oxygen diffusion into the bulk is negligible at room temperature in comparison with the rate of surface processes.

Anomaly in the rate of oxygen absorption, *i.e.* the rate is increased due to the oxide nucleation at the surface, has been observed at 923 K and at oxygen pressure of 6.7×10^{-5} Pa and at 973 K at pressure of 1.3×10^{-4} Pa.[28] As compared with the results at room temperature, the increase in the relative height of the Auger peak suggests that oxide nucleation occurs at 873 K at oxygen pressures greater

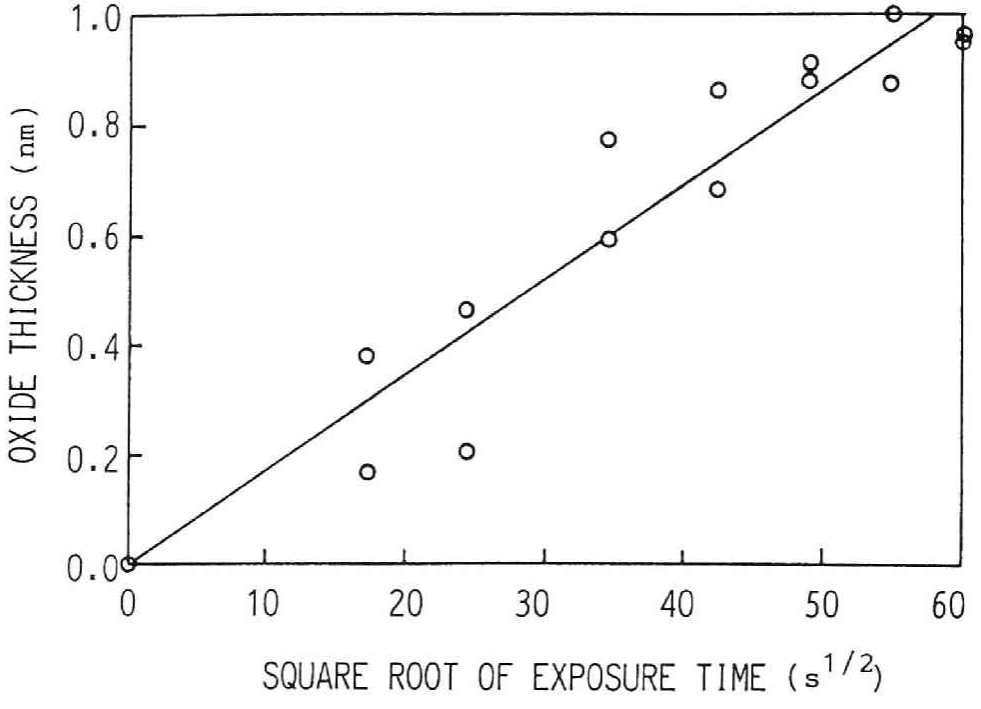

Fig. 6-7. Growth of the oxide film by oxidation at 773 K and 1.3×10^{-5} Pa as a function of the square root of the oxygen exposure in time.

than 6.7×10^{-5} Pa.

The shift of the kinetic energy of the Auger peak of zirconium by oxidation has been measured *in situ* at 773 K and 873 K under a constant oxygen pressure of 1.3×10^{-5} Pa. The kinetic energies of the Auger peaks of zirconium at 773 K after oxygen exposure of 3600 s are decreased by 2.2 eV in the $M_{45}N_1N_{23}$ transition, 1.5 eV in the $M_{45}N_{23}N_{23}$ transition and 1.4 eV in the $M_{45}N_1V$ transition. Although these values of the energy shift are slightly less than those in the measurement at room temperature, the values measured are in agreement with those estimated above on the basis of the assumption that the hole-hole interaction energy is negligible.

In the $M_{45}N_{23}V$ transition a new peak at the energy lower by 6.5 eV was observed after the exposure of 300 s and no changes in energy of the peak at 145 eV were found. By using the result of the decrease in the peak-to-background height of the $M_{45}N_{23}V$ Auger transition the oxide thickness on metal zirconium is estimated. Fig. 6-7 shows the oxide thickness as a function of the square root of time of the oxygen exposure. It has been found that the rate of oxide growth is almost parabolic, *i.e.* the oxide thickness is proportional to the square root of time. This parabolic growth rate can be explained by our absorption model[26,28] in which the absorption rate by the oxide-covered surface is limited by a oxygen diffusion with a moving boundary of oxide/metal interface. The coefficient of the parabolic growth rate k_p (the oxide thickness is given by $k_p t^{1/2}$) is found to be 1.7×10^{-2} nm·s$^{-1/2}$.

The kinetic energies of the Auger electron of zirconium have not been changed significantly by oxidation at 873 K and at 1.3×10^{-5} Pa. The peak split of the $M_{45}N_{23}V$ transition at the energy lower by 6.5 eV was not

observed within the detection limit of the AES. This means that almost the whole surface of zirconium remains in α-zirconium because of the fast diffusion of oxygen into the bulk. The decreases in the peak-to-peak height of the $M_{45}N_1N_{23}$ transition, the $M_{45}N_{23}N_{23}$ transition and the $M_{45}N_1V$ transition are less than 15 % by oxidation in comparison with those for the clean surface. The oxide thickness estimated by the decrease in the metal $M_{45}N_{23}V$ Auger peak is found to be less than 0.1 nm.

EELS

Oxidation at Room Temperature

Fig. 6-8 shows the second derivative of the electron energy loss spectra as a function of oxygen exposure in Langmuir. Metallic zirconium with a clean surface was oxidized at room temperature and at a constant oxygen pressure of 1.3×10^{-5} Pa. It has been found that the loss energies for the clean surface are 6.5 eV(peak A), 15.5 eV(peak B), 22.4 eV(peak C), 27.7 eV(peak D), 35.8 eV(peak E), 42.1 eV(peak F) and 53.4 eV(peak G) and that the loss energies for the oxide-covered surface after oxygen exposure for 100 L are 6.4 eV(peak H), 12.4 eV(peak I), 19.0 eV(peak J), 25.6 eV(peak K), 32.8 eV(peak L), 39.7 eV(peak M) and 54.8 eV(peak N).

The intensity of the second derivative loss peak B is the greatest for the clean surface. It has been reported that the loss peak B is caused by a collective excitation of valence electrons.[4,18-22] Frandon *et al.* have measured the electron energy loss spectra in the transmission mode for clean surface by using a 20 keV electron beam.[18] By using the Kramers-Kronig analysis they have shown that real part of the

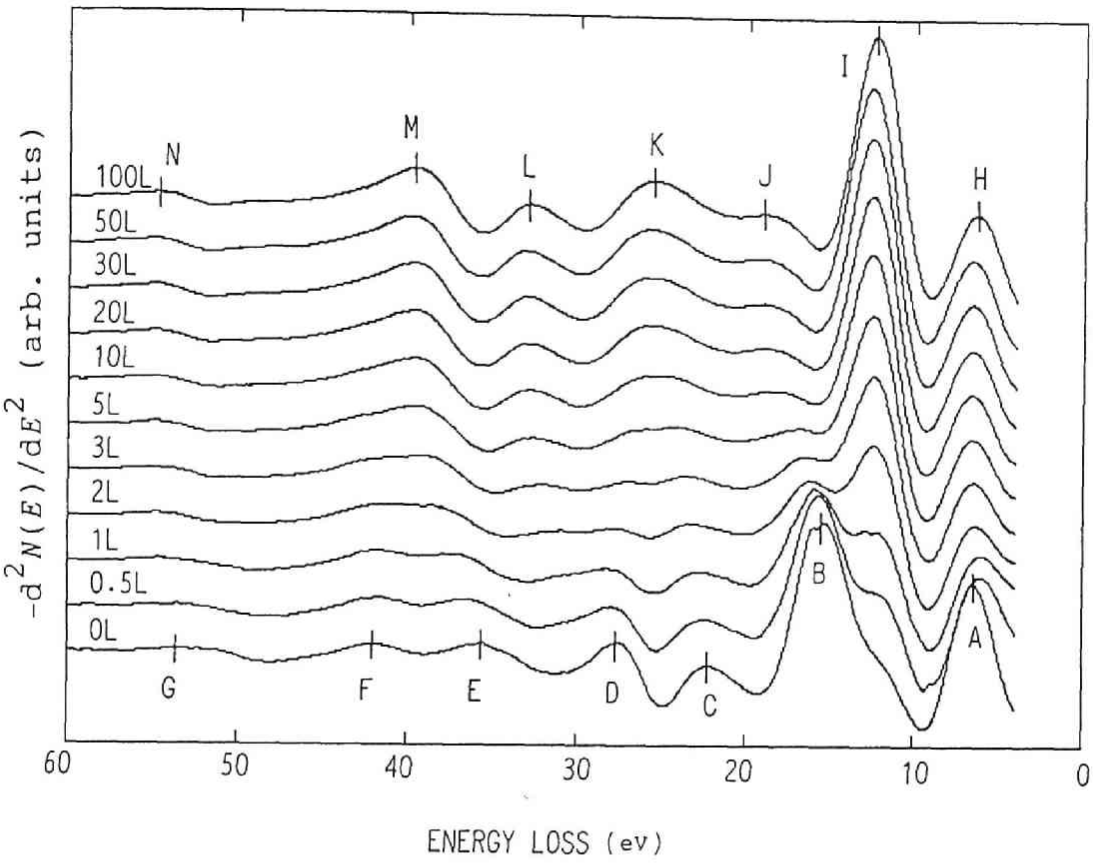

Fig. 6-8. Change in the electron energy loss spectra of zirconium by oxidation at room temperature as a function of oxygen exposure in Langmuir.

dielectric constant is zero and the imaginary part becomes small at the loss energy of 16.9 eV and concluded that the loss is caused by the bulk plasmon. The energy of bulk plasmon in the zero-th order approximation is given by

$$\hbar\omega_p = \hbar(ne^2/\varepsilon_0 m)^{1/2} \qquad (6\text{-}4)$$

where n, e, m and ε_0 are the electron density, the electron charge, the electron rest mass and the permittivity of free space. The number of valence electrons per zirconium atom is four and the energy calculated by eqn. (6-4) is 15.4 eV. The loss energy of peak B is in good agreement with that calculated. The great intensity of this peak B supports the collective feature of the loss.

The physical origin of the energy loss of the peak I, of which the intensity is the greatest for the oxide-covered surface, has been a subject of controversy.[4,18,21] It has been reported that the loss is due to a plasmon excitation,[4,18-19] an interband transition[20-21] and a collective excitation which includes an exciton creation.[32] We will assign this energy loss to a plasmon collective excitation which includes creation and annihilation of electron-hole pairs by the interband transition between the oxygen 2p valence band and the zirconium 4d conduction band.[33] The reasons for this assignment are as follows:

(i)At this loss energy the real part of the dielectric constant is zero and the imaginary part becomes smaller. We have calculated the dielectric constant by the Kramers-Kronig analysis. In the calculation we have used the data of $\mathrm{Im}(-1/\varepsilon)$ determined by Frandon *et al.*[18] The real part ε_1 and the imaginary part ε_2 of the

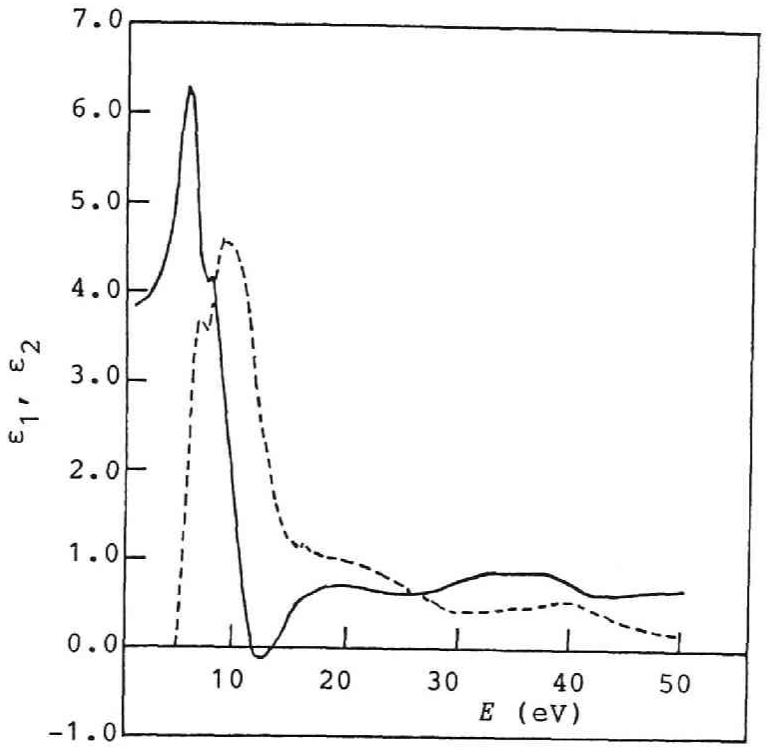

Fig. 6-9. Real part ε_1 (——) and imaginary part ε_2 (- - -) of the dielectric constant for zirconium oxide calculated from th data given by Frandon *et al.* [18]

dielectric constant as a function of loss energy are shown in Fig. 6-9. The zero of ε_1 and the small value of ε_2 suggest that a collective excitation occurs at this energy. Thus it seems that the explanation by the interband transition is not justified.

(ii)Horie has discussed the relation between an exciton and a plasmon in insulators by the use of an electron-hole pair approximation.[33] He has shown that a plasmon-like collective excitation occurs if the wave functions of the excited electron and the hole left are not localized but rather extended, *i.e.* the electrons are excited from the valence band to the conduction band. The measured optical energy gap between the valence band and the conduction band in the monoclinic zirconium oxide[34] is 4.99 eV and the gap determined by a band calculation is 4.51 eV in the monoclinic phase.[35] If the transition of the peak I is caused by the exciton collective excitation, an exciton line at the energy less than 5 eV should be observed. In our measurement loss peaks were not observed at the energy less than 5 eV but at the loss energy of 6.4 eV(loss peak H). The energy loss of the peak H may be caused by the interband transition from the oxygen 2p valence band to the zirconium 4d conduction band. This means that the plasmon-like collective excitation is induced by the electron-hole pair which has an extended wave function.

From the above discussion we may conclude that the energy loss of the peak I is caused by the plasmon-like collective excitation. According to the theory by Horie,[33] the energy of the plasmon in insulator is given by

$$(\hbar\omega)^2 \simeq \hbar^2 (n_{0\times} e^2 / \varepsilon_0 m) + E_{gap}^2 \qquad (6\text{-}5)$$

where the first term of the right-hand side of the eqn. (6-5) represents the plasmon energy of the free electron, n_{ox} is the electron density of the oxide and E_{gap} is the energy gap between the valence band and the conduction band. From the eqn. (6-5) and the plasmon energy measured, n_{ox} is estimated to be *ca.* 2 electrons per oxygen ion. The value is equal to the valency of the oxygen ion in the zirconium oxide. This fact suggests that the number of the valence electrons which induce the plasmon excitation is less than the total number of valence electrons (6 electrons per oxygen ion).

We will assign the other energy losses to the single electron excitation from an occupied electron level to an unoccupied level. In Fig. 6-10 the electronic structure from the 4s level to the valence band are shown by using the data described below. The energies of the core levels have been determined from the XPS measurements for the clean and the oxide-covered surfaces.[11-17,30] The density of the occupied states of the valence band has been determined from the UPS measurements for the clean and the oxide-covered surfaces.[12] The density of the unoccupied states for the clean surface has been measured by the bremsstrahlung isochromat spectroscopy(BIS). The density of states of metallic zirconium[36-38] and zirconium oxide in the monoclinic phase[35] have been calculated by several investigators. The energy level of the calculated oxygen 2p valence band is determined so that the energy level of the band is in agreement with that measured by the UPS.[12]

As shown in Fig. 6-10, the assignments are as follows. Peak A: from the occupied valence band to the unoccupied valence band above E_F. Peaks D, E and F: from the N_{23} level to the unoccupied valence band just above E_F. 8 eV and 14 eV above E_F, respectively.

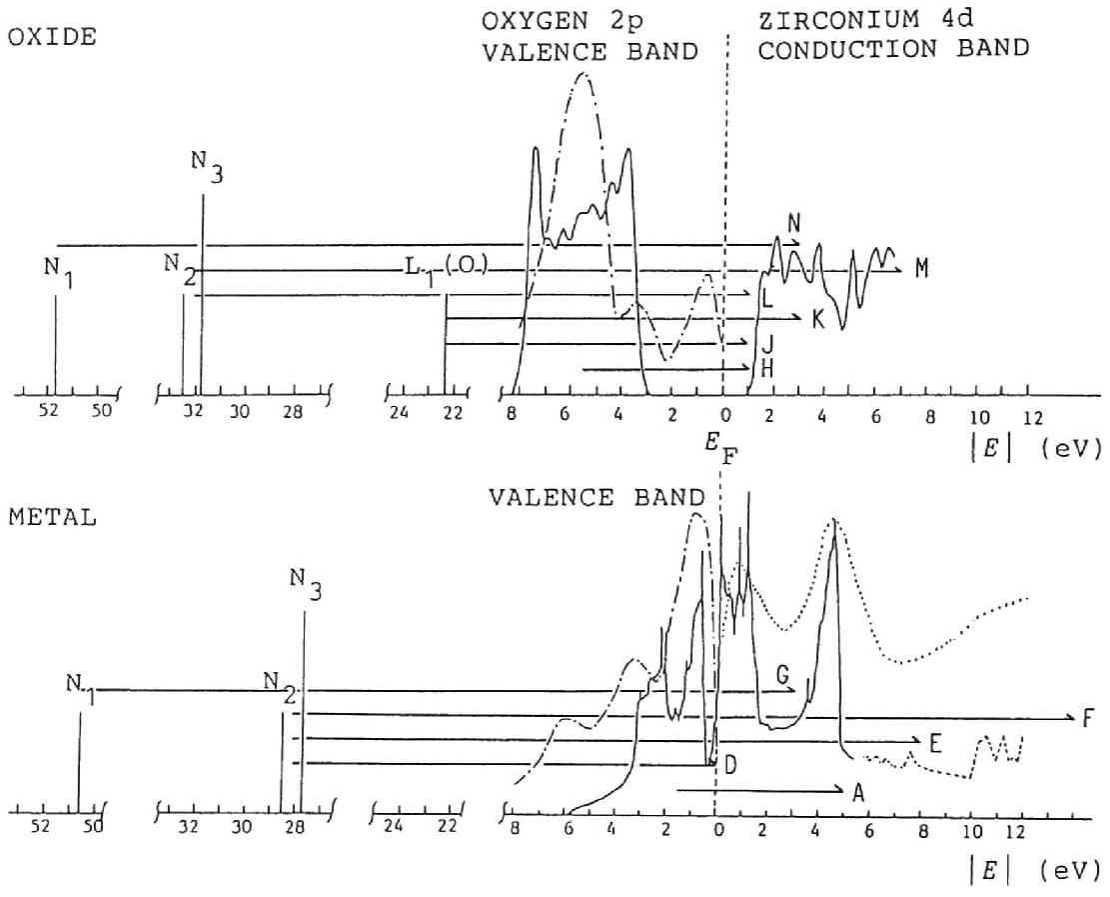

Fig. 6-10. Electronic structures of metallic zirconium and zirconium oxide. The core states are shown by the use of the results of the XPS measurement.[11-17,30] The band structure of the metallic zirconium are shown by the use of the results of the UPS measurement(—·—), [12] the BIS measurement (·····)[36] and the band calculation (– – –)[36] (——)[37]. The band structure of the oxide is shown by the use of the UPS measurement (—·—)[12] and the band structure calculation (——).[35] Assignments of the electron energy loss peaks of A-N are shown in the figure.

Peak G: from the N_1 level to the unoccupied valence band 3 eV above E_F. The peak C can not be explained. Peak H: from the valence band to the bottom of the conduction band. Peaks J and K: from the oxygen L_1 level to the conduction band bottom and 3 eV above the bottom, respectively. Peaks L and M: from the N_{23} level to the conduction band bottom and 7 eV above the bottom, respectively. Peak N: from the N_1 level to the conduction band.

Recently Vanini *et al.* have suggested that the independent electron description of the transition from the N_{23} level to the unoccupied valence band breaks down for the energy loss of metallic zirconium and that the transition is described in terms of an isolated atomic model.[22] In our assignments the fact that the excited energy level in the unoccupied valence band is not in good agreement with the maxima of the density of states may be caused by the loss mechanism suggested by Vanini *et al.*[22] However, we have assigned the energy losses based on the band model, because the hole-hole interaction energy is found to be negligible in the calculation of the kinetic energy of the Auger electron.

Oxidation at High Temperatures

Metallic zirconium with a clean surface was exposed to oxygen at temperatures of 773 K and 873 K and under a constant oxygen pressure of 1.3×10^{-5} Pa. The electron energy loss spectra were measured *in situ*. Fig. 6-11 and Fig. 6-12 show the electron energy loss spectra of zirconium at 773 K and 873 K as a function of time of oxygen exposure.

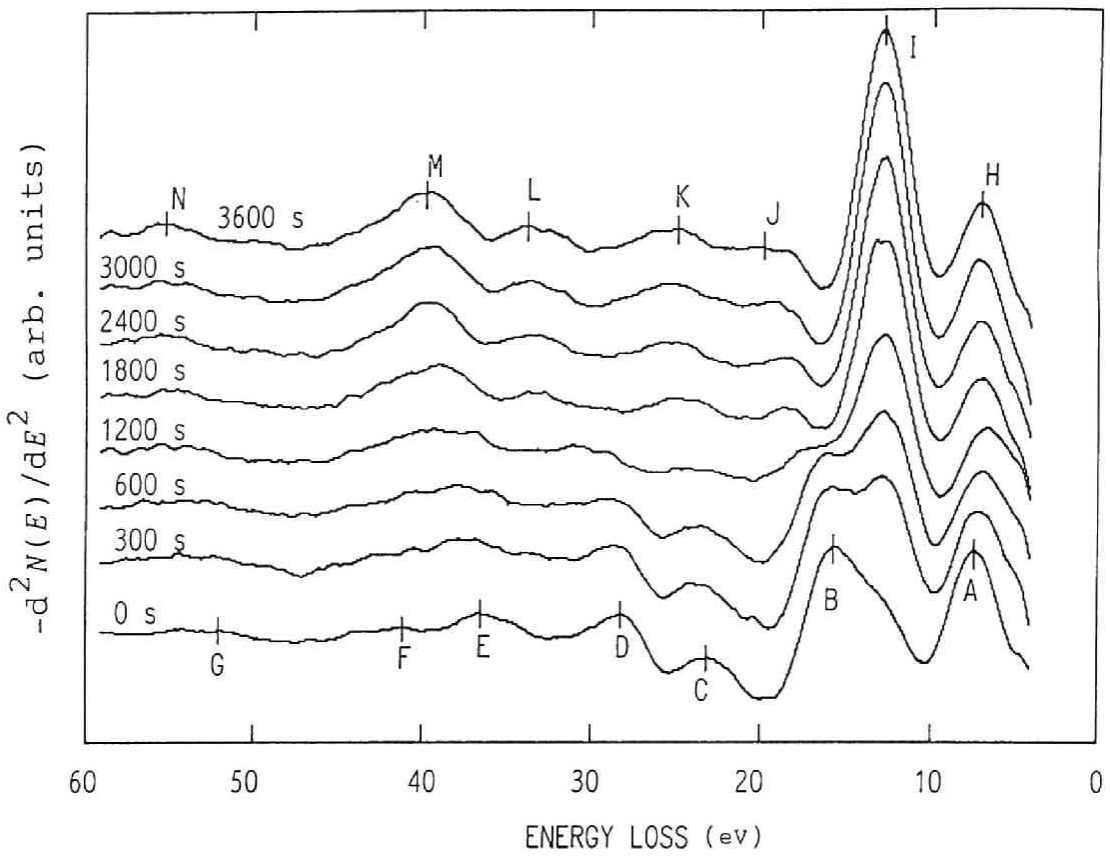

Fig. 6-11. Change in the electron energy loss spectra of zirconium by oxidation at 773 K and at 1.3 × 10^{-5} Pa as a function of oxygen exposure in time. Assignments of the peaks of A-N are identical with those of the results at room temperature.

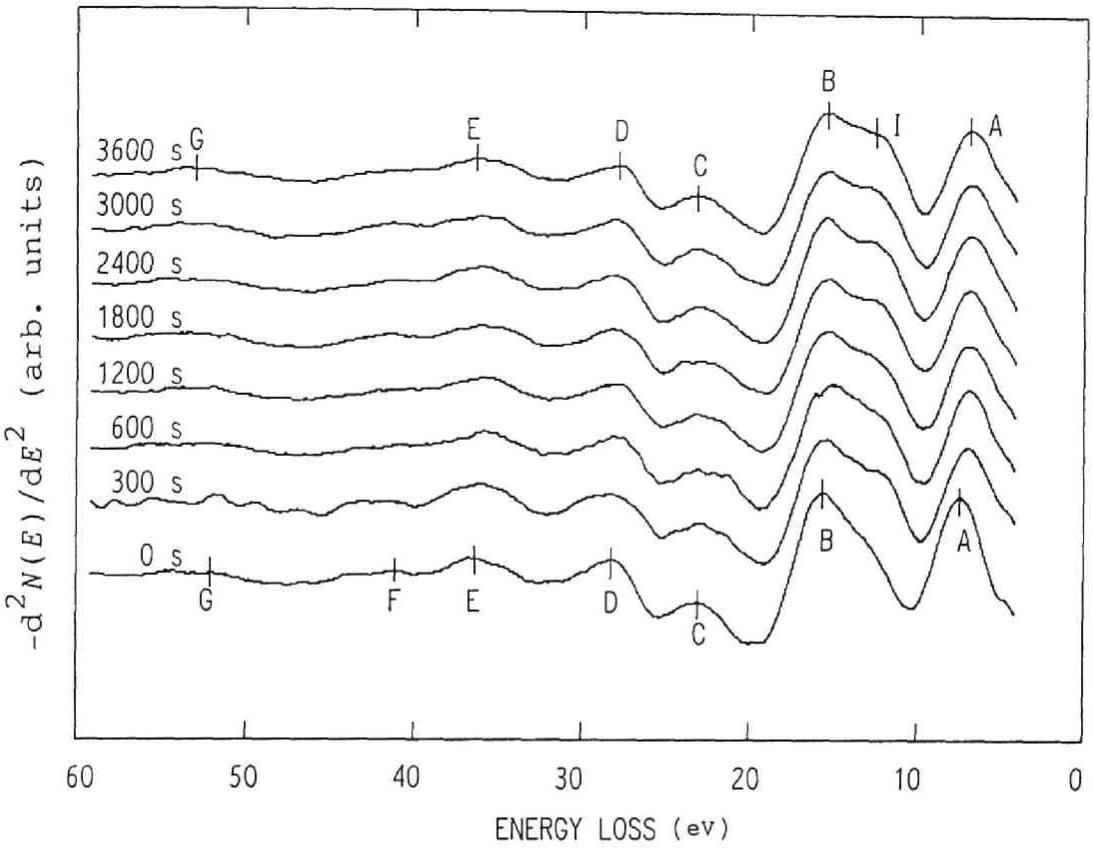

Fig. 6-12. Change in the electron energy loss spectra of zirconium by oxidation at 873 K and at 1.3×10^{-5} Pa as a function of oxygen exposure in time. Assignments of the peaks of A-G and I are identical with those of the results at room temperature.

Because of the diffusion of oxygen into the bulk the change in spectra, which is remarkably observed at the loss energy of plasmon, by oxidation at 773 K occurred slower than that at room temperature. The change in the spectra from the metal to the oxide was completed within 1800 s, which is in good agreement with the results of the Auger spectra at 773 K and 1.3×10^{-5} Pa. The loss energies and the intensities of the second derivative loss peaks for the clean and the oxide-covered surface are the same as those of oxidation at room temperature. Thereby the assignments of the peaks A-N may be the same as those of the peaks in the measurement at room temperature.

Although no significant change in the kinetic energy of Auger electron by oxidation at 873 K and at 1.3×10^{-5} Pa was observed, a peak of the plasmon loss for the oxide-covered surface was observed at the shoulder of the metal plasmon peak.(See the peak I in Fig. 6-12) This may be due to the surface sensitivity of the energy loss spectroscopy in comparison with the Auger electron spectroscopy. In our measurement the EELS has been found to be more sensitive to the contaminants at the surface. In addition the observed plasmon loss for the oxide surface may be correlated with the above-mentioned oxide thickness of less than 0.1 nm which was estimated by the decrease of the metal $M_{45}N_{23}V$ Auger peak in the measurement at 873 K and at 1.3×10^{-5} Pa. No significant changes in the loss energies and the intensities of the other loss peaks by oxidation at 873 K were observed.

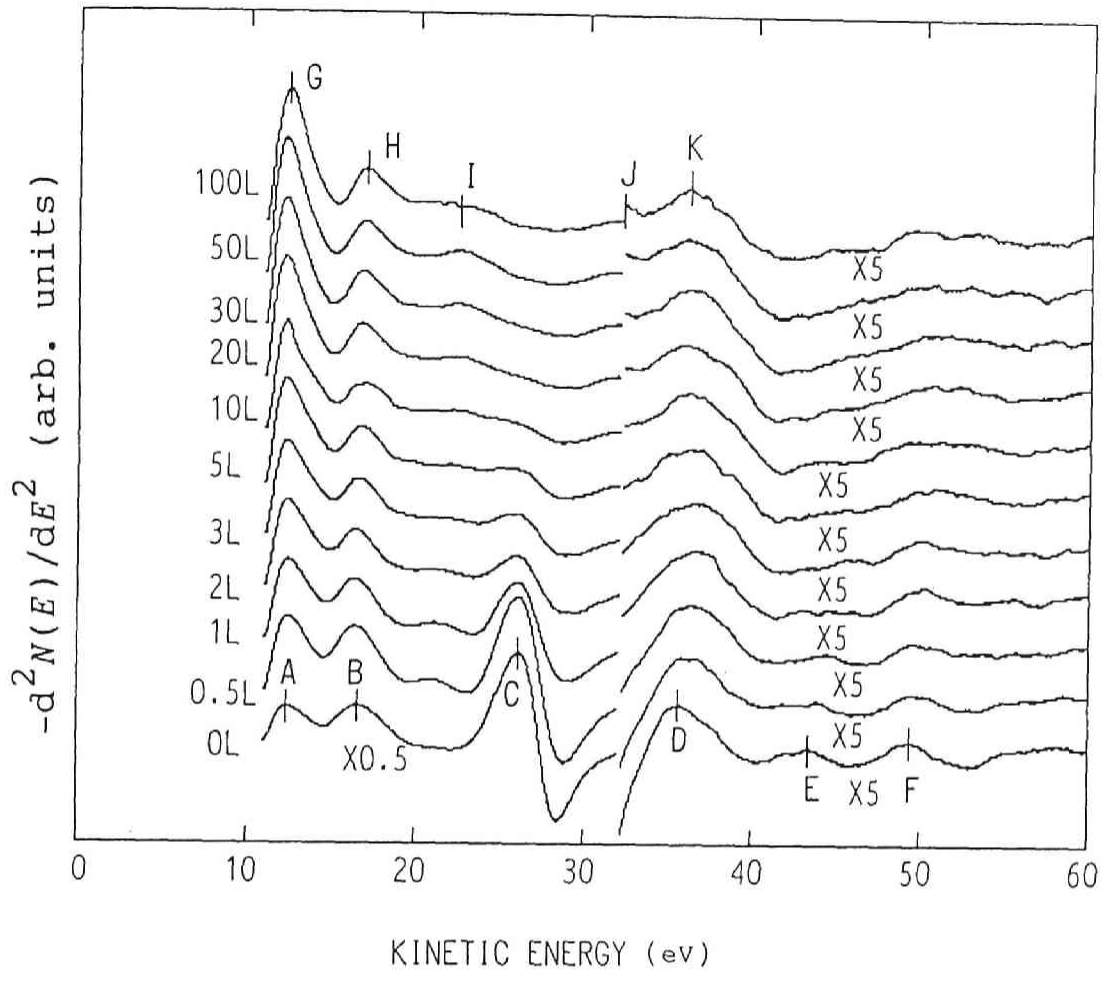

Fig. 6-13. Change in the secondary electron emission spectra of zirconium by oxidation at room temperature as a function of oxygen exposure in Langmuir. The kinetic energy is relative to the Fermi energy of the metallic zirconium.

SES

Oxidation at Room Temperature

Fig. 6-13 shows the change in the second derivative of the secondary electron emission spectra of zirconium by oxidation at room temperature as a function of oxygen exposure in Langmuir. The metallic zirconium was oxidized under a constant oxygen pressure of 1.3×10^{-5} Pa. The work function of the spectrometer *ca.* 5 eV is added to the measured kinetic energy in order to show the kinetic energy relative to Fermi energy of metallic zirconium. The kinetic energies of the peaks of the spectra are 12.4 eV(peak A), 16.4 eV(peak B), 26.1 eV(peak C), 35.6 eV(peak D), 43.4 eV(peak E) and 49.3 eV(peak F) for the clean surface and 12.3 eV(peak G), 16.6 eV(peak H), 21.7 eV(peak I), 32.3 eV(peak J) and 36.1 eV (peak K) for the oxidized surface.

Willis *et al.* have shown that some peaks observed in the SES correlate closely with the final-density-of-states maxima above the vacuum level, *i.e.* the maxima in the density of unoccupied states above the Fermi level.[39] In our spectra the peaks A, B, G and H may correspond to the density-of-states maxima 12.4 and 16.4 eV above E_F for the clean surface and 12.3 and 16.6 eV above E_F for the oxide-covered surface, respectively. Speier *et al.* have measured the density of unoccupied states up to 12 eV above E_F by BIS and shown a good agreement with the density-of-states calculated by a band theory.[36] As shown in Fig. 6-10, the density-of-states maximum exists at energy 10 eV above E_F. This maximum may correspond to the peak A. The density-of-states 12 eV above the

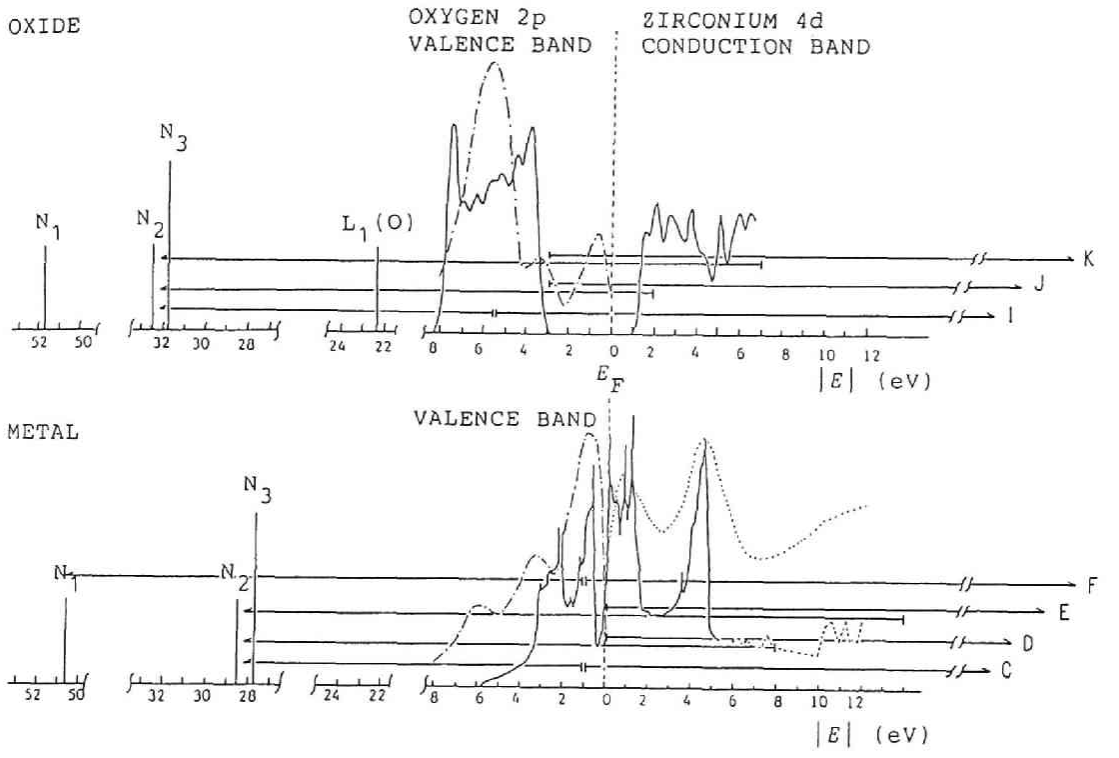

Fig. 6-14. Assignments of the peaks of the secondary electron emission.

Fermi level for the clean surface and that 6 eV above the bottom of the conduction band for the oxide have not been reported, and comparison is impossible.

Our assignments of the other SES peaks are shown in Fig. 6-14. The peaks C and I are the $N_{23}VV$ Auger peak(super Coster-Kronig transition) for the clean surface and the oxide-covered surface, respectively. The kinetic energy, which was estimated on the basis of a negligibly weak hole-hole interaction, of the $N_{23}(M)V(M)V(M)$ transition for the clean surface (25.7 - 26.5 eV relative to E_F) and that of the $N_{23}(O)V(O)V(O)$ transition for the oxide-covered surface (19.8 - 20.6 eV relative to E_F) are in good agreement with the kinetic energies measured. The peak F is the N_1VV Auger peak(super Coster-Kronig transition) for the clean surface, because the kinetic energy of the $N_1(M)V(M)V(M)$ transition estimated (48.6 eV relative to E_F) is in good agreement with the kinetic energy measured.

Recently a few investigators have reported that the secondary electron emission of the peaks D, E, J and K can be explained by autoionization emission.[19-20] This assignment was mainly due to the fact that the peaks measured are broad and the autoionization emission is observed in other 3d and 4d transition metals. When an excited electron above the Fermi level deexcites to the core hole state, the electron transfers the energy directly to an electron at the Fermi level for the clean surface and to a electron at the top of the valence band for the oxide surface. Since this transition occurs in a short period, a lifetime broadening of the emission peak is induced.[19-20] From the law of energy conservation the peaks D and F may be explained by the autoionization emission in which the excited electrons at energies 8 eV and 14 eV above E_F deexcite to the

N_{23} core hole state and the electrons transfer their energies to the electrons at E_F. The peaks J and K may be explained by the autoionization emission in which the excited electrons at the energy of the bottom of the conduction band and 6 eV above the bottom of the conduction band deexcite to the N_{23} core hole state in the oxide and the electrons transfer their energies to the electrons at the top of the valence band. The fact that the energies at the above-mentioned excited states are in good agreement with those observed in our EELS measurement supports this assignment, *i.e.* the excited states of peaks D, E, J and K in the secondary electron emission spectra were observed as the corresponding peaks E, F, L and M in the electron energy loss spectra, respectively (see Fig. 6-10 and Fig. 6-14).

Oxidation at High Temperatures

The secondary electron emission spectra were measured *in situ* at 773 K and 873 K under a constant oxygen pressure of 1.3×10^{-5} Pa as a function of exposure time. The kinetic energies and the intensities of the second derivative peaks (not shown) for the clean surface and the oxide-covered surface after the exposure for 3600 s are the same as those measured at room temperature. The change in energies and intensities with time was just the same way as the change in those of the Auger spectra and the energy loss spectra at 773 K and 1.3×10^{-5} Pa, *i.e.* the spectra of the metal was changed to that of oxide in 1800 s and no significant change was observed after 1800 s.

At 873 K the intensity of the second derivative peak of the $N_{23}VV$ transition was decreased by 30 % at the exposure of 3600 s, as compared

with that for the clean surface.(not shown) This may be due to a peak broadening by oxidation because the kinetic energy of this peak was not changed. The significant changes in the kinetic energy and the intensities of the other peaks were not observed by oxidation at 873 K and at oxygen pressure of 1.3×10^{-5} Pa.

Conclusion

The oxidation of zirconium at room temperature depends on the exposure in Langmuir, *i.e.* the product of oxygen pressure and time. The oxide thickness estimated is *ca.* 1 nm after exposure for 100 L at room temperature. The kinetic energies of the peaks of the Auger electron spectra are explained by the electronic structure of the substrate on the assumption that the hole-hole interaction is negligible. The energy losses measured for the clean and the oxidized surface are explained by the single electron excitation and the collective excitation of plasmon. The peaks which correspond to the density of unoccupied states, the Auger peaks and the autoionization peaks are observed in the secondary electron emission spectra. The changes in the Auger, the electron energy loss and the secondary electron emission spectra by oxidation at high temperatures depend on the surface oxidation states which are determined by the dynamic competition between the surface processes such as the adsorption and the transfer of the adatom into the bulk and the diffusion process of oxygen into the bulk. The oxide growth rate is found to be parabolic at high temperature of 773 K and at 1.3×10^{-5} Pa.

References for Chapter 6

1. J. S. Foord, P. J. Goddard and R. M. Lambert,
   Surf. Sci., 1980, 94, 339.
2. G. N. Krishnan, B. J. Wood and D.Cubicciotti,
   J.Electrochem.Soc., 1981, 128, 191.
3. P. Sen, D. D. Sarma, R. C. Budhani, K. L. Chopra and C. N. R. Rao,
   J. Phys. F, 1984, 14, 565.
4. K.-O. Axelsson, K.-E.Keck and B. Kasemo, *Surf. Sci.* 1985, 164, 109.
5. J. M. Sanz, C. Palacio, Y. Casas, J. M. Martinez-Duart,
   Surf. Inerface Anal., 1987, 10, 177.
6. B. Jungblut, G. Sicking, T. Papachristos,
   Surf. Interface Anal., 1988, 13, 135.
7. T. Tanabe and M. Tomita, *Surf. Sci.*, 1989, 222, 84.
8. K. C. Hui, R. H. Milne, K. A. R. Mitchell, W. T. Moore and M. Y. Zhou,
   Solid State Commun., 1985, 56, 83.
9. P. C. Wong and K. A. R. Mitchell, *Can. J. Phys.*, 1987, 65, 464.
10. P. C. Wong, K. C. Hui, B. K. Zong and K. A. R. Mitchell,
    Solid State Commun., 1987, 62, 293.
11. B. W. Veal, D. J. Lam and D. G. Westlake,
    Phys. Rev. B, 1979, 19, 2856.
12. R. L. Tapping, *J. Nucl.Mater.*, 1982, 107, 151.
13. D. P. Valyukhov, M. A. Golubin, D. M. Grebenshchikov and V. I. Shestopalova, *Sov. Phys. Solid State*, 1982, 24, 1594.
14. P. E. West and P. M. George, *J. Vac. Sci. Technol.*, 1987, A5, 1124.
15. L. Kumar, D. D. Sarma and S. Krummacher,
    Appl. Surf. Sci., 1988, 32, 309.

16. C. O. De González and E.A. García, *Surf. Sci.*, 1988, 193, 305.

17. C. Morant, J. M. Sanz, L. Galán, L. Soriano and F. Rueda, *Surf. Sci.*, 1989, 218, 331.

18. J. Frandon, B. Brousseau and F. Pradal, *Phys. Stat. Sol. (b)*, 1980, 98, 379.

19. C. Palacio, J. M. Sanz and J. M. Martinez-Duart, *Surf. Sci.* 1987, 191, 385.

20. P. Aebi, M. Erbudak, A. Leonardi and F. Vanini, *J. Electron Spectrosc. Relat. Phenom.*, 1987, 42, 351.

21. G. R. Corallo, D. A. Asbury, R. E. Gilbert and G. B. Hoflund, *Phys. Rev. B*, 1987, 35, 9451.

22. F. Vanini, M. Erbudak and P. Aebi, *Solid State Commun.*, 1988, 66, 589.

23. M. Yamamoto, S. Naito, M. Mabuchi and T. Hashino, *J. Chem. Soc. Faraday Trans.*, 1990, 86, 157.

24. K. Griffiths, *J. Vac. Sci. Technol.*, 1988, A6, 210.

25. M. Yamamoto, S. Naito, M. Mabuchi and T. Hashino, to be published.

26. H. Takeuchi, S. Naito, M.Yamamoto and T. Hashino, *J. Chem. Soc. Faraday Trans.* 1, 1988, 84, 4235.

27. M. Yamamoto, S. Naito, M. Mabuchi and T. Hashino, *J. Phys. Chem.*, 1989, 93, 5203.

28. M. Yamamoto, S. Naito, M. Mabuchi and T. Hashino, *J. Chem. Soc. Faraday Trans.*, in press.

29. H. Kato, Y. Sakisaka, M. Nishijima and M. Onchi, *Surf. Sci.*, 1981, 107, 20.

30. *Handbook of Chemistry and Physics*, ed. R. C. Weast, M. J. Astle and W. H. Beyer (CRC, Florida, 67th edn, 1986),

pp. F163-F166.

31. M. P. Seah and W. A. Dench, *Surf. Interface Anal.*, 1979, 1, 3.

32. G. Marletta and S. Pignataro, *Chem. Phys. Lettters*, 1986, 124, 414.

33. C. Horie, *Prog. Theor. Phys.*, 1959, 21, 113.

34. J. G. Bendoraitis and R. E. Salomon, *J. Phys. Chem.*, 1965, 69, 3666.

35. F. Zandiehnadem, R. A. Murray and W. Y. Ching,
Physica B, 1988, 150, 19.

36. W. Speier, J. C. Fuggle, R. Zeller, B. Ackermann, K. Szot, F. U. Hillebrecht and M. Campagna, *Phys. Rev. B*, 1984, 30, 6921.

37. O. Jepsen, O. K. Andersen and A. R. Mackintosh,
Phys. Rev. B, 1975, 12, 3084.

38. P. Blaha, K. Schwarz and P. H. Dederichs,
Phys. Rev. B, 1988, 38, 9368.

39. R. F. Willis, B. Fitton and G. S. Painter,
Phys. Rev. B, 1974, 9, 1926.

Conclusion

Oxidation of transition metals has been a practical problem of corrosion. However, the microscopic mechanism of the oxidation of transition metals, at high temperatures in particular, has not been investigated in detail. In the present work the mechanism of the oxidation of zirconium has been clarified by studying the kinetics of oxygen absorption by zirconium at high temperatures and at low oxygen pressures and the oxidation states at the zirconium surface by the use of SIMS, AES, EELS, SES and the work function method.

The summary of this work are as follows.

1. The rate of oxygen absorption by the oxide-covered surface is proportional to the square root of oxygen pressure. Based on the assumption of the local equilibrium between the adsorption and the desorption process, the pressure dependence of the rate is explained by the diffusion of oxygen into the bulk with a moving boundary of the oxide/metal interface. The activation energy for the transfer of oxygen adatoms on the oxide-covered surface into the bulk is evaluated to be $(1.0 \pm 0.1) \times 10^{-19}$ J per O atom. The changes in the resistivity of zirconium by oxidation are in agreement with that calculated by the same model as used for oxygen absorption.

2. The rate of oxygen absorption by α-zirconium is almost proportional to the oxygen pressure. The absorption rate is limited by the adsorption of oxygen gas. The absorption rate is explained by using a modified Langmuir model in which the absorption processes comprises three successive steps: the dissociative adsorption of oxygen molecules on the

zirconium surface with an interaction between adatoms, the transfer of adatoms at the surface sites to the outermost bulk sites and the diffusion of oxygen atoms into the bulk. The following kinetic parameters are determined. The activation energy for the adsorption is (7.4 ± 0.6) × 10^{-20} J per O atom. The interaction between the adatoms is attractive and the energy is -4 × 10^{-21} J per O-O pair. The adsorption site has a potential energy lower by (2.2 ± 0.1) × 10^{-19} J per O atom than in the bulk. The linear relation between the effective emissivity and the oxygen concentration at the surface of α-zirconium has been found.

3. Secondary ion mass spectroscopy(SIMS) has been used to investigate the chemical composition of the zirconium surface at low oxygen pressures and at high temperatures. Existence of three sequential stages of the increase in the yields of the secondary ions Zr^+, ZrO^+ and ZrO_2^+ has been observed: (i) the first stage in which the surface remains as α-zirconium and the yields increase slowly; (ii) the second stage in which nucleation of oxide causes rapid increase in the yields; (iii) the final stage in which the surface is covered with the oxide and the yields show saturation. The surface remains as α-zirconium longer at lower oxygen pressures and at higher temperatures. The increase in the yields of the Zr^+ ion is interpreted to be caused by the formation of oxide at the surface. By means of the resonance tunnelling theory, the reason for the increase is explained by the downward energy shift of the highest occupied electronic level of the substrate. The depth profile is found to be determined by the dynamic competition between transport of oxygen at the surface and diffusion of oxygen into the bulk.

4. An anomaly in the rate of oxygen absorption has been observed at the stage of nucleation of the surface oxide, *i.e.* the rate of oxygen absorption is increased anomalously by the formation of oxide at the surface. The rate of oxygen absorption at the nucleation stage is numerically evaluated by using a model in which nucleation and growth of oxide at the surface is approximated by an autocatalytic reaction. The calculated oxide coverage is in good agreement with that obtained from the SIMS measurement. The activation energy for the decomposition of the quasi two-dimensional oxide at the surface is evaluated to be $(7.0 \pm 0.5) \times 10^{-20}$ J.

5. Three stages of the change in the work function are found: decrease at the initial stage, increase at the second stage and saturation at the final stage. By using SIMS, it is shown that the three stages of the change in the work function correspond to the oxidation stage of oxygen adsorption, the stage of oxide nucleation and the stage of oxide growth, respectively. The initial decrease in the work function is caused by the oxygen adsorption at the surbsurface site. The potential of oxygen at the metal surface is calculated by the effective medium theory. One of the reasons for the incorporation of oxygen to the subsurface is that metallic zirconium has a low incorporation barrier of oxygen from the surface site to the subsurface site. The downward energy shift of the chemical potential by the oxide formation is the cause of the increase in work function at the second and the final stage.

6. The change in the kinetic energies of the Auger and the secondary electrons and the change in the energy losses by the single electron excitations with the progress of the oxidation of zirconium are explained by the downward energy shift of the core levels and the valence band of

zirconium. The energy loss by the collective excitation of plasmon is also observed in the electron energy loss spectra for the metal and the oxide-covered zirconium surfaces. The increase in the relative peak-to-peak height of the oxygen Auger transition and of the zirconium Auger transition, which is a measure of the oxygen concentration at the surface, shows the evidence that the dynamic competition between the surface processes and diffusion process in the the bulk occurs in the oxidation of zirconium at high temperatures and low oxygen pressures. The rate of oxide growth estimated from the Auger electron spectra is found to be parabolic at high temperatures.

In conclusion, the oxidation of zirconium has been shown to go through the three stages: the adsorption of oxygen, nucleation of oxide and growth of oxide. The results of the rate of oxygen absorption at high temperatures and low oxygen pressures, of the chemical composition determined by SIMS and AES and of the change in the electronic structure obtained by AES, EELS, SES and the work function method show a conclusive evidence for the existence of the three stages.

Acknowledgments

The author would like to express his gratitude for the guidance and encouragement received from Professor T. Hashino, Kyoto University. The author is also grateful to Associate Professor S. Naito, Dr. M. Mabuchi, Messrs H. Takeuchi, Y. Maeno and T. Satake for their helpful discussions. The works in Chapters 1 and 5 were greatly assisted by the effort of Messrs H. Takeuchi and Y. Maeno, respectively.

He would like to thank Messrs O. Hashitomi, T. Tuchiyama and Y. Nishinosono for their skillful technical assistance throughout the course of this work.

He also wishes to acknowledge valuable discussions with the members of Institute of Atomic Energy, Kyoto University, especially with Dr. T. Kawai, Dr. Y. Ohta, Messrs K. Yura, M. Kikuchi, T. Sakka, M. Kimura, K. Kagawa, M. Fujiwara, T. Maeda, Y. Ashida and A. Kaneda.